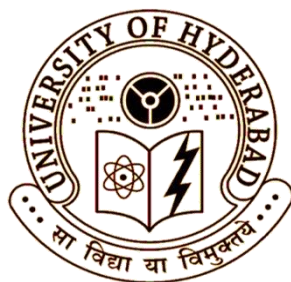

Studies of Polybutadiene diol based Water Dispersible Polyurethanes and their Nanocomposites

A Thesis Submitted for the Degree of

DOCTOR OF PHILOSOPHY



BY

Kuruma Malkappa

**School of Chemistry
University of Hyderabad
Hyderabad-500 046
INDIA**

December 2015

**Dedicated
To
My Parents and Teachers**

CONTENTS

Declaration	i	
Certificate	ii	
Preface	iii	
Acknowledgement	iv	
Common Abbreviations	vi	
CHAPTER-1	Introduction	1–33
1.1 HISTORY OF POLYURETHANE (PU)		1
1.2. SYNTHESIS OF POLYURETHANES		1
1.2.1. The importance of polyols		2
1.2.2. Importance of diisocyanates		3
1.3 PROPERTIES OF POLYURETHANES		5
1.3.1 Thermal Properties		6
1.3.2 Mechanical Properties		6
1.3.3 Film formation and hydrophobic properties		7
1.4 POLYURETHANE APPLICATIONS		8
1.4.1 Adhesives and binders		9
1.4.2 Textile industry		9
1.4.3 Shape memory		9
1.4.4 Tissue engineering		10
1.4.5 Insulating materials		11
1.4.6 Biomedical applications		11
1.4.7 Coating and Painting		11
1.5 WATER DISPERSIBLE POLYURETHANES		11
1.5.1 Anionic PU dispersions		12
1.5.2 Cationic PU dispersions		12
1.5.3 Non-ionic PU dispersions		12
1.5.4 Particle morphology and stability		14
1.6 STRUCTURE PROPERTY RELATIONSHIP OF PU		15

1.7 HYDROXYL TERMINATED POLY BUTADIENE (HTPB)	17
1.8 POLYMER NANOCOMPOSITES	20
1.8.1 Polymer clay composites	20
1.8.2 Polymer-Titanium/Silica Nano composites	23
1.9 AIM OF THE THESIS	24
1.10 REFERENCES	25
CHAPTER-2 Material and Experimental Methods	35—42
2.1. MATERIALS	35
2.2. CHARACTERIZATION METHODS	35
2.2.1 Spectroscopic studies	35
2.2.1.1. FT-IR Study	35
2.2.1.2. NMR Study	35
2.2.2 X-Ray Diffraction studies	35
2.2.2.1. WAX Study	35
2.2.2.2 SAX Study	36
2.2.3. Mechanical strength measurement	36
2.2.3.1. Dynamic Mechanical Analysis	36
2.2.3.2. Universal Testing Measurement	36
2.2.4. Microscopic Studies	38
2.2.4.1. FESEM Study	38
2.2.4.2. AFM Study	38
2.2.4.3. TEM Study	38
2.2.5. Thermal analysis	38
2.2.5.1. TG-DTA Study	38
2.2.5.2. DSC Analysis	38
2.2.6. Contact angle measurement	39
2.2.7. Particle size analysis	39
2.2.8. Antibacterial activity	39
2.2.9. Hydroxyl value Measurement	39

2.3. REFERENCES	40
CHAPTER-3	
Simultaneous improvement of tensile strength and elongation: An unprecedented observation in case of HTPB polyurethanes	43–61
3.1. INTRODUCTION	43
3.2. SYNTHESIS	44
3.2.1. Synthesis of HTPB-DNB	44
3.2.2. Synthesis of Polyurethane	45
3.3. CHARECTERIZATION	46
3.4. RESULTS AND DISCUSSION	46
3.4.1. Synthesis and Spectroscopic Studies of Polyurethanes	46
3.4.2. Tensile properties	49
3.4.3. X-ray studies	52
3.4.4. Morphological study	56
3.4.5. Thermal Study	57
3.5. CONCLUSION	59
3.6. REFERENCES	60
CHAPTER 4	
Hydrophobic, water dispersible polyurethane: Role of polybutadienediol structure	63 – 86
4.1. INTRODUCTION	63
4.2. SYNTHESIS	64
4.2.1. Preparation of Water-Dispersible Polyurethanes	64
4.2.2. Preparations of PU Films from Water-Dispersible PU (WDPU)	66
4.3. CHARECTERIZATION	66
4.4. RESULTS AND DISCUSSION	67
4.4.1. Synthesis of Water Dispersible PUs	67

4.4.2. FT-IR Study	68
4.4.3. Stability and Morphological Studies of Synthesized PU Dispersions	70
4.4.4. Preparation of Film from WDPUs and Their Characterizations	74
4.4.5. Thermogravimetric Analysis	74
4.4.6. Tensile Properties of PU	76
4.4.7. Thermal Transitions and Modulus of PUs	78
4.4.8. Surface Hydrophobicity of PU Films	81
4.5. CONCLUSION	84
4.6. REFERENCES	85
 CHAPTER 5	
Functionalized polybutadiene diol Based hydrophobic, water dispersible polyurethane nanocomposites: Role of Organoclays structure	89 – 115
 5.1. INTRODUCTION	89
5.2. SYNTHESIS	90
5.2.1. Organic modification of kaolinite clay	90
5.2.2. <i>In-situ</i> preparation of water dispersible polyurethane/clay nanocomposite	90
5.2.3. Preparations of PU films from WDPUs/clay composites	91
5.3. CHARACTERIZATION	91
5.4. RESULTS AND DISCUSSION	93
5.4.1. Preparation of WDPUs/clay composite	93
5.4.2. FT-IR study	95
5.4.3. Solid-state NMR study	97
5.4.4. X-ray diffraction study	99
5.4.5. Morphology study	101
5.4.6. Tensile properties	103
5.4.7. Thermal stability	106

5.4.8. Thermal transitions	107
5.4.9. Surface hydrophobicity of nanocomposite films	110
5.5. CONCLUSION	112
5.6 REFERENCES	113
 CHAPTER 6 Organic/Inorganic hybrid nanocomposites of water dispersible polyurethanes for antibacterial coating	 117 – 139
 6.1. INTRODUCTION	 117
6.2. SYNTHESIS	118
6.2.1. Preparation of TiO ₂ (core)-SiO ₂ (shell) nanoparticles	118
6.2.2. Preparation of water dispersible PU (WDPU) nanocomposite with TiO ₂ (core)-SiO ₂ (shell) particles	118
6.2.3. Preparations of PU films from WDPU/TiO ₂ -SiO ₂ nanocomposites	120
6.3. CHARECTERIZATION	120
6.4. RESULTS AND DISCUSSION	120
6.4.1. Synthesis of HTPB-DNB WDPU and its nanocomposites with TiO ₂ (core)/SiO ₂ (shell) particles	120
6.4.2. Spectroscopic study of WDPU/TiO ₂ -SiO ₂ nanocomposites	124
6.4.3. Wide angle X-ray diffraction (WAXD) studies	126
6.4.4. FE-SEM studies	127
6.4.5. Tensile properties of WDPU/TiO ₂ -SiO ₂ nanocomposites	128
6.4.6. Thermo-mechanical studies of WDPU/TiO ₂ -SiO ₂ nanocomposites	130
6.4.7. Surface hydrophobicity of WDPU/TiO ₂ -SiO ₂ nanocomposite films	134
6.4.8. Antibacterial activity	135
6.5. CONCLUSION	137
6.6 REFERENCES	138

CHAPTER 7	Summary and Conclusion	141-145
7.1. Summary		141
7.1. Conclusion		143
7.1. Scope of Future Work		144
<i>Publication and Presentation</i>		149-150

DECLARATION

I hereby declare that the matter embodied in the thesis entitled “*Studies of Polybutadiene diol based Water Dispersible Polyurethanes and their Nanocomposites*” is the result of investigations carried out by me in the School of Chemistry, University of Hyderabad, Hyderabad, India under the supervision of **Prof. Tushar Jana** and it has not been submitted elsewhere for the award of any degree or diploma or membership, etc. This work is free from plagiarism. I hereby agree that my thesis can be submitted in Shodhganga/**INFLIBNET**

In keeping with the general practice of reporting scientific investigations, due acknowledgements have been made wherever the work described is based on the findings of other investigators. Any omission or error that might have crept in is regretted.

A report on plagiarism from the University library is enclosed.

December 2015

Kuruma Malkappa

Regd. No: 10CHPH18

UNIVERSITY OF HYDERABAD
Central University (P.O.), Hyderabad-500046, INDIA

Professor Tushar Jana
School of Chemistry
University of Hyderabad



Web: <http://chemistry.uohyd.ac.in/~tj/>

Tel: 91-40-23134808 (Office)
91-40-65555187 (Home)
91-9440127016 (Mobile)
Fax: 91-40-23012460
E-mail: tusharjana@uohyd.ac.in
tjscuoh@gmail.com

CERTIFICATE

This is to certify that the work described in this thesis entitled “***Studies of Polybutadiene diol based Water Dispersible Polyurethanes and their Nanocomposites***” has been carried out by **Mr. Kuruma Malkappa** under my supervision and the same has not been submitted elsewhere for any degree.

Dean
School of Chemistry
University of Hyderabad
Hyderabad-500 046
India

Prof. Tushar Jana
(Thesis supervisor)

PREFACE

The present thesis entitled “***Studies of Polybutadiene diol based Water Dispersible Polyurethanes and their Nanocomposites***” has been divided into seven chapters. **Chapter 1** includes brief introduction of PUs, synthetic procedures of PUs and different types of water dispersible PUs and the structure property relationships of PUs. In addition, the advantages and importance of water dispersible PUs in various applications and mainly coating applications are discussed. **Chapter 2** deals with the details of materials source which were used for all the working chapters and the experimental procedure for characterization of all synthesized polymers and nanocomposites. **Chapter 3** In this chapter, a series of solvent-based PUs were synthesized from HTPB and modified HTPB (HTPB-DNB) as polyols using different types of diisocyanates. The structural properties of the resulting PUs were characterized by using different instrumental techniques which revealed that the formation of extra H-bonding network between the dinitrobenzene and urethane backbone is the driving force for superior tensile properties in case of modified HTPB-PUs. **Chapter 4** explores the novel methods for synthesis of water dispersible PUs from two different butadiene diols namely HTPB and HTPB-DNB. Hard segment content variation found to be the best choice to control several important properties including hydrophobicity of the PU surface. **Chapter 5** describes the preparation of clay nanocomposites of water dispersible PUs with two different types of clays (Cloisite-30B and Kao) by an *in-situ* method. The influence of incorporation of clay, on the properties of water dispersible PUs were evaluated. **Chapter 6** describes the formation of nanocomposites of water dispersible PUs with TiO₂/SiO₂ core-shell nanoparticles by *in-situ* process and the effect of nanosized core-shell nanoparticles on the properties of water dispersible PUs and their antibacterial applications were studied. **Chapter 7** summarizes the findings of the present investigations, presents concluding remarks and the future scopes of the current study.

December, 2015

Kuruma Malkappa

ACKNOWLEDGEMENT

I would like to express my most sincere appreciation to my research and thesis supervisor, Professor. Tushar Jana, for his generous support, technical guidance, constant cooperation and encouragement throughout the course of my research at University of Hyderabad. He has been quite helpful to me in both academic and personal fronts. It has been great pleasure and fortune to work with him who introduced me to the field of Polymer Chemistry. His discipline, working style and honesty for the research have paved a new path in my career. I am also indebted to him for the work freedom during the last five years.

I would like to thank the former and present Deans, School of Chemistry for their constant inspiration and for allowing me to avail the available facilities. I am extremely thankful individually to all the faculty members of the school for their kind help and cooperation at various stages.

I am very grateful acknowledge to the members of my Ph.D. doctoral committee Dr. P. K. Panda and Dr. K. Muralidharan for their encouragement and support throughout my research career.

Financial assistance from ACRHEM, University of Hyderabad and CSIR, New Delhi for providing research fellowship as well as various instrumental facilities, is sincerely acknowledged.

I felt very lucky and proud to have labmates like Arindamda, Arunda, Sandipda, Muralida, Mousumidi, Sudhanshu, Niranjana, Jayaprakash, Bikas, Shuvra, Raju, Narasimha, Kondareddy, Rambabu, Moumitha and Harilal in my Ph.D life. Arindamda, Arunda and Sandipda are very much like elder brothers in lab they are always with me in my problematic time and also thankful to them for their support and help at the initial stage of my research. My special thanks to M. Sc project students Srinu, Balaji, Keertireddy, Swetha, Srikanth, Appalanaidu, saibal, Chandrakala, Venkatesh and Ajay Krishnan

I sincerely acknowledge Dr. Rohini Kumar of IICT, Hyderabad for helping with UTM experiments and also sincerely thank Centre for Nanotechnology, UoH for allowing me to use the TEM facility. I also would like to express special thanks Dr. Ramanuj Narayana, Senior Scientist of IICT Hyderabad for allowing us to do contact angle and particle size analyzer experiments. I would also like to express my sincere gratitude to Prof. Ch. Venkata Ramana, School of Life Science allowing me to do the antibacterial activity test of my samples. I thank Suresh and Tushar for helping me with the antibacterial activity experiment, and also Nagaraju for helping in particle size analyzer and contact angle measurement at IICT.

I sincerely acknowledge all my teachers starting from the school, to the college and to the University for teaching me all the discipline, values and education throughout my academic career. My special thanks to Ram Singh, Babu Singh, S. Krishna Reddy, Mohan Reddy, Beechi Reddy and Dr. D. S. R. Rajender Singh for their kind help and valuable suggestions and supported me a lot to reach this stage.

I also thank all non-teaching staff for their timely help. I thank Mr. Thurab Syed, Smt. Vijayalakshmi for their help in recording NMR spectra. I thank Mr. Shetty, Mr. Vijay Bhaskar, Mr. Dilip, Mr. Sai, Mr. Sharma, Mr. Jayaram, Mr. Durgesh, Mr. Shetty, Mr. Joseph, Mr. Sambashiva Rao and Mr. Venkatesh for their cooperation.

I would also like to express my sincere thanks to all my friends in HCU with whom I have some wonderful memories in Hyderabad throughout my Ph.D. life.

I am really lucky for my close association with include Ravikiran, Raghav, Santhosh, Sravan, Surender, G.M., Sathis, Kumar, Chandu, Thirupathi Reddy, Ramu, Raghu, Ranjith, Rajkumar, Ajay, Suman, Rahul, Balraj, Sayappa Goud, Bhaskar, Manmohan, Srinivas Reddy for their help and encouragement in various stages of my life.

Words are not enough to express appreciation, gratitude earnest feelings to my wife Dhana Laxmi for giving me her constant mental support and encouragement in the last period of my Ph.D life and my little princess, Himaakshitha who is a blessing in the guise of daughter.

My beloved parents and all my family members without their sacrifice and mental support I would not have reached to this stage of my life. I am greatly obligated to my parents for their spiritual guidance and stay as a philosopher of my life.

**December, 2015
University of Hyderabad
Hyderabad-500 046
India**

Kuruma Malkappa

Common Abbreviations

CA	Contact Angle
DCM	Dichloromethane
DMAc	N,N-dimethyl acetamide
DMF	N,N-dimethyl formamide
DMSO	Dimethyl sulfoxide
DMA	Dynamic Mechanical Analyzer
DSC	Differential Scanning Calorimeter
DLS	Dynamic light scattering
DBTDL	Dibutyltin dilaurate
FTIR	Fourier transform infrared spectroscopy
FESEM	Field Emission Scanning Electron Microscopy
HTPB	Hydroxyl Terminated Polybutadiene
HTPB-DNB	Hydroxyl Terminated Polybutadiene Dinitrobenzene
HTPB-PU	Hydroxyl Terminated Polybutadiene Polyurethane
HTPB-DNB-PU	Hydroxyl Terminated Polybutadiene dinitrobenzene Polyurethane
H ₁₂ MDI	4,4'-Diisocyanato dicyclohexyl methane
IPDI	Isophoron diisocyanate
M _n	Number average Molecular weight
M _w	Weight average Molecular weight
MDI	Methylene diphenyl diisocyanate
MW	Molecular weight
NMR	Nuclear magnetic resonance
NMP	N-methyl-2-pyrrolidone
PDI	Polydispersity Index
PU	Polyurethane
SAXD	Small angle X-ray diffraction
T	Temperature
2,4-TDI	2,4-Toluene diisocyanate
2,6-TDI	2,6-Toluene diisocyanate
TEM	Transmission Electron Microscopy
TEOS	Tetraethyl orthosilicate
T _g	Glass transition temperature
TGA	Thermogravimetric analyzer
UTM	Universal Testing Measurement
WAXD	Wide-angle X-ray diffraction

CHAPTER 1

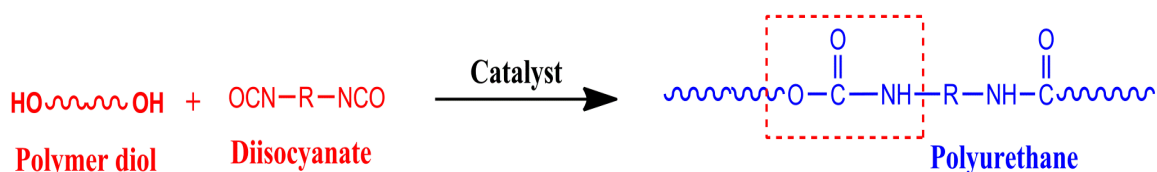
Introduction

1.1. HISTORY OF POLYURETHANES

In 1937, the German scientist prof. Otto Bayer was found out that the poly addition of the diols and diisocyanates in the presence of the catalyst forms polyurethane (PU) in appropriate conditions.¹⁻⁴ During the time of World War II, small-scale PUs were used for the purpose aircraft coating but the same time diisocyanates are not available on the market. After the World War II, some research groups in various countries like U.S.A and U.K focused their research activities and interests in PUs but the commercial development was very slow. During this time, the German chemical industries utilized Prof. Otto Bayer expertise in the PUs chemistry and developed the elastomers and foams^{5,6} Among various chemical industries, the DuPont and ICI first recognized the important property of the PU materials. Production of commercial flexible PU foams from toluene diisocyanate (TDI) and polyols was started in 1954. After that in the year 1960, around 4500 metric tons of flexible PU foams were synthesized. The isocyanate reaction offers the opportunity to prepare tailor-made PU products such as fibres, rubbers etc. In 1969, Bayer developed rigid foams through reaction injection moulding method, which obtained more stiffness mainly for thermal insulating applications. Throughout the sixties, significant improvement in chemical research, its uses and processing technology led to a broad range of commercial applications of PUs in many market areas. The introduction of thermoplastic PUs extended the present processing techniques to injection moulding and extrusion for plentiful applications. To prepare PUs one of the essential starting materials is high molecular weight polymerdiol and the maximum polymer diols are viscous liquids. In 1956, the Dupont introduced the first commercial availability of polyether polyol. In 1960, CTPB (Carboxyl terminated poly butadiene) was used for propellant applications and at the same time, HTPB (Hydroxyl terminated polybutadiene) was developed. The first test for rocket propellant applications with HTPB as a binder was carried out in 1972, showed better advantages over CTPB including high solid loading, desirable mechanical and ageing properties.

1.2. SYNTHESIS OF POLYURETHANES

Polyurethane (PU) is most versatile polymeric materials which can be readily synthesised by the reactions between the polyols and diisocyanates in the presence of suitable conditions and catalyst (Scheme 1.1). A brief description of raw materials which are required for the synthesis of PUs and about the general chemistry involving PU synthesis are discussed in the next few sections. The property of the PUs largely depends on the structures and functionalities of polyols and diisocyanates.



Scheme 1.1. General reaction scheme for the synthesis of polyurethane

1.2.1. The importance of polyols

The substance, which moderate molecular weight (within 10,000 Daltons) and more than one hydroxyl functional group at the terminal position called as polyols. This is one of the important raw materials in the synthesis of PUs mainly depend on the molecular weight, functionality, viscosity and degree of crosslinking of the polyols. The polyols may contain different functionalities along with hydroxyl groups such as ester, ether, amides, acrylic and other functionalities.⁷ For better properties such as combined physicochemical and biodegradability, Papageorgiou et al.⁸ have synthesized the combined aromatic and aliphatic ester copolymer diols containing polyurethanes. The aliphatic part offers the elastic nature because increases in the aliphatic content, the elastic nature increases while it decreases the tensile strength and young modulus. However, most of the well known polyurethanes (PUs) are synthesized from different kinds of polymer polyols based in petrochemicals as solvent which are environmentally toxic. Because of the environmental concerns, recently several methods have been developed for synthesis of water-dispersible PUs in which water is used as a solvent.^{9,10} Generally, polyols are produced by ring-opening polymerization of cyclic esters, cyclic ethers as ethylene oxide, tetrahydrofuran or propylene oxide and cyclic lactams etc. There are different polymer polyols to the synthesis of PUs for various applications. For example to the synthesize biodegradable and shape memory applications, the polylactam and polylactone are used as the polymer diols.^{11,12} Some commonly used polyol structures are shown in the Figure 1.1.¹³

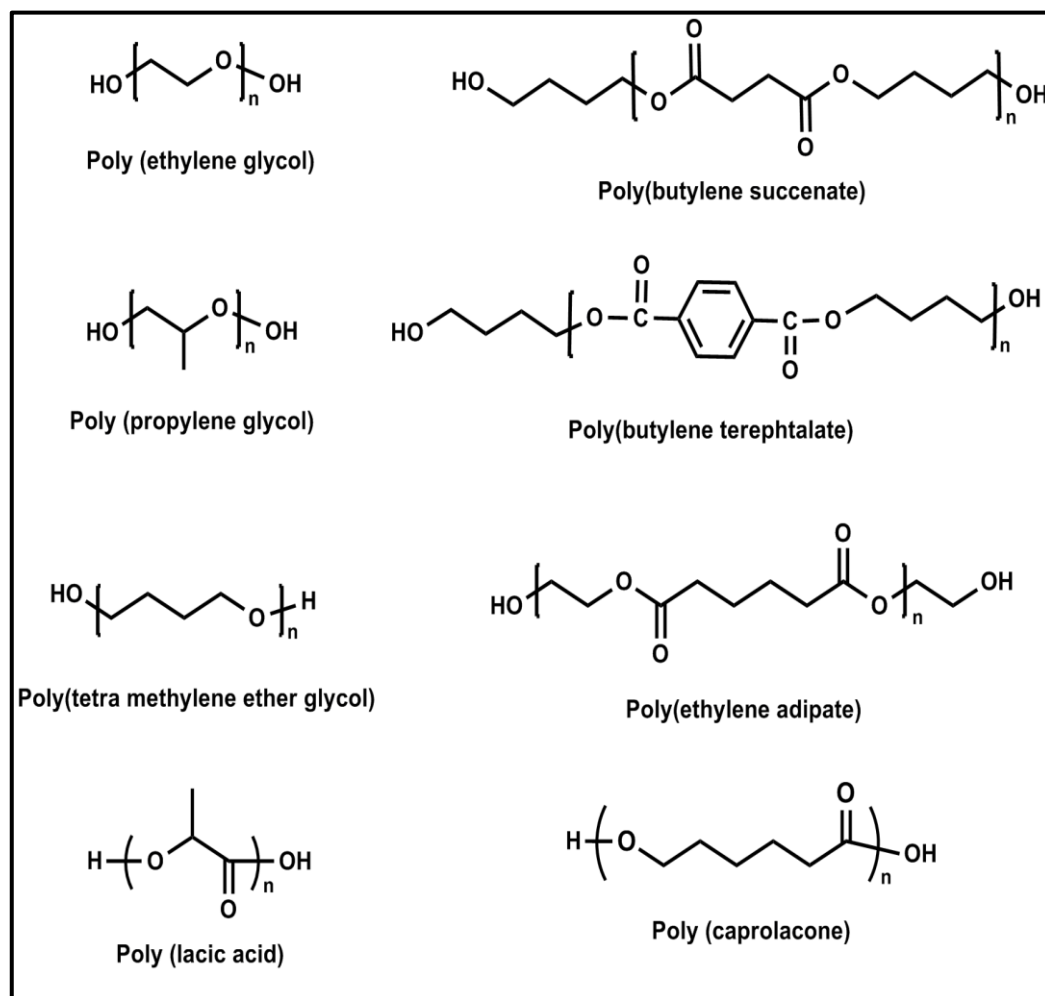


Figure 1.1. Commonly used polymer diol structures.¹³

1.2.2. Importance of diisocyanates

The diisocyanate is one of the most important organic compounds which is used for the synthesis of PUs. The chemical structure of diisocyanate contains cumulative double bonds with N, C and O in the sequence such as $\text{O}=\text{C}=\text{N}-\text{R}-\text{N}=\text{C}=\text{O}$, where R can be aromatic, aliphatic, cyclic or acyclic compound. Because of the vast industrial importance of PUs, we need to study diisocyanate chemistry thoroughly and understand the properties and their reactivity. Diisocyanates are highly reactive and hence readily produce urethane groups without any by-products formation. An isocyanate contains two or more $-\text{NCO}$ functional groups for one molecule and is called as diisocyanes or polyisocyanate respectively.

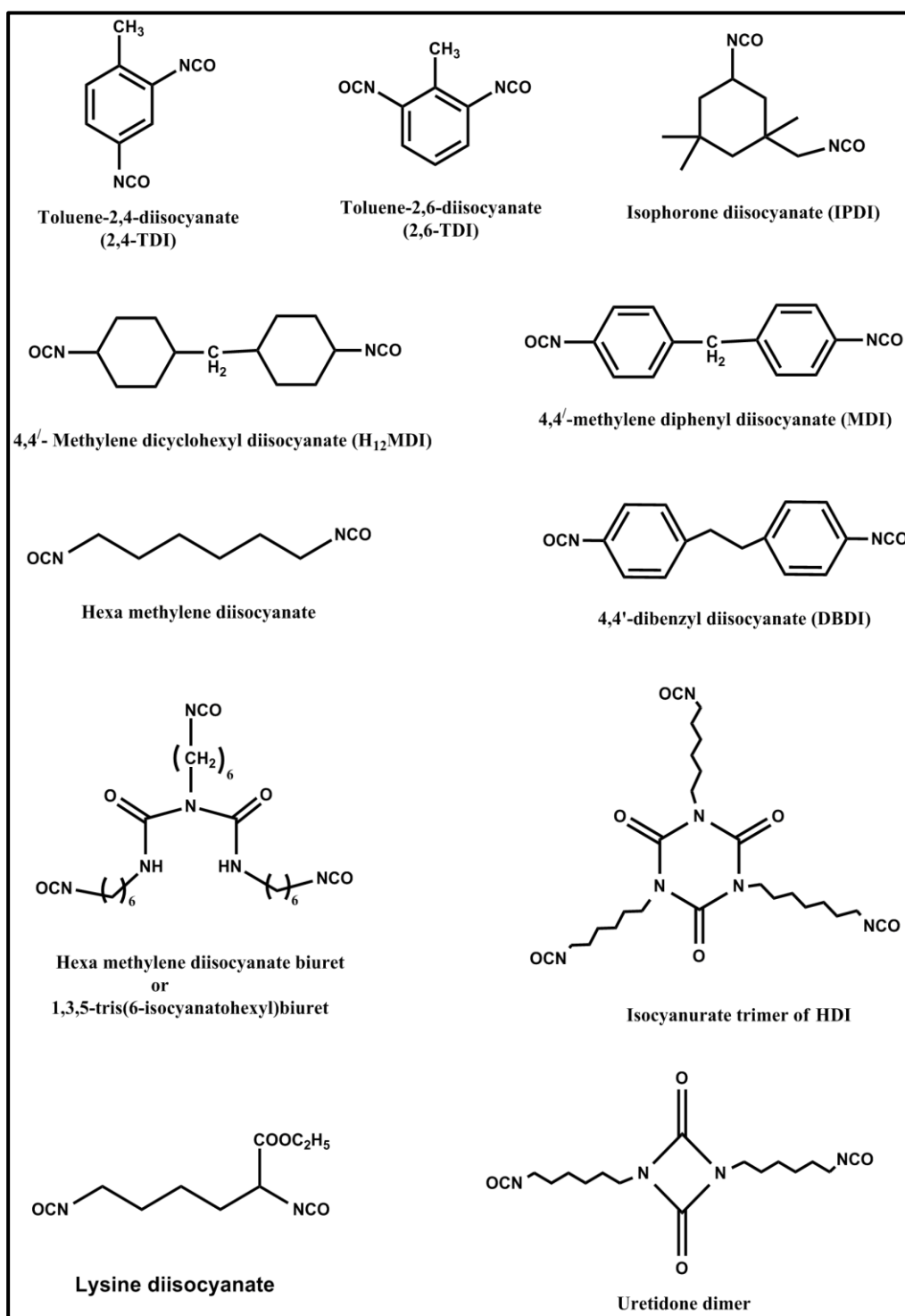


Figure 1.2. Some commonly used diisocyanate and triisocyanate structures.^{13,14}

All diisocyanate are liquids or solids in nature and highly reactive and it undergo reaction across the double bond -C=N of the -NCO group. The reactivity of the isocyanates are mainly depended on the electron density of the central carbon atom of the isocyanate. The low electron density of central carbon atom containing compounds are highly reactive and that is why the aromatic diisocyanates are highly reactive than aliphatic because of resonance structures. Therefore, the electrophilic nature of the aromatic diisocyanates can alter through different substituents on an aromatic ring like electron withdrawing or donating groups. The reactivity of diisocyanates plays an important role for the synthesis of PUs because of the possibility of formation of dimers, trimers and higher oligomers and also possible to formation of polymers. In addition, the number of cross-linking reactions may take place, and primarily depends on the reaction conditions such as temperature, catalysts, and the structure of the alcohols, amines and diisocyanates. Structures of commonly used some isocyanate structures are shown in Figure 1.2 which include toluenediisocyanate (TDI), 4,4'-dicyclohexyl methane diisocyanate (H_{12}MDI), 4,4'-methylene diphenyl diisocyanate (MDI), isophorone diisocyanate (IPDI) and hexa methylene diisocyanate (HDI) and also some triisocyanate structures. The most commonly used isocyanates are TDI and IPDI but compared to TDI, IPDI has some advantages because it is not toxic, average reactivity and aliphatic. For PU synthesis, the IPDI is widely used in the preparation of light stable coating PUs. The two isocyanate groups of IPDI have different reactivity because of different steric hindrance and attached to different carbons that are primary and secondary carbons.

1.3. PROPERTIES OF THE POLYURETHANES

The PU contains urethane and urea linkages between the two monomers and therefore, PU exhibit several intra and inter molecular interactions which results PU has strong affinity to form hydrogen bonding between the urethane -N-H and carbonyl -C=O groups in the PU chains. Generally PUs are mechanically strong and thermally and chemically stable owing to the cross linking (both physical and chemical). Also the PUs exhibits the flexibility and durability because of high molecular weight long chain diols. Most of the PUs contain excellent abrasion resistance, durability and impact resistant. All these properties typically depend on starting materials such as polyols and diisocyanates. Therefore we can able to control the required property of the PUs by changing the lengths of the soft and hard block content and changing the order of hard and soft segment block in PU synthesis. Because of these properties and advantages, the PUs are widely used in various field. The PUs are not soluble most of the solvents, because of high crosslinking and it is soluble only in few high polar

solvents like dimethyl formamide (DMF), dimethyl acetamide (DMAc), dimethyl sulfoxide (DMSO) and N-methyl pyrrolidone (NMP).

1.3.1. Thermal Properties

The PUs are widely used in different fields because of that lot of research work have been carried out to understand the thermal degradation and to improve the thermal stability of the PUs. Thermo gravimetric analyser (TGA) is an useful instrument to evaluate the thermal stability of the PUs. Majority of the literature reported that PUs start degradation around 180 to 200° C in the presence of nitrogen atmosphere and degradation temperature varies with PU structure.¹⁵ For example PUs which are used for industrial thermal insulating applications starts degradations above 250° C. The thermal degradation temperature can be affected by altering polyols and diisocyanates.¹⁶⁻¹⁸ Compared to solvent-based PUs, the water dispersible PUs are very useful for coating applications and also widely used for various applications because of environmental regulation. In recent years the coating industries are focusing to develop the fire-resistant PUs, water dispersible PUs considering fire safety and health hazardous.^{19,20} Kim et al.¹⁹ reported polyimide containing water dispersible PU which was synthesised to increase the thermal stability. Since, the polyimide has an unyielding heat resistant therefore polyimide containing PUs are thermally more stable. PUs are elastic in nature and show the T_g at the sub ambient temperature range at around -60° to -70° C. Differential scanning calorimetry (DSC) and dynamic mechanical analyser (DMA) commonly used to measure the T_g . Generally, the PUs exhibit thermodynamic immiscibility, which resulted into micro phase separation between the hard block and soft block, and hence display two T_g values. That is one T_g for soft segment at lower temperature side and another T_g for hard segment at higher temperature range.²¹⁻²⁴

1.3.2. Mechanical Properties

The urethane bonds which are derived from diisocyanate and chain extender provide the rigidity or strength, and the urethane bond which is derived from the polyols and diisocyanates is responsible for the elastic property of the PU materials. Both physical and chemical crosslinking that take place in the PU chain greatly influence the mechanical property of PUs. Generally, the PUs show abrasion resistant, high impact resistant, durability and flexibility. Due to environmental concern the conventional solvent based PUs are replaced by aqueous PUs in many research groups are focused on synthesis of water dispersible PUs and to increase the mechanical properties. Gunduz et al.²⁵ reported PU dispersions containing different ionic groups such as tartaric acid and dimethylol propionic acid which are introduced into the PU back bone and they observed that in case of tartaric acid containing

PUs show better mechanical properties than dimethylolpropionic acid because of more crosslinking. Polyester polyol PUs have certain advantages, compared to polyether polyol PUs with respect to mechanical strength and oil resistant but the polyether polyol PUs have the certain advantage such as hydrolytic stability.²⁶ Many research groups have reported that with increase the –NCO/-OH ratio, the mechanical strength increases because of the increasing crosslinking. The branching in isocyanates or polyols also increases the crosslinking which further increases the mechanical strength and cohesive forces of the PUs.^{27,28} Hourston et al.²⁹ explored that the importance of neutralization step, the degree of neutralization, the type of ionic component, and the type of counter ions for their effect on the mechanical, particle size and colloidal properties of the PUs dispersions. Various research groups reported that with different types of polyols and diisocyanates, different ionic groups and different types of neutralizations of their properties such as thermal, mechanical, particle morphology and hydrophobic properties can be altered.³⁰⁻³³

1.3.3. Film formation and hydrophobic properties

The PUs can form good films because of some strong physical interactions between the PU chains such as the hydrogen bonding interactions and Van der Waals forces. In the case of solvent based PUs electrostatic forces are present and in the event of water-dispersible PUs the ionic attractions are present. Mainly, the water dispersible PUs can forms a good film with more toughness at low temperature conditions because of the association of PU colloids and water-swollen particles morphology. The hydrophobic property is an important phenomenon in coating applications and this property can be measured with the help of water contact angle measurement. Hydrophobicity is a surface property and this property mainly influenced by the surface energy and microstructure of the surface or geometrical arrangement of the film surface.³⁴⁻³⁸ The roughness of the film, also helps increasing in the contact angle.³⁹⁻⁴² Based on water contact angle measurement the film surfaces are divided in to three types that is hydrophilic, hydrophobic and super hydrophobic. Suppose the water contact angle of the film surface is less than 90° it has called as hydrophilic and above 90° it has called as hydrophobic and if more than 150°, called super hydrophobic. Nowadays vast research is going on for the development of the hydrophobic and super hydrophobic PU dispersion surfaces. Two methods that are often used are first, is to create the rough hydrophobic surface and the second one is to reduce the surface energy. To reduce surface energy, fluorine-containing long alkyl chain compounds introduced into the PU backbone through the covalent bonds formation. Zhang et al.⁴³ synthesised PU dispersions by introducing trifluoroethyl methacrylates through crosslinking and they observed that excellent film forming, hydrophobic and mechanically stable are shown in Figure 1.3 which is useful

for hydrophobic coating applications. Such type of fluorinated PUs are widely used for antifouling, anti-fogging and microelectronic applications.^{44,45} Various methods have been developed to fabricate hydrophobic and super hydrophobic PU dispersions and these are micelles deposition on surface of block copolymer and polydimethylsiloxane containing block copolymers.⁴⁶

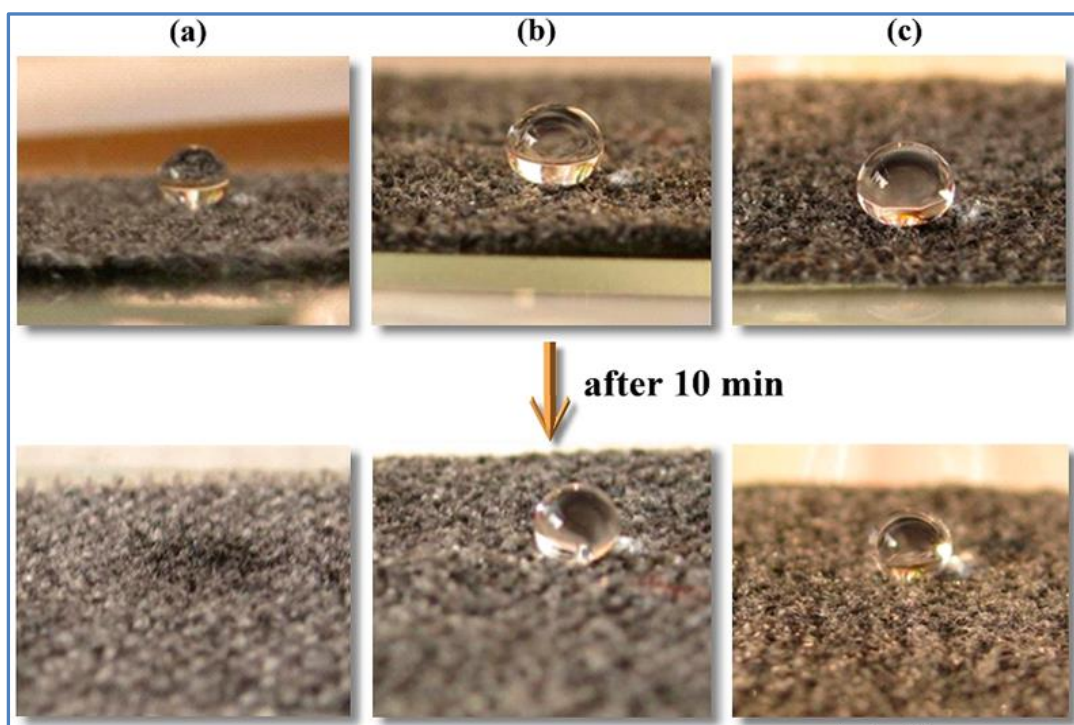


Figure 1.3. The photographs of cotton absorbing water droplets before and after 10 minutes (a) Uncoated water dispersible PU (b) Coated with fluorinated acrylic water dispersible PU (c) coated with aziridine-cross linked fluorinated acrylic water dispersible PU⁴³

1.4. POLYURETHANE APPLICATIONS

PUs have attracted varieties of applications in numerous fields due to thermal stability, mechanical strength and also other physical properties. PU materials usually display durability, flexibility, abrasion resistance and impact resistant. Because of these properties PUs are used in various fields such as composite wood, leather, rubbers, building and constructions, automotive etc. Hydroxyl terminated polybutadiene (HTPB) based PUs are widely used in rocket propellant applications.



Figure1.4. An overview of polyurethane applications including rocket propellant applications (Adapted from Google Images internet).

1.4.1. Adhesives and binders

Adhesives are widely used in varieties of industrial applications such as constructions, automotive, furniture, textiles, aircraft, electronic and electrical applications. Some specific adhesives are used in medical applications such as in wounds drying and dental reconstructions.⁴⁷⁻⁴⁹

1.4.2. Textile industry

Water dispersible PUs has non-flammability, excellent tensile strength, abrasion resistant and also flexibility at lower temperature. Because of these advantages PU dispersions are predominantly used in textile coating applications.^{50,51} The acrylic PU emulsions also useful for textile coating resins because of their crosslinking, which improved the final property of textile materials.^{52,53}

1.4.3. Shape memory

The PUs that is able to show phase deformation at different conditions such as temperature, light, pH, electricity and humidity can be utilized for shape memory. However, most of the PUs is reported temperature deformation. This PUs are a kind of shrinkable applications suppose temperature, pH, light etc. The shape memory PUs are used in the field of bio-medical applications for some device

such as orthopaedic, nerve regeneration, cardiovascular applications.⁵⁴⁻⁵⁷ And also some shape memory alloys are used especially in technical applications transducers, sensors and medical implants.⁵⁸⁻⁶⁰

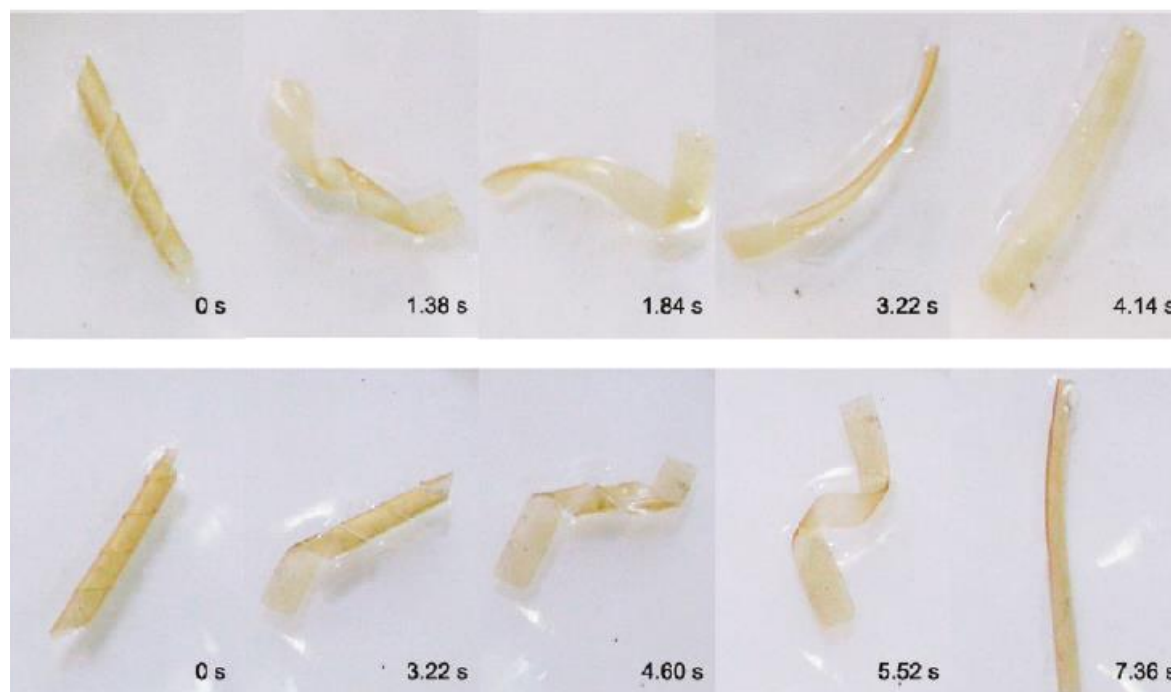


Figure 1.5. Transitions from the temporary spiral shapes to the permanent linear shapes of polymers of different composition.⁵⁴

1.4.4. Tissue engineering

In this application the biodegradability, nontoxicity and cell growth properties are important. Most of the PUs are biocompatible, biodegradable and good mechanical properties such as tensile strength, more elastic nature, abrasion resistant and tear strength. Hence, PU materials are very much useful in tissue engineering applications⁶¹⁻⁶³ Guan et al⁶⁴ synthesized highly porous poly (ether urethane urea), with PCL and 1,4-diisocyanatobutane (BDI) and putrescine which is highly biodegradable and good for tissue engineering applications. Because BDI could release a polyamine which helps for the cell growth and propagation. Several research groups have synthesized PUs for various tissues engineering applications.⁶⁵⁻⁶⁹

1.4.5. Insulating materials

The rigid PU foams are used as insulating materials, such as insulating boards for roofing, metal-faced panels, and walls.^{70,71}

1.4.6. Biomedical applications

PU's have high toughness, flexibility, abrasion resistant, and tear strength and biocompatibility. Generally, the most of the PU's are non-toxic and hydrolytic resistant with the biological fluids due to crosslinking. Therefore, PU's applications are limitless in biological applications. Such as artificial heart valves,⁷² vascular devices,⁷³ aortic valves,⁷⁴ tissues replacing,⁷⁵ artificial bones⁷⁶ and drug delivery applications.⁷⁷

1.4.7. Coating and Painting

The PU's are widely used in coating applications because of high thermal stability and excellent mechanical properties such as high toughness, tensile strength, elasticity, good abrasion resistant, tear resistant and impact resistant. Most of the PU's have good film forming nature, water resistant and chemical stability. However, PU's are solvent based and many reports are available with different polyols and different diisocyanate contents. Nowadays, all over the world the coating industries are attracted by water based PU dispersions because of certain advantages over the solvent-based PU's. That is mainly the environmentally friendly, less expensive, low viscosity and non-flammable. Therefore, there is no environmental pollution since after coating while drying they do not elute any organic solvent. So, present researchers all over the world, focussed on replacement with water dispersible PU's and also try to further improvement in the thermal, mechanical and also flame retardant properties of the water dispersible PU's so as to utilize as a high performance coating material.

1.5. WATER DISPERSIBLE POLYURETHANES

Paul Schlack, first synthesised PU water dispersions in 1943, under vigorous stirring the diisocyanates emulsified with the same amount of diamines resultant to be an excellent dispersed polyurea suspension as the product.⁷⁸ Further introduction of the specific ionomer or emulsifier into the polymer backbone resulted to the PU product which is more stable and good dispersions obtained. The properties such as the emulsions stability and film formation, thermal and mechanical properties also enhanced which are very useful.⁷⁹ The properties of the PU dispersions and film properties are highly depends on the chemical compositions and reaction conditions. With varying the chemical

compositions in the PU synthesis, such as soft and hard segment variations the physical properties can be altered and tuned. The percentage of the ionic group not only affecting the emulsion stability and particle size, but it is also affecting the hardness and flexibility of the final PU material⁸⁰ Based on the type of ionic group which is introduced in the PU chain for mainly water dispersions. The PU dispersions are classified into three types and these are anionic, cationic and non-ionic. The mechanisms of the particle formation in the water dispersible PU synthesis are shown in the Figure 1.6.⁸⁴

1.5.1. Anionic PU dispersions

To prepare anionic PU dispersions, one has to introduce the diol bearing carboxylic acid such as dimethylol propionic acid or tartaric acid then the acid group presence subsequently neutralized with tertiary amine.^{80,97} The groups which is having diol with anionic functional groups such as sulphonates or diaminosulfonates etc can also be used.⁸¹

1.5.2. Cationic PU dispersions

Introduction of cationic monomer like dimethylol amine and phosphorous containing compounds into the polymer backbone and followed by the amine group neutralization with acids results cationic PU dispersions.^{85,82,98}

1.5.3. Non-ionic PU dispersions

Non-ionic dispersions of PU are prepared without using any ionic centre or emulsifier but it is stabilized with inbuilt ionic centres. These ionic centres are mostly oriented at the surface of the particles.⁸³ These types of dispersions have certain advantages over ionic dispersions such as stable against frost, pH changes, electrolytes and high mechanical strength. However, these PU dispersions has some disadvantages like these are more sensitive to water, swelling, hydrolytically decomposition which makes the dispersions turbidity and softened.

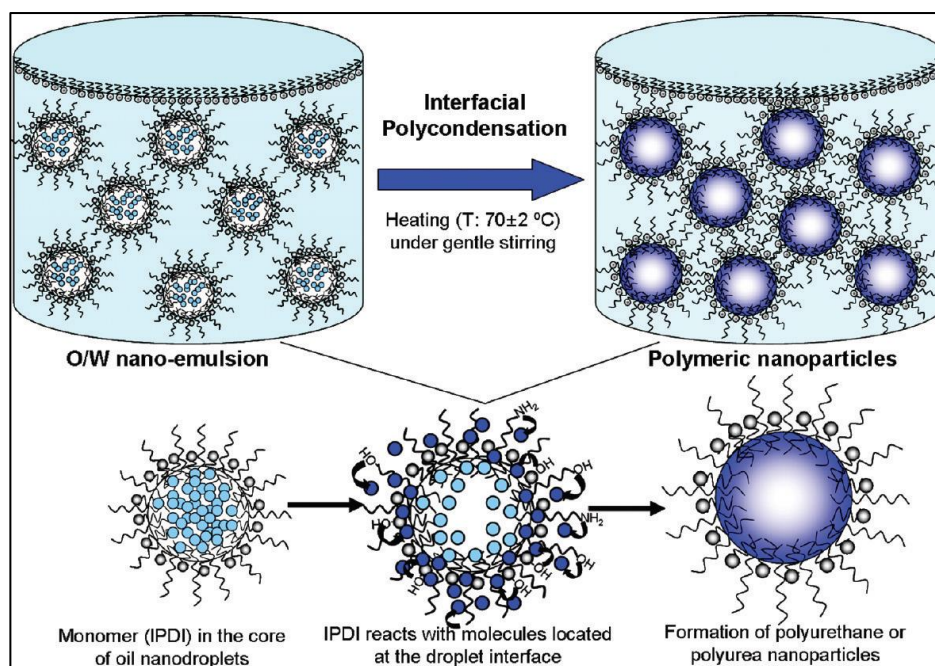


Figure 1.6. The mechanism of water dispersible polyurethanes and polyurea nanoparticle formation⁸⁴

There are no reports based on HTPB-PU dispersions but large number of reports exists on other polymer diols based PUs such as polytetramethylene oxide (PTMO), polycaprolactone (PCL), polyethyleneoxide (PEO), polylacticacid (PLA) and some renewable polyols such as castor oil, soybean oil and cardinal oil etc. In the preparation of PU dispersions, the ionic groups play the important role that we can create introducing to the PU chains either in the hard segment or in the soft segment which is capable of the formation of ionic charges upon neutralization, subsequently water addition to forms PU dispersions. Generally, the ionic groups such as salts of carboxylates or sulfonate groups commonly introduced in the hard segment PU chains through chain extenders.⁸⁵⁻⁸⁷ But Xia et al⁸⁸ designed and prepared PU dispersions, with ionic group contains in soft segments such as hydroxyl terminated poly (caprolactone) diols containing sodium sulfonate group in soft segment. Recently, the water dispersible PU nanoparticles have been synthesised using different compositions of biodegradable polymer diols (PCL and PLA), used as a soft segment and they find out that the nanoparticle was swelling with temperature dependency. Such type of nanoparticle phenomenon is excellent for particularly drug delivery applications.⁸⁹ Mao et al.⁹⁰ successfully prepared water-dispersible PUs covalently bonded anthraquinone dyechromophore via introducing micromolecule Disperse Red 91 to the PU skeleton and termed as coloured polymers. This idea was first raised by

Kuhn,⁹¹ this offers the excellent thermal, mechanical, solvent resistant and migration stability due to presence of dye chemically bonded to the PU skelton.^{92,93} These coloured PU dispersions are more useful for textile coatings, printing ink, cosmetics and photoelectricity materials, etc.⁹⁴

Larocket al.⁹⁵⁻⁹⁸ research group have extensively developed environmental friendly water dispersible PUs from renewable source polyols, like soybean oil and castor oil. They successfully prepared a series of anionic⁹⁷ and cationic⁹⁸ PU dispersions to introduce the appropriating ionomer into the polymer backbone using soybean oil as a polyol contains different hydroxyl functionality and different hard segment content, and also the properties of the resulting PU dispersions was demonstrated. Further, to improve the thermal and mechanical properties purpose, the same research group have developed a novel method to prepare hybrid latex PU dispersions. It can be attributed to extensively grafting and interpenetration between the PU and the acrylics, resulting in the core-shell particle morphology and high thermal and mechanical properties was observed, due to highly miscible of hybrid latexes.⁹⁵ After that, a variety of new soybean oil-based water dispersible PU/polystyrene-butyl acrylate hybrid latexes with core-shell structures have been synthesized via emulsion polymerization. Polymerization kinetics, the particle size of latexes, thermal and mechanical properties of the resulting hydride latexes have been studied.⁹⁹

1.5.4. Particle morphology and stability

The water dispersible PU particles have an open type and water-swollen structures designate as particles of ionic polymer in aqueous solutions. According to Satguru et al.¹⁰⁰ they proposed a preliminary model of PU particles as shown in Figure 1.7A. Based on this model, the PU particles are spherical and water swollen morphology because of the water rich areas are present inside the particles. Several factors can affect the particle morphology of PU dispersions such as molecular weight of starting compounds, steric hindrance, stabilizing group, the concentration of solvent, and the reaction conditions. The stability of the PU dispersions and the properties are highly depending on the particle size and the forces which present between the particles. If the particle size is more, the PU dispersions are not stable for longer time. Goa et al.¹⁰¹ proposed a micelle structure in water when styrene-4-vinylpyridine methyl iodide block copolymer is used. This type of micelle structures has a large hydrophobic group present at core side and hydrophilic groups present at corona side. Such type of micelles they have considered as crew-cut micelles and the proposed model structures is shown in Figure 1.7B.

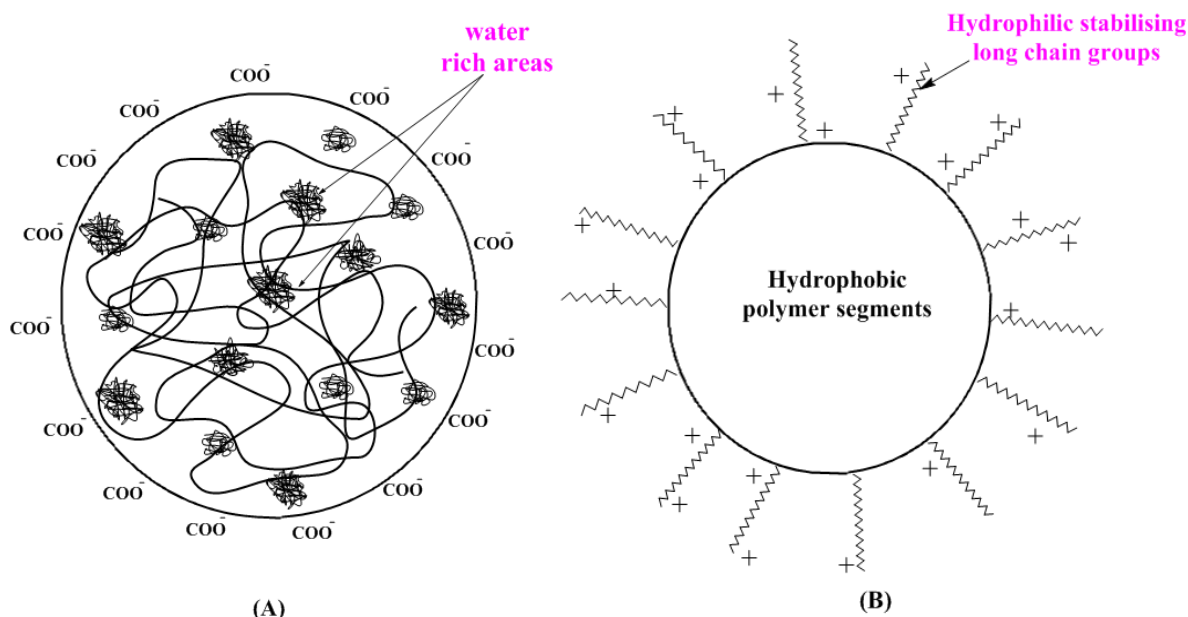


Figure 1.7. Possible particle morphology of water dispersible polyurethanes ionomeric colloids (Adapted from references 100, 101)

1.6. STRUCTURE-PROPERTY RELATIONSHIP OF PU

PU is a type of copolymer consists of an alternating hard segment and soft segment of which the soft segment is responsible for flexible nature and the hard segment is responsible for the strength of the PUs. The general hard and soft segmented PU structure is presented in Figure 1.8. Most of the cases soft segments are the amorphous in nature and it exhibit lower T_g value hence it is called as a soft segment and provides the elastic property to the PU. The most of the hard segments are crystalline in nature and it is responsible for the higher T_g value. This attributes the hardening in room temperature conditions. Therefore, it is called hard segment and it provides strength to the PUs.¹⁰² Because of this reason the PU chains exhibit certain amount of degree of thermodynamically immiscibility and the micro-phase separation between the hard block and soft block. Hence these two phases degree of immiscibility control the required properties such as the chemical and physical properties and can be altered by changing the concentrations and the lengths of hard and soft segments.¹⁰³⁻¹⁰⁵ In the water dispersible PUs can also exhibit phase separation, macrodomain formations and phase mixing are possible similar to solvent based PUs. Kim et al.¹⁰⁶ explained that the structure property relationship of water dispersible PUs with different types of polyols and diisocyanate structures and demonstrated the effects of structure on physicochemical properties such

as phase separation, phase mixing and mechanical properties. The soft segment having large enough chain length and lower T_g value are more phase separation and also it may crystallize. Compared to polyether polyol PUs, polyester polyols PUs show better mechanical properties, because of strong hydrogen bond formation between the urethane -N-H and carbonyl group of polyester polyols leads to the additional interactions between the soft and hard segment results in being higher phase mixing.¹⁰⁷ In between two PU-copolymer chains dipole-dipole and hydrogen-bonding interactions are present resulting to be significantly phase separated then the soft segment is randomly distributed in the PU polymer chains therefore the polymers are high elastic in nature, and this elastic property is an important in shape memory applications. This shape memory property also depends, on the structure of the starting compounds of PU. Suppose in PU backbone, the aromatic ring is present then along with those interactions extra induced dipole-dipole interaction also exist and such type of polymers are excellent for shape memory application. The chain extenders such as ethylene diamine and butanediol also differentiating the shape memory property because of urea and urethane linkages in the PU backbone. The two factors are involving in the shape memory polymers that are shape recovery and shape retention.^{108,109} The hydrogen bonding, crystallization and dipole-dipole interactions are providing the shape retention and shape recovery comes from the phase transformations of the soft segment that are from glassy to rubbery nature.

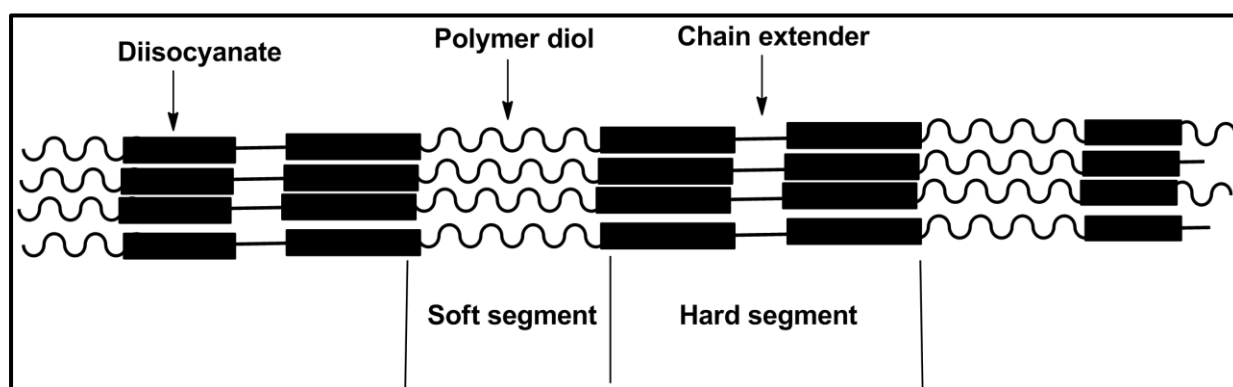


Figure 1.8. Schematic representation of common segmented polyurethane structure

The morphology of the PU largely depends on the processing methods, structure of the monomers and their reactivity. The morphology of the PU plays a significant role in understanding the structure-property relationships of the PUs. In PU, generally physical crosslinking takes place through interactions between the two PU chains driven by hydrogen bonding and Van der Waals interactions

which results into may phase separation, ordering and subsequently the crystal nature may be increase.¹¹⁰⁻¹¹² The ratio of the -NCO/-OH also affects the phase separation. The higher ratio of -NCO/-OH increases the cross-linking and hydrogen bond formation and hence enhances the phase separation.¹¹³ In PUs, the hydrogen bonding is an important factor to the formation of phase separation and morphology. Higher the hydrogen bonding between the two phases more will be the degree of phase mixing. Otherwise, the hydrogen bonds are only controlled by the hard segment which is possible to enhance the crystallization and hence phases separation. The Bonart and Clough¹¹⁴ first introduced and reported this kind of two-phase morphology of PUs and recognized this phenomenon with the help of small angle X-ray scattering (SAXS) study since this is an important tool to confirm the segmental phase separation and phase mixing. After that Koutsky and Cooper¹¹⁵ was also observed two-phase microstructure in case of polyester and polyether containing polyurethanes with the help of transmission electron microscopy (TEM). Later Chen-Tsai et al. and Serrano et al. proved the two phase morphology of different percentage of hard segment containing PUs with SAXS and TEM analysis.¹¹⁶⁻¹¹⁸ But the nature of the soft segment can also influences the compatibility with hard segment and it has been observed that if the soft segment is more polar then it is more compatible with the hard segments. For example, the polyester polyols are more polar than polyether polyols, therefore polyester polyols containing PUs are having additional compatibility with hard segment. Many researchers have reported verities of specific kind of morphology and they have tried to explain those morphology as the influence of different types of physical interactions. A large number of reports have been available on morpalogy of PUs, based on different structural variations and property differences, for example effects of diisocyanate, polymer diol and chain extender structures on morphology of PUs.¹²⁰⁻¹²²

1.7. HYDROXYL TERMINATED POLYBUTADIENE (HTPB)

HTPB is a viscous liquid polymer and it has excellent physicochemical and mechanical properties such as hydrolytic stability, low-temperature flexibility, chemical resistant, adhesives to different kind of substrates, high elongation and electrical insulating properties.¹¹⁹ The properties of the HTPB, such as viscosity, molecular weight and other properties are highly depends on the reaction conditions by which it is produced and these are temperature, type of initiator and polarity of solvent, etc. Generally, HTPB is prepared by anion polymerization¹²⁰ and free radical polymerization¹²¹ from 1,3-butadiene in the presence of H₂O₂ as an initiator and alcohols are used as a solvent. Zhou et al.¹²² reported that compared to free radical polymerization, the anion polymerization process is the best method to preparation of HTPB with high percentage of 1,4-content and narrow (polydispersity index)

PDI distribution, low glass transitional temperature and this may be the best choice to prepare new material with high processability and high flexibility. To synthesis the high molecular weight of HTPB, some reports suggested that the isopropanol as a solvent can be used. HTPB is extensively using in many areas not only in rocket propellant applications which include coating, sealants, adhesives and advanced materials. Terminal hydroxyl group can used to be synthesize the (A-B-A)_n block copolymer,¹²³ cross-linked elastomers^{124,125} and toughened resins.^{126,127} Since 1981, coating industries have developed many protecting coatings using HTPB, especially for Navy materials and showed that this coat had good protection against the sea water,¹²⁸ because of its excellent mechanical properties including at lower temperature conditions. HTPB is a viscous liquid polymer and widely using as a binder for rocket propellant applications all over the world, because of some specific interesting properties such as:

- 1) It has high loading capacity up to 85%.
- 2) It can able to store longer time and T_g is -70° C
- 3) It is contains the excellent flow characteristics.
- 4) High decomposition temperature >200° C
- 5) Good mechanical properties

However, HTPB has major drawbacks since it cannot provide any energy to the explosive composites while burning. Therefore it is an inert binder. Thus, in recent years several efforts have been made to modify HTPB with energetic groups such as -NO₂, -N₃, -ONO and O, N-containing cyclic compounds such as azoles, oxytaners, azitidiens into its polymer backbone through covalent bond formation without disturbing the HTPB properties.¹²⁹ In our research group several modifications of HTPB with different energetic groups have been reported.^{130, 131} To enhance the burning rate of the propellant the iron containing compounds such as ferrocene moiety covalently bonded to the HTPB backbone.¹²⁹ Some of the modified HTPB structures are shown in Figure 1.9

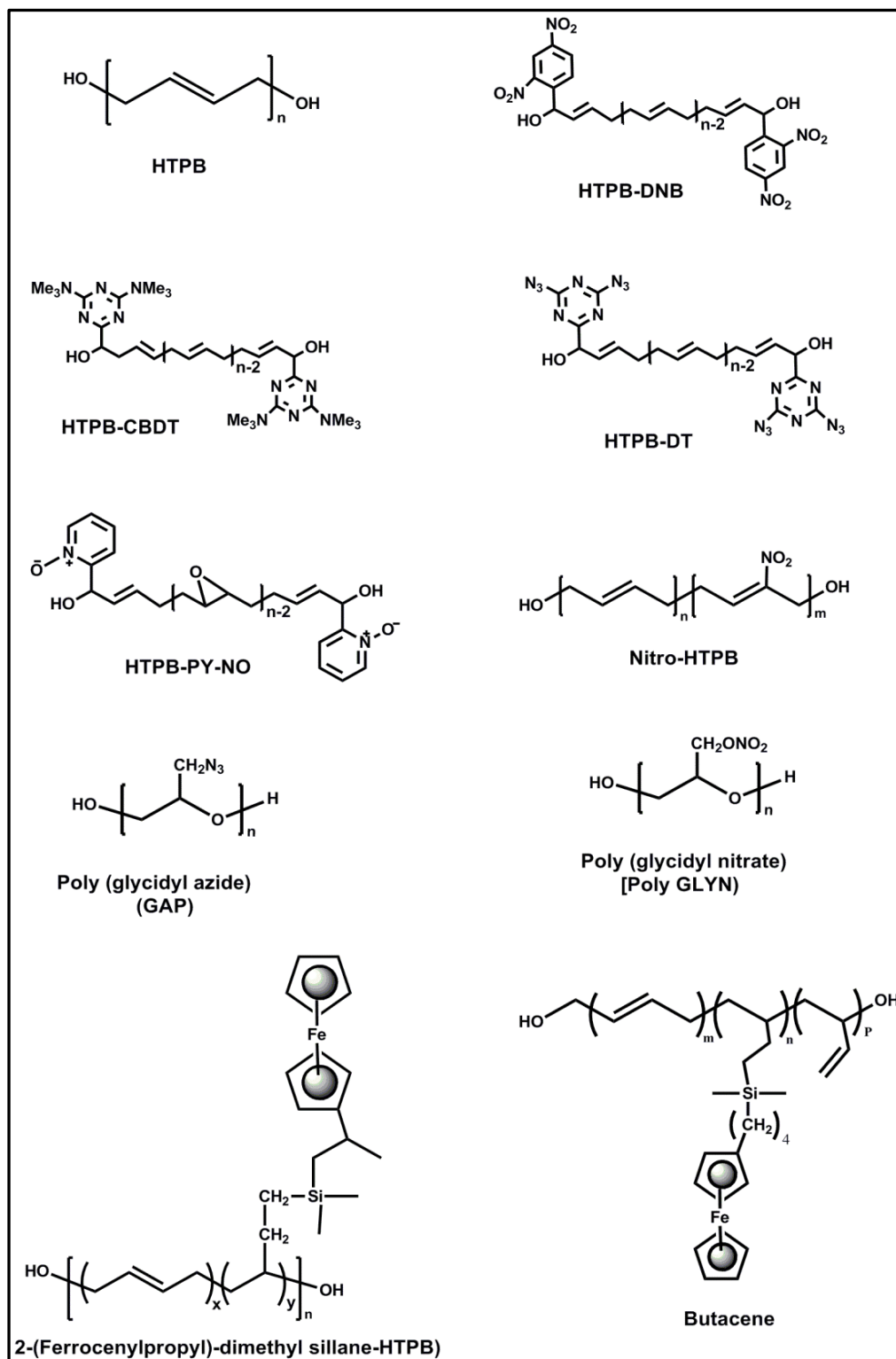


Figure 1.9. Some structures of modified HTPB polymer diols. ¹²⁹⁻¹³¹

1.8. POLYMER NANOCOMPOSITES

The material which is prepared with the combination of multiple phases within a single polymer matrix called as a composite, and these generally display enhanced physical properties compared to those of individual components. In the composite materials one of the phase is a continuous phase which is polymer matrix and other phases called as dispersed phase which is nanofiller or reinforcing material. In the recent years, polymer nanocomposite materials have come to the forefront and it has recognised as one of the frontier area of research in the field of polymeric materials. Generally polymer composites are prepared by introducing the nanofillers into the polymer matrix and these nanofillers are embedded in the microscopic levels in the polymer matrix. The advantages of the nanofillers are that the enhancement of the overall properties such as thermal, mechanical and other properties of the polymer material with a low-cost efficiency. In recent years methods have been developed to formulate the nanocomposite materials of water dispersion of PU introducing the nanofillers into the polymer (PU) matrix. These nanocomposite PU dispersions materials are being used for high performance applications due to the unique combination of properties of organic/inorganic hybrid material. Also, these materials are utilized for various structural and functional applications such as coatings, painting, electronics, biomedical, optical lenses, optical fibres and insulating materials etc.

1.8.1. Polymer Clay nanocomposite

Polymer composites with different types of the organically modified clays have been widely studied and their properties were explored because of their low cost, high surface area, easy availability, unique layered structured and also it offers many other advantages in comparison to other nanofillers. Different types of layered silicates are available with various crystalline sizes and aspect ratios. Generally, the clay surface consists of inorganic hydrophilic substances and therefore it is not compatible with the polymer for making nanocomposites. Hence, one has to modify with an organophilic substances which is compatible with the organic polymer to yield polymer nanocomposites. This type of organic modifications modifies the regular inorganic hydrophilic clay to organophilic clay and also increases the distance between the basal planes of the clays silicate layers. Then the polymer chains are easily enter in the between silicate layers resulting the new type of polymer materials which is called as polymer-organo clay nanocomposites.¹³²⁻¹³⁵

Most of the inorganic clays contain sodium ions in between the silicate layers, and hence the modification is possible by exchange of the sodium ions with quaternary alkyl ammonium ion, phosphonium ion etc.¹³⁶⁻¹³⁸ Montmorillonite (MMT) clay is the most extensively studied and used nanoclay. Often the sodium ions of MMT in between the silicate layers, exchanged with quaternary ammonium ions of the modifier. This montmorillonite clay commonly known as Cloisite clay and this is commercially available in different types depending on the type of modifier used.¹³⁹ Among these, Cloisite-30B clay is one of the modified Cloisite clay in which methyl, tallow, and bis-2-hydroxyethyl quaternary ammonium are present where tallow is (65% C₁₈, 30% C₁₆, and 5% C₁₄) and chloride is present as anion.¹⁴⁰ Kaolinite (Kao) clay is one kind of the illite clay and this clay structure contains the repeating units of tetrahedron-octahedron-tetrahedron layers. Therefore, it is called as layered alumino-silicate clay. This Kaolinite clay have been extensively used to prepare polymer nanocomposites.¹⁴¹ The Kao clay contains hydroxyl functional groups between each silicate layers which is derived from the tetrahedral sheet of silica oxide and octahedral sheet of the aluminium oxide. Because of this hydroxyl functionality it is possible to modify with any organic solvents such as dimethyl formamide or dimethyl sulfoxide etc.^{136,142,143} The clay structures of montmorillonite and Kaolinite are shown in Figure 1.10.

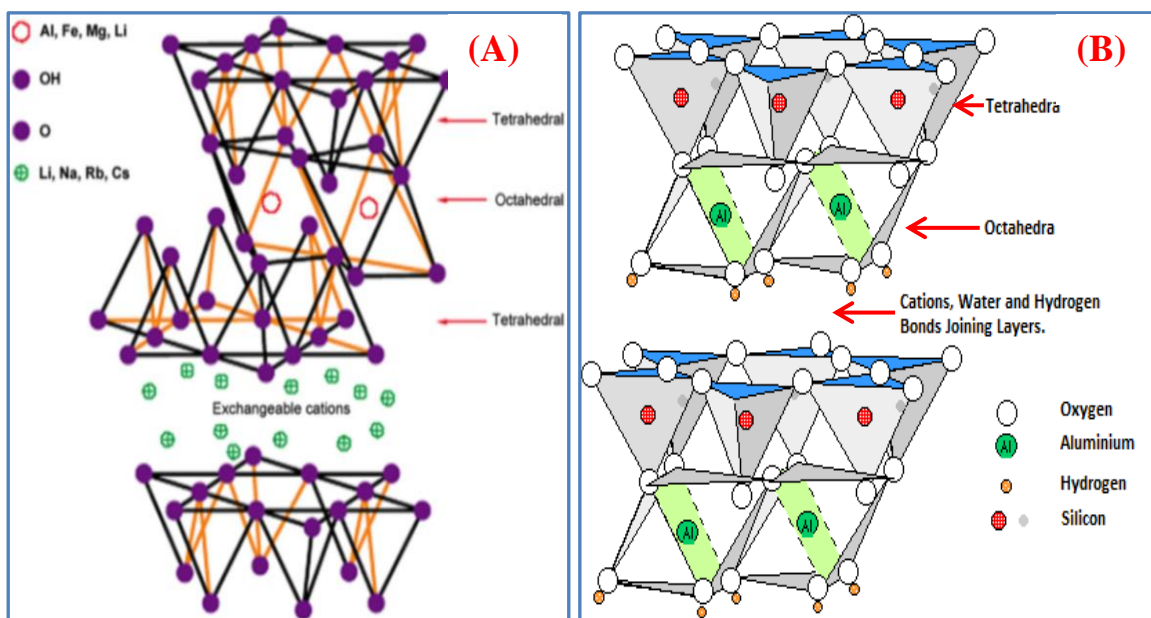


Figure 1.10. Structures of (A) Montmorillonite (B) Kaolinite (Adapted from Google image)

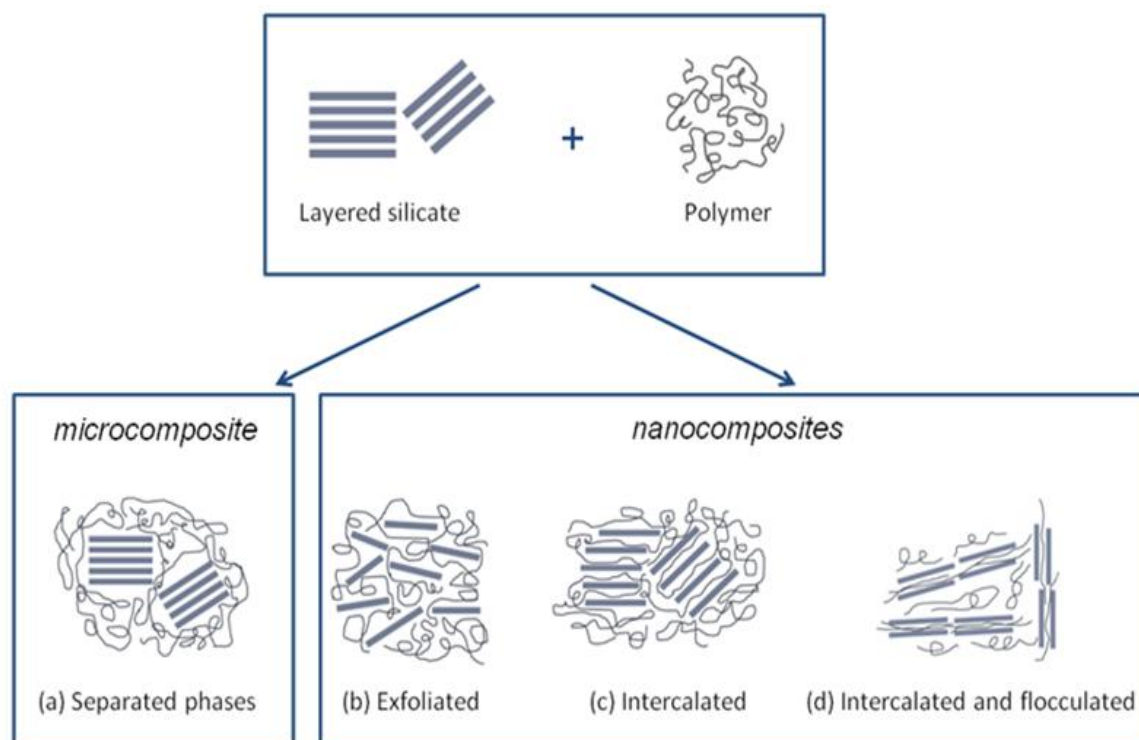


Figure 1.11. The possible structure formation of polymer/organoclay nanocomposite (Adapted from Google image).

Polymer clay nanocomposite was first prepared by the Toyota research group in 1980 which made the significant changes in the field of polymer nanocomposites. The first made polymer-nanocomposite was Nylon-6/MMT clay composite and it was demonstrates that the significantly improvement in thermo-mechanical properties of nanocomposites compared to neat Nylon-6.¹⁴⁴ The polymer/clay nanocomposites can be classified into four categories, based on the position and nature of the organoclay dispersion in the polymer matrix and these include intercalated, intercalated and flocculated, exfoliated and aggregated as shown in the Figure 1.11. Generally, the polymer-clay composites can be prepared by three different methods and those are solution-mixing or blending, *in-situ* synthesis and, melt mixing polymerization. Among these varieties of techniques, the *in-situ* method is the best method to prepared clay nanocomposite with water dispersible PU (WDPU). Compared to solvent-based PU/Clay composites, WDPU/Clay composite system behaves differently because the ionic interactions in WDPU. Therefore in absence of ionic interactions the most of the solvent-based PU/Clay composites are intercalated structure and on the otherhand WDPU/Clay

composites are exfoliated structures owing to the strong ionic attractions between anionic WDPUs and cationic clay platelets.¹⁴⁵⁻¹⁴⁹ Wang et al.¹⁵⁰ were first reported that the preparation and properties of segmented PU/clay composites. Several authors have prepared PU/clay composites by using varieties of organically modified clays such as laponite,¹⁵¹⁻¹⁵³ hallosite,¹⁵⁴ bentonites,¹⁵⁵ etc. Compared to neat PUs, clay nanocomposite PUs are better for coating applications because of their unique properties of organic and inorganic hybrid materials.

1.8.2. Polymer Titanium/Silica Nanocomposites

The performance of polymers can be improved by introducing nanoparticles into the polymer matrix owing to the interactions between the inorganic nanoparticles and organic polymer matrix resultant into a new type of polymer material with better properties. There are many number of interesting inorganic nano-sized particle with potentially unique properties such as silica,¹⁵⁶ Titanium,¹⁵⁷ zinc,¹⁵⁸ silveroxides¹⁵⁹ and carbon nanotubes,¹⁶⁰ graphene,¹⁶¹ fullerenes¹⁶² etc. Among these TiO₂ has attracted great attention of researchers because of their outstanding and interesting physical and chemical properties. It has been widely used in many fields such as solar cell applications,¹⁶³ photo catalytic degradation of organic pollutants,¹⁶⁴ water splitting into H₂-devices,¹⁶⁵ self-cleaning applications,¹⁶⁶⁻¹⁶⁸ antibacterial and antifogging applications,¹⁶⁹⁻¹⁷¹ and also used as a white pigments in paint,¹⁷² plastics,¹⁷³ ceramics,¹⁷⁴ cosmetics and several industrial pharmaceutical applications.¹⁷⁵ Among these varieties of applications, the self-cleaning and antibacterial applications are the essential in the field of coating applications. The self-cleaning properties are two types that are hydrophobic and hydrophilic self-cleaning. In hydrophobic self-cleaning, the dust particles were removed by rolling of the water droplets on the surface of the films whereas in hydrophilic self-cleaning water droplets are sitting on the surface of the film and fast spreading on their surface of the film and, removes the impurities and dust particles in the presence of sunlight. Several authors have prepared super hydrophobic and super hydrophilic material with appropriate TiO₂ nanoparticles surface modifications.¹⁷⁶⁻¹⁷⁹ Fujima et al.¹⁸⁰ prepared super hydrophilic thin films with stepwise deposition of the core-shell TiO₂/SiO₂ nanoparticles on glass surface. Zhou, et al.¹⁸¹ fabricated the super-hydrophobic thin film by using perfluorooctyltrichlorosilane modified TiO₂ nanoparticles coated on a glass substrate. Compared to TiO₂ nanoparticles, the silica coated on surface of TiO₂ nanoparticles (TiO₂/SiO₂ core-shell nanoparticles) exhibited better properties such as antiviral, photo-catalytic, antifogging, antibacterial, methanol activation and self-cleaning properties.¹⁸²⁻¹⁸⁷ Because of the interactions between the positive charge of TiO₂ and negative charge of SiO₂ nanoparticles produces a new type of materials which contains new catalytic active sites and also it enhances the thermal and

mechanical properties due to in the presence of supporting SiO₂ part.¹⁸⁸ Therefore, the thermo-mechanical properties of the core-shell nanoparticles composite polymers are very high compared to neat polymer due to the interactions between the shell component and polymer matrix.

1.9. AIMS OF THE THESIS

The above discussion in this chapter about the HTPB and modified HTPB (HTPB-DNB) offers countless opportunities to study and develop new PU and their composite for verities of applications. Although the presence of enormous kinds of literature on the varieties of PU polymer materials, we find out that there are several reports on solvent-based PUs but not many reports on “PU water dispersions”. Also we have elucidated that the advantages and the importance of PU water dispersions, over the solvent based PUs. Throughout the discussions, we have realized that compared to HTPB-PUs, HTPB-DNB-PUs shows better properties. In Chapter 3, we have synthesised solvent-based PUs using different diisocyanates and HTPB, and HTPB-DNB used as polymer diols. We have found out and investigated the influence on the properties of PU because of dinitrobenzene functionality at the terminal position of HTPB. Even though a vast amount of works of literature related to HTPB-PU synthesis is available, unfortunately there is no study has been concentrating on the effect of such terminal modification of HTPB which can influence mechanical properties of PUs. In Chapter 4, we have further used HTPB and HTPB-DNB as polymer diols to the synthesis water dispersible PUs with varying the percentage of hard segment contents. All the water dispersible PUs, we could observed that the particles morphology, storage stability and also we prepared films and we carried out all the required properties of coating material such as mechanical, thermal, and hydrophobic properties and how it influences the percentage of hard segment content on properties of PUs films. A large number of reports exist based on different types of polyols but not exist any reports on HTPB based water dispersible PUs. Compared to HTPB-PUs, HTPB-DNB-PU dispersions shows better properties, so we are keeping this concept in mind we have prepared composites of HTPB-DNB water dispersible PUs in next two chapters (Chapters 5 and 6) to explore the properties of HTPB-DNB-PU nanocomposite. We have synthesised clay nanocomposite and TiO₂-SiO₂ core-shell nanocomposites of HTPB-DNB water dispersible PUs to improve the several properties which we discussed in Chapter 5 and Chapter 6. Therefore the thesis mainly deals with synthesis and characterization of HTPB and modified HTPB based water dispersible PUs and their nanocomposites which have potential use for coating applications. The aim and objective of each chapter of this thesis are elaborated in the introductory part of the individual chapters.

1.11. REFERENCES

- (1) O. Bayer, *Angew. Chem.*, **1947**, A59, 257
- (2) O. Bayer, E. Muller, S. Petersen, H. P. Piepenbrink, E. Windemuth, *Rubber Chem. Technol.*, **1950**, 23, 812
- (3) T. Lieser, *U.S. Patent. 2266*, **1941**, 777
- (4) A. E. Christ, W. E. Hanford (to du Pont), *U.S. Patent. 1940*, 233639
- (5) P. Pinten (to A. G. Dynamit), *Ger. Pat. 932 633*, **1943**
- (6) Mark S. M. Alger. *Polymer Science Dictionary*, Springer. **1967**, p. 569
- (7) Szymczyk, A.; Senderek, E.; Nastalczyk, J.; Roslaniec. *Z. Eur. Polym. J.* **2008**, 44, 436–443
- (8) Papageorgiou, G. Z.; Vassiliou, A. A.; Karavelidis, V. D.; Koumbis, A.; Bikiaris, D. *Macromolecule*, **2008**, 41, 1675.
- (9) Kong, Xi.; Suresh S. N. Gogo, S.; Karak, N. *ACS Sustainable Chem. Eng.* **2014**, 2, 2730–2738
- (10) Lligadas, Li, Y.; Noordover, B. A. J.; Benthem, R. A. T. M.; Koning, C. E. *ACS Sustainable Chem. Eng.* **2014**, 2, 788–797
- (11) Paderni, K.; Pandini, S.; Passera, S.; Pilati, F.; Toselli, M.; Messori, M. *J Mater Sci*, **2012**, 47, 4354–4362
- (12) Nampoothiri, K. M.; Nair, N. R.; John, R. P. *Bioresource Technology*, **2010**, 101, 8493–8501
- (13) Madbouly, S. A.; Otaigbe, J. U. *Progress in Polymer Science*, **2009**, 34, 1283–1332
- (14) Peter, A.; Edwards.; Striemer, G.; Webster, D. C. *Progress in Organic Coatings*, **2006**, 57, 128–139
- (15) (a) Sreedhar, B.; Chattopadhyay, D. K.; Karunakar, S. H. M.; Sastry, A. R. K. *Journal of Applied Polymer Science*, **2006**, 101, 25–34 (b) Jayakumar, R.; Lee, Y. S.; Nanjundan, S. *J. Appl. Polym. Sci.* **2004**, 92, 710–721
- (16) Dick, C.; Dominguez-Rosado, E.; Eling, B.; Liggat, J. J.; Lindsay, C.I.; Martin, S.C.; Mohammed, M.H.; Seeley, G.; Snape, C.E. *Polymer*, **2001**, 42, 913–923.
- (17) Dominguez-Rosado, E.; Liggat, J. J.; Snape, C. E.; Eling, B.; Pochtel, J. *Polym. Degrad. Stability*, **2002**, 78, 1–5.
- (18) Olivia, D.; Nair, M.; Davis, P.; Brent.; Bradley, J.; Sparks.; Derek L.; Patton.; Savin, D. A. *ACS Appl. Mater. Interfaces*, **2014**, 6, 6088–6097
- (19) Lee, M.H.; Choi, H.Y.; Jeong, K.Y.; Lee, J.W.; Hwang, T.W.; Kim. B.K. *Polym. Degrad. Stab.* **2007**, 92, 1677.

- (20) (a) Liu, J.; Ma, D. *J. Appl. Polym. Sci.* **2002**, *84*, 2206. (b) Qin, X.; Yang, X.; Wang, X.; Wang, M. *J. Polym. Sci. A: Polym. Chem.* **2005**, *43*, 4469.
- (21) Qia, H.; Liua, F.; Zhanga, N.; Chena, Yi.; Yangb, H.; Wangb, Z. *Progress in Organic Coatings*, **2012**, *73*, 33–41
- (22) Wanga, L.F.; Jib, Q.; Glassb, T.E.; Wardb, T.C.; McGrathb, J.E.; Mugglic, M.; Burnsd, G.; Sorathiae, U. *Polymer*, **2000**, *41*, 5083–5093
- (23) Subramani, S.; Lee, J.; Choi, S.; Kim, J. *J. Polym. Sci. Part B: Polym. Phys.* **2007**, *45*, 2747–2761
- (24) Park, J. H.; Park, K. D.; Bae, Y. H. *Biomaterials*, **1999**, *20*, 943–953
- (25) Gunduz, G.; Kisakurek, R. R. *Journal of dispersion science and technology*, **2004**, *25*, 217–228
- (26) Park, S. H.; Chunga, I. D.; Hartwig, A.; Kim, B. K. *Colloid. Surf A: Physicochem. Eng. Aspects*, **2007**, *305*, 126–131
- (27) (a) Jang, J. Y.; Jhon, Y. K.; Cheong, I. W.; Kim, J. H. *Colloid. Surf A: Physicochemical and Engin. Aspects*, **2002**, *196*, 135–143 (b) Tien, Y.I.; Wei, K.H. *Polymer*, **2001**, *42*, 3213–3221 (c) Tawa, T.; Ito, S. *Polymer J*, **2006**, *38*, 686–693
- (28) Negim, E.M.; bekbayeva, L.; Mun, G.A.; Abilov, Z. A.; Saleh, M. I. *World applied science journal*, **2011**, *14*, 402–407
- (29) Hourston, D. J.; Williams, G. D.; Satguru, R.; Padget, J. C.; Pears, D. *Journal of Applied Polymer Science*, **1999**, *74*, 556–566
- (30) Kim, B. K.; Kim, K.; Jeon, H. M. *J. Appl. Polym. Sci.* **1994**, *53*, 371–378
- (31) Lee, S. Y.; Lee, J. S.; B. K. Kim, *Polym. Inter*, **1997**, *42*, 67–76
- (32) Abouzahr, S.; Wilkes, G. L.; *J. Appl. Polym. Sci.* **1984**, *29*, 1695.
- (33) Chun, B. C. Cho, T. K.; Chung, Y. *European Polymer Journal*, **2006**, *42*, 3367–3373 (shape memory)
- (34) Esteves, A. C. C.; Lyakhova, K.; van der Ven, L. G. J.; van Benthem, R. A. T. M.; de With, G. *Macromolecules*, **2013**, *46*, 1993–2002
- (35) Motlagh, N. V.; Sargolzaei, J.; Shahtahmassebi, N. *Surf. Coat. Techn.* **2013**, *235*, 241–249
- (36) Nelson, M. A.; Long, T. E. *Macromol. Chem. Phys.* **2014**, *215*, 2161–2174
- (37) Wankhede, R. G.; Moreyc, S.; Khanna, A.S.; Birbilis, N. *Appl. Surf. Sci.* **2013**, *283*, 1051–1059
- (38) (a) Wanling Wu.; Zhu, Q.; Qing, F.; Han, C. C. *Langmuir*, **2009**, *25*, 17–20 (b) Kannan, A. G.; Choudhury, N. R.; Dutta, N. *ACS Appl. Mater. Interfaces*, **2009**, *1*, 336–347

- (39) Nystrom, D.; Lindqvist, J.; Ostmark, E.; Hult, A.; Malmstro, E. *Chem. Commun.*, **2006**, 3594–3596
- (40) Xiong, D.; Liu, G.; Hong, L. *Chem. Mater.* **2011**, *23*, 4357–4366
- (41) (a) Guo, Z.; Zhou, F.; Hao, J.; Liu, W. *J. AM. CHEM. SOC.*, **2005**, *127*, 15670–15671 (b) Qu, Li.; Vaia, R. A.; Dai, Li. *ACS Nano*, **2011**, *5*, 994–1002
- (42) Wang, Z.; Zhu, Li.; Li, W.; Liu, H. *ACS Appl. Mater. Interfaces*, **2013**, *5*, 4808–4814
- (43) Zhao, J.; Zhou, T.; Zhang, J.; Chen, H.; Yuan, C.; Zhang, W.; Zhang, A. *Ind. Eng. Chem. Res.* **2014**, *53*, 19257–19264
- (44) Cui, X.; Zhong, S.; Wang, H. *Colloids Surf. A.* **2007**, *303*, 173–178
- (45) Xiao, X.; Wang, Y. *Colloids Surf. A.* **2009**, *348*, 151–156
- (46) (a) Zhaofeng, Wu.; Wang, H.; Tian, X.; Cui, P.; Dinga, X.; Yea, X. *Phys. Chem. Chem. Phys.*, **2014**, *16*, 6787–6794 (b) J. T. Han, X. R. Xu, K. W. Cho, *Langmuir*, **2005**, *21*, 6662. (c) Zhao, N.; Xie, Q. D.; Weng, L. H.; Wang, S. Q.; Zhang, X. Y.; Xu, J. *Macromolecules*, **2005**, *38*, 8996
- (47) Okamoto, Y.; Klemarczyk, P. T. *J. Adhesion*, **1993**, *40*, 81
- (48) Clearfield, H. M., et al. *J. Adhesion*, **1989**, *29*, 81
- (49) Lunsford, L. R., *Symposium on Adhesives for Structural Applications, New York, Inter science*, **1962**
- (50) Mooney, C. L.; Schwartz, P. *Text. Res. J.* **1985**, *55*, 449–452
- (51) Sengupta, A.K.; Sarkar, B.P. *Text. Res. J.*, **1972**, *42*, 268–271
- (52) Johnson, L.; Samms, J. J. *Coated Fabrics*, **1997**, *27*, 48
- (53) Skoko, M. *Tekstil*, **1998**, *47*, 345–349
- (54) Guo, B.; Chen, Y.; Lei, Y.; Zhang, Li.; Zhou, W. Y.; Rabie, A. B. M.; Zhao, J. *Biomacromolecules*, **2011**, *12*, 1312–1321
- (55) Nair, D. P.; Cramer, N. B.; Scott, T. F.; Bowman, C. N.; Shandas, R. *Polymer*, **2010**, *51*, 4383–4389.
- (56) Serrano, M. C.; Chung, E. J.; Ameer, G. A. *Adv. Funct. Mater.* **2010**, *20*, 192–208.
- (57) Yakacki, C. M.; Gall, K. *Adv. Polym. Sci.* **2010**, *226*, 147–175.
- (58) Ping, P.; Wang, W.; Chen, X.; Jing, X. *Biomacromolecules*, **2005**, *6*, 587–592
- (59) Kleinhans, G.; Starkl, W.; Nuffer, K. *Kunststoffe*, **1984**, *74*, 445.
- (60) Kleinhans, G.; Heidenhain, F. *Kunststoffe*. **1986**, *76*, 1069.
- (61) Fray, M. E.; Prowans, P.; Puskas, J. E.; Altstadt, V. *Biomacromolecules*, **2006**, *7*, 844–850

- (62) Ritchie, R. O.; Dauskart, R. H.; Yu, W.; Brendzel, A. M. *J. Bio. Mater. Res.* **1990**, *24*, 189-206.
- (63) Renz, R.; Altstaedt, V.; Ehrenstein, G. W. *J. Reinf. Plast. Compos.* **1988**, *7*, 413-434.
- (64) J. J. Guan, K. L. Fujimoto. *Biomaterials*, **2005**, *26*, 3961-3971.
- (65) J. Y. Zhang, E. J. Beckman. *Tissue Engineering*, **2002**, *8*, 771-785.
- (66) Z. H. Zhou, J. M. Ruan, *Journal of University of Science and Technology*, **2008**, *15*, 290-298.
- (67) S. A. Guelcher, *Biomaterials*, **2008**, *29*, 1762-1775.
- (68) S. A. Guelcher, K. Gallagher, *Acta Biomaterialia*, **2005**, *1*, 471-484.
- (69) K. D. Kavlock, T. W. Pechar, *Acta Biomaterialia*, **2007**, *3*, 475-484.
- (70) Abdel Hakim, A. A.; Nassar, M.; Emam, A.; Sultan, M. *Materials Chemistry and Physics*, **2011**, *129*, 301-307
- (71) Demharter, A. *Cryogenics*, **1998**, *38*, 113-117
- (72) Ruijian, Xu.;Evangelos, M.; Alan, J.S.; JamesRunt. *Macromolecules*,**2001**, *34*, 337-339.
- (73) Kolff, W.J.; Yu, L.S.; The return of elastomer valves. *Ann Thorac Surg*, **1989**, *48*, 598
- (74) Sabine, H.; Daebritz.; Bemd, F.; Benita, H.; Joerg, S.; Groetzner, J.; Ruediger, A.; Bruno, J. M.; Jorg, S.; Sachweh. *Eur. J. Cardio-thor, Surg.* **2004**, *25*, 946-952.
- (75) *Tissue Engeneering*, **2010**, Part-A, Vol-16.
- (76) Apostolovic, B.; Deacon, S. P.; Duncan, R.; Klok, H. A. *Biomacromolecules*, **2010**, *11*, 1187-1195.
- (77) Du, J. Z.; Du, X. J.; Mao, C. Q.; Wang, J. *J. Am. Chem. Soc.* **2011**, *133*, 17560-17563
- (78) (a) Schlack, P. *Bobingen AG ffir Textilfasern*, DBP 920 512 (16.6.43) (b) Hansson, A.; Union Chimique-ChemischeBedrijven, DOS, 2 146 888, **1970** (c) Ney, E. A.; Regos, N.; Labb, P. *J. Elastomers Plast*, **1976**, *8*, 210.
- (79) (a) Reischl, A.; Dieterich, D. *Farbenf. Bayer, DOS 1 595 687*,**1966** (b) Dieterich, D.; Miller, E.; Bayer, O.; Peter, J. *DBP 1 495 693* (30.8.62)
- (80) (a) Milligan, C. L. *U. S. Pat.3 412 054* (31.10.66)(b) Carbide, U.; Keberle, W.; Oertel, G. *U. S. Pat.3 539 483* (20. 3. 1967) (c) Bayer, A. G.; Remley, K. H. *DOS 1 816 246* (22. 12.67)
- (81) (a) Keberle, W.; Dieterich, D.; Bayer, A. G. *DBP 1 495 847* (8.12.64) (b) Keberle, W.; Dieterich, D.; O. Bayer, Bayer A. G. *DBP 1 237 306* (26.9.64), (c) Keberle, W.; Thoma, W.; Bayer, A. G. *Pat. 1 280 750* (23.8.69)
- (82) Zhang, M.; Hemp, S. T.; Zhang, M.; Allen, M. H.; Carmean, R. C.; Moore, R. B.; Long, T. E. *Polym.Chem*, **2014**, *5*, 3795

- (83) (a) Lorenz, O.; Reinmüller, K. H.; Fonck, N.; *Kautsch. GummiKunstst*, **1980**, 33, 527. (b) Lorenz, O.; Budde, V.; Wirtz, W. *Angew. Makromol. Chem*, **1979**, 83, 113.
- (84) Morral-Ruiz, G.; Solans, C.; Garcia, M. L.; Garcia-Celma, M. J. *Langmuir*, **2012**, 28, 6256–6264
- (85) Wen, T. C.; Wang, Y. J.; Cheng, T. T.; Yang, C. H. *Polymer*, **1999**, 40, 3979.
- (86) Saetung, A.; Kaenhin, L.; Klinpituksa, P.; Rungvichaniwat, A.; Tulyapitak, T.; Munleh, S.; Campistron, I.; Pilard, J. F. *J. Appl. Polym. Sci.* **2012**, 124, 2742.
- (87) Choi, S. H.; Kim, D. H.; Raghu, A. V.; Reddy, K. R.; Lee, H. I.; Yoon, K. S.; Jeong, H. M.; Kim, B. K. *J. Macromol. Sci. Phys.* **2012**, 51, 197.
- (88) Xia, J.; Xu, Y.; Gong, C.; Gao, D. *J. Appl. Polym. Sci.* **2014**, DOI: 10.1002/APP.39657
- (89) Ou, C.; Su, C.; Jeng, U.; Hsu, S. *ACS Appl. Mater. Interfaces*, **2014**, 6, 5685–5694
- (90) Mao, H.; Wang, C.; Wang, Y. *New J. Chem*, **2015**, 39, 3543–3550
- (91) (a) Kuhn, H. H. *US Pat*, **1964**, 3157633. (b) Kuhn, H. H. *US Pat*, **1969**, 3449319.
- (92) Altomare, A.; Ciardelli, F.; Solaro, R. *Macromol. Symp*, **2004**, 218, 353–362.
- (93) Maradiya, H. R.; Patel, V. S. *J. Appl. Polym. Sci.* **2002**, 84, 1380–1389.
- (94) Marechal, E. *Prog. Org. Coat*, **1982**, 10, 251–287.
- (95) Lu, Y.; Larock, R. C. *Biomacromolecules*, **2007**, 8, 3108–3114.
- (96) Lu, Y.; Larock, R. C.; *J. Appl. Polym. Sci.* **2008**, Accepted.
- (97) Yongshang, Lu.; Y.; Larock, R. C. *Biomacromolecules*, **2008**, 9, 3332–3340
- (98) Yongshang, Lu.; Y.; Larock, R. C. *Progress in Organic Coatings*, **2010**, 69, 31–37
- (99) Yongshang, Lu.; Xia, Y.; Larock, R. C. *Progress in Organic Coatings*, **2011**, 7, 336–342
- (100) Satguru, R.; Mahon, M.; Padget, J.; Coogan, R. G. *J. Coat. Tech*, **1994**, 66, 47–55.
- (101) Gao, Z.S.; Varshney, S.K.; Wong, S.; Eisenberg, A. *Macromolecules*, **1994**, 27, 7923–7927
- (102) Garrett, J. T.; Runt, J. *Macromolecules*, **2000**, 33, 6353–6359
- (103) Szymczyka, A.; Nastalczyka, J.; Sablong, R.J.; Roslaniec, Z. *Polym. Adv. Technol.* **2011**, 22, 72–83
- (104) Wang, Li.; *Eur. Polym. J.* **2005**, 41, 293–301
- (105) L. Rueda-Larraz, Arlas, B. F.; Tercjak, A.; Ribes, A.; Mondragon, I.; Eceiza, A. *European Polymer Journal*, **2009**, 45, 2096–2109
- (106) Kim, B. K.; Lee, Y. M. *Colloid PolymSci*, **1992**, 270, 956–961
- (107) Abouzahr, S.; Wilkes, G. L. *J Appl Polym Sci*, **1984**, 29, 2695
- (108) Yoo, S. R.; Lee, H. S.; Seo, S. W. *Polymer (Korea)*, **1997**, 21, 467–79.

- (109) Chun, B. C.; Cho, T. K.; Chung, Y. *Eur. Polym. J.*, **2006**, *42*, 3367–3373
- (110) Liu, C. D.; Chun, S. B.; Mather, P. T.; Zheng, L.; Haley, E. H.; Coughlin, E. B. *Macromolecules*, **2002**, *35*, 9868–9874.
- (111) Elabd, Y. A.; Sloan, J. M.; Barbari, T. A. *Polymer*, **2000**, *41*, 2203–2212.
- (112) Dearth, R. S.; Mertes, H.; Jacobs, P. J. *Progress in organic coatings*, **1996**, *29*, 73–79
- (113) Desai, S.; Thakore, I.M.; Sarawade, B. D.; Devi, S. *Eur. Polym. J.*, **2000**, *36*, 711–725.
- (114) (a) B. Bonart. *J. Macromolec. Sci. Phys.*, **1968**, *B2*, 115. (b) Clough, S. B.; Schneider, N. S.; King, A. O. *J. Macromol. Sci. Phys.*, **1968**, *B2*, 641
- (115) Koutsky, J. A.; Hien, N. V.; Cooper, S. L. *J. Polym. Sci.*, **1970**, *B8*, 353
- (116) MacKnight, M. Xu, W. J.; Chen-Tsai, C. H. Y.; Thomas, E. L. *Polymer*, **1987**, *28*, 2183
- (117) Chen-Tsai, C. H. Y.; Thomas, E. L.; MacKnight, W. J.; Schneider, N. S. *Polymer*, **1986**, *27*, 659
- (118) Serrano, M.; MacKnight, W. J.; Thomas, E. L.; Ottino, J. M. *Polymer*, **1987**, *28*, 1667
- (119) Zhou, Q.; Jie, S.; Li, B. *Polymer*, **2015**, *67*, 208–215
- (120) Chen, J.; Pan, G.; Qi, Y.; Yi, J.; Bai, H. *J. Polym. Sci.* **2010**, *28*, 715–720.
- (121) Brosse, J. C.; Derouet, D.; Epailard, F.; Soutif, J. C.; Legeay, G.; Dusek, K. Springer, Berlin, **1986**, *81*, 167–223.
- (122) Zhou, Q.; Jie, S.; Li, B. *Ind. Eng. Chem. Res.* **2014**, *53*, 17884–17893
- (123) (a) Lee, I.; Bates, F. S. *Macromolecules*, **2013**, *46*, 4529–4539 (b) Lee, I.; Panthani, T. R.; Bates, F. S. *Macromolecules*, **2013**, *46*, 7387–7398.
- (124) Saramolee, P.; Lopattananon, N.; Sahakaro, K. *Eur. Polym. J.*, **2014**, *56*, 1–10.
- (125) Martinez, H.; Hillmyer, M. A. *Macromolecules*, **2014**, *47*, 479–485.
- (126) Thomas, R.; Sinturel, C.; Pionteck, J.; Puliyalil, H.; Thomas, S. *Ind. Eng. Chem. Res.* **2012**, *51*, 12178–12191.
- (127) Thomas, R.; Yumei, D.; Yuelong, H.; Le, Y.; Moldenaers, P.; Weimin, Y.; Czigany, T.; Thomas, S. *Polymer*, **2008**, *49*, 278–294.
- (128) Gouranlou, F. *Asian Journal of Chemistry*, **2007**, *19*, 1645–1647
- (129) (a) Cho B, Si-Tae N.; *J. Appl. Polym. Sci.* **2011**, *121*, 3560–3568 (b) AlaviNikje M, A.; Hajifatheali H. *Polym. Bull.* **2012**, *68*, 973–982. (c) Cho, B.; Noh, S. *J. Appl. Polym. Sci.* **2011**, *121*, 3560–3568
- (130) Shankar, R. M.; Roy, K. T.; Jana, T. *J. Appl. Polym. Sci.* **2009**, *114*, 732–741.

- (131) (a) Shankar, R. M.; Saha, S.; Meera, K. S.; Jana, T. *Bull. Mater. Sci.* **2009**, 32, 507-514 (b) Shankar, R. M.; Roy, K. T.; Jana, T. *Bull. Mater. Sci.* **2011**, 34, 745–754.
- (132) Chanchal Chakraborty.; Pradip K. Sukul.; Kausik Dana.; Sudip Malik.; *Ind. Eng. Chem. Res.* **2013**, 52, 6722–6730
- (133) Lee H. T.; Li-Huei Lin. *Macromolecules*, **2006**, 39, 6133-6141.
- (134) SadokLetaief, Jerome Leclercq, YunLiu, and Christian Detellier.; *Langmuir*, **2011**, 27, 15248–15254
- (135) SadokLetaief, Tamer A. Elbokl, Christian Detellier.; *J. Colloid. Interf. Science*, **2006**, 302, 254–258.
- (136) Ghosh, S.; Sannigrahi, A.; Maity, S.; Jana, T. *J. Phys. Chem. C*, **2011**, 115, 11474–11483
- (137) Liff, S. M.; Kumar, N.; Kinley, M. G. H. *Nat. Mater.* **2007**, 6, 76–83.
- (138) Maiti, P.; Nam, P.H.; Okamoto, M.; Hasegawa, N.; Usuki, A. *Macromolecules*, **2002**, 35, 2042
- (139) (a) Cervantes, J. M.; Rodriguez, J. V. C.; Vazquez-Torres, H.; Garfias-Mesias, L. F.; Paul, D. R. *Thermo chimica Acta*, **2007**, 457, 92–102. (b) Finnigan, B.; Casey, P.; Cookson, D.; Halley, P.; Jack, K.; Truss, R.; Martin, D. *Inter. J. Nanotech*, **2007**, 4, 496-515
- (140) Barmar M.; Barikani M.; Fereidounnia M. *Iran. Polym. J.* **2006**, 15, 709-714
- (141) Gardolinski, J. E.; Careera, L. C. M.; Cantao, M. P.; Wypych, F. *J. Material sci*, **2000**, 35, 3113
- (142) Thompson, J. G.; Cuff, C. *Clay Clay Miner.* **1985**, 33, 490
- (143) Zhu, J.; Morgan, A. B.; Lamelas, F. J.; Wilkie, C. A. *Chem. Mater*, **2001**, 13, 3774
- (144) Kojima, Y.; Usuki A.; Kawasumi M.; Okada A.; Fujushima A.; Kurauchi T.; Kamigaito O. *J. Mater. Res*, **1993**, 8, 1185–1189
- (145) Qian, Y.; Lindsay, C. I.; Macosko, C.; Stein, A. *ACS Appl. Mater. Interfaces*, **2011**, 3, 3709–3717
- (146) Lee, H.; Lin, L. *Macromolecules*, **2006**, 39, 6133-6141
- (147) Chivrac, F.; Pollet, E.; Averous, L. *Polym. Adv. Techn*, **2010**, 21, 578–583
- (148) Jeong, E. H.; Yang, J.; Hong, J. H.; Kim, T. g.; Kim, J. H.; Youk, J. H. *E. Polym. J*, **2007**, 43, 2286–2291
- (149) Subramani, S.; Lee, J.; Choi, S.; Kim, J. H. *J. Polym. Sci: Part B: Polym. Physics*, **2007**, 45, 2747–2761
- (150) Wang, Z.; Pinnavaia, T. J. *Chemistry of Materials*, **1998**, 10, 3769-3771

- (151) Korley, L. T. J.; Liff S. M.; Kumar, N.; McKinley, G. H.; Hammond, P.T.; *Macromolecules*, **2006**, 39, 7030-7036
- (152) Liff, S. M.; Kumar, N.; McKinley, G. H. *Nature Material*, **2007**, 6, 76-83
- (153) Sormana J. L., Chattopadhyay S., Meredith J. C. *Journal of Nanomaterials*, **2008**, article ID 869354, 9 pages
- (154) Abdullayev, E.; Abbasov, V.; Tursunbayeva, A.; Portnov, V.; Ibrahimov, H.; Mukhtarova, G.; Lvov, Y. *ACS Appl. Mater. Interfaces*, **2013**, 5, 4464–4471
- (155) Fiayyaz, M.; Zia, M. K.; Zuber, M.; Jamil, T.; Khosa, M. K.; Jamal, M. A. *Korean J. Chem. Eng.* **2014**, 31, 644-649
- (156) Chattopadhyay, D.K.; Muehlberg, A. J.; Webster, D. C. *Progress in Organic Coatings*, **2008**, 63, 405–415
- (157) Pei Liu, Haijin Liu, Guoguang Liu, Kun Yao, Wenying Lv. *Appl. Surf. Sci.* **2012**, 258, 9593–9598
- (158) Xue-Yong Ma, Wei-De Zhang. *Polym. Degrad. Stab.* **2009**, 94, 1103–1109
- (159) Liu, H.; Song, J.; Shang, S.; Song, Z.; Wang, D. *ACS Appl. Mater. Interfaces*, **2012**, 4, 2413–2419
- (160) (a) Liao, I.; Tan, M.; Sridhar, I. *Materials and Design*, **2010**, 31, S96–S100 (b) Wang, T.; Yu, C.; Yang, C.; Shieh, Y.; Tsai, Y.; Wang, N. *J. Nanomater.* **2011**, article ID 814903, 9 pages
- (161) (a) Kim, H.; Miura, Y.; Macosko, C. W. *Chem. Mater.* **2010**, 22, 3441–3450 (b) Hsiao, S.; Chen-Chi, M.; Liao, W.; Wang, Y.; Li, S.; Huang, Y.; Yang, R.; Liang, W. *ACS Appl. Mater. Interfaces*, **2014**, 6, 10667-10678
- (162) Chopra, S.; Alam, S. *J. Appl. Polym. Sci.* **2013**, 128, 2012-2019
- (163) Jang, S. R.; Lee, C.; Choi, H.; Ko, J. J.; Lee, J.; Vittal, R.; Kim, K. *J. Chem. Mater.* **2006**, 18, 5604–5608
- (164) Harrison S. Kibombo, Dan Zhao, AndraGonshorowski, Sridhar Budhi, Miles D. Koppang, and Ranjit T. Koodali. *J. Phys. Chem. C* **2011**, 115, 6126–6135
- (165) (a) Osterloh, F. E. *Chem. Mater.* **2008**, 20, 35–54. (b) Nowotny, J.; Bak, T.; Nowotny, M. K.; Sheppard, L. R. *J. Phys. Chem. B* **2006**, 110, 18492–18495.
- (166) Pinho, L.; Mosquera, M. J. *J. Phys. Chem. C* **2011**, 115, 22851–22862.
- (167) Pinho, L.; Mosquera, M. J. *Appl. Catal., B: Environ.* **2013**, 134, 25–221
- (168) Pakdel, E.; Daoud, W. A.; Wang, X. G. *Appl. Surf. Sci.* **2013**, 275, 397.
- (169) Tan, A. W.; Pingguan-Murphy, B.; Ahmad, R.; Akbar, S. A. *J. Mater. Sci.* **2013**, 48, 8337

- (170) Liu, K. S.; Jiang, L. *Annu. Rev. Mater. Res.* **2012**, *42*, 231
- (171) Tricoli, A.; Righettoni, M.; Pratsinis, S. E. *Langmuir*, **2009**, *25*, 12578.
- (172) Zhang, M.Q.; Rong, M. Z.; Yu, S. L.; Wetzel, B.; Friendrich, K. *Wear*, **2002**, *253*, 1086–1093.
- (173) Shukla, R. K.; Sharma, V.; Pandey, A. K.; Singh, S.; Sultana, S.; Dhawan, A. *Toxicol In Vitro* **2011**, *25*, 231–241
- (174) Chen, X.; Mao, S. S. *Chem. Rev.* **2007**, *107*, 2891
- (175) Liu, H.; Ma, L.; Zhao, J.; Liu, J.; Yan, J.; Ruan, J.; Hong, F. *Biol Trace Elem Res*, **2009**, *129*, 170–180
- (176) Wier, K. A.; McCarthy, T. J. *Langmuir*, **2006**, *22*, 2433
- (177) Nosonovsky, M.; Bhushan, B. *Nano Lett*, **2007**, *7*, 2633
- (178) He, B.; Patankar, N. A.; Lee, J. *Langmuir*, **2003**, *19*, 4999
- (179) Koishi, T.; Yasuoka, K.; Fujikawa, S.; Ebisuzaki, T.; Zeng, X. C. *Proc. Natl. Acad. Sci. U.S.A.* **2009**, *106*, 8435
- (180) Zhang, X. T.; Sato, O.; Taguchi, M.; Einaga, Y.; Murakami, T.; Fujishima, A. *Chem. Mater.* **2005**, *17*, 696.
- (181) Xu, L.; Geng, Z.; He, J.; Zhou, G. *ACS Appl. Mater. Interfaces*, **2014**, *6*, 9029–9035
- (182) Michael V. Liga, Samuel J. Maguire-Boyle, Huma R. Jafry, Andrew R. Barron, Qilin Li. *Environ. Sci. Technol.* **2013**, *47*, 6463–6470
- (183) Ren, Y.; Chen, M.; Zhang, Y.; Wu, L. *Langmuir*, **2010**, *26*, 11391–11396
- (184) Tricoli, A.; Righettoni, M.; Pratsinis, S. E. *Langmuir*, **2009**, *25*, 12578
- (185) Mallakpour, S.; Zeraatpisheh, F.; Sabzalian, M. *EXPRESS Polymer Letters*, **2011**, *5*, 825–837
- (186) Greene, D.; Serrano-Garcia.; Govan, J.; Yurii, K. *Nanomaterials*, **2014**, *4*, 331–343
- (187) Tapan, N. A.; Mustain, W. E.; Gurau, B.; Sandi, S.; Prakash, J. *J. New. Mater. Electrochemical Systems*, **2004**, *7*, 281–286
- (188) Zhu, J.; Wei, S.; Haldolaarachchige, N.; Young, D. P.; Guo, Z. *J. Phys. Chem. C*, **2011**, *115*, 15304–15310

CHAPTER 2

Materials and Characterization Techniques



This chapter describes the source of all the materials and characterization techniques used for the working Chapters 3 to 6. These are briefly discussed below.

2.1. MATERIALS

The hydroxyl terminated polybutadiene (HTPB) was received as a gift sample from HEMRL, Pune, India, and used as received. The HTPB sample has the following physical characteristics: number average molecular weight ($M_n = 5210$), polydispersity index (PDI) = 2.53, viscosity at 29°C = 2680 cP and hydroxyl value = 42.60 mg KOH/gm. 1-Chloro-2,4-dinitrobenzene (DNCB), methyl ethyl ketone (MEK), triethyl amine (TEA) and butane diol (BDO) were purchased from SRL India and used as received. Isophorone diisocyanate (IPDI), toluene-2,4-diisocyanate (2,4-TDI), toluene-2,6-diisocyanate (2,6-TDI), dibutyltindilaurate (DBTDL), dimethylol propionic acid (DMPA), tetraethyl orthosilicate (TEOS), titanium dioxide (TiO_2) anatase nanoparticles and kaolinite (Kao) nano clay were received from Sigma-Aldrich and used without further purification. Cloisite-30B nano clay was purchased from Southern Clay Products, USA. Hydroxyl terminated polybutadiene (HTPB) was dried in vacuum oven at 70°C for one day before use.

2.2. CHARACTERIZATION METHODS

2.2.1. Spectroscopic studies

2.2.1.1. FT-IR Study

FT-IR spectra of PU films (thickness around 0.3 mm) were measured on FT-IR spectrometer (Nicolet 5700) at resolution of 0.5 cm^{-1} with an average of 64 scans.

2.2.1.2. NMR Study

All the ^{13}C CP-MAS measurements of PU films were carried out using a 400 MHz NMR (Bruker) spectrometer and ^1H -NMR spectra were recorded using Bruker AV 400 MHz NMR spectrometer at room temperature using $\text{DMSO-}d_6$ as NMR solvent to confirm the chemical structures of all the PUs.

2.2.2. X-Ray Diffraction Studies

2.2.2.1. WAX Study

The powder diffraction (WAXD) patterns of the PU films were collected from an X-ray generator (model PW 1729, Philips) with Cu K_α radiation source at voltage 40 kV and 30 mA current.

The diffractograms data were collected at a scan rate of 0.6°/minute in the 2θ range 2 to 80°. The PU films were fixed on a glass slide for the collection of data.

2.2.2.2. SAX Study

The small angle X-ray diffraction (SAXD) experiment of the PU films were carried out on a Hecus X-ray diffractometer with Cu K $_{\alpha}$ radiation ($\lambda = 1.5418 \text{ \AA}$) source operated at voltage of 50 kV and 1 mA current.

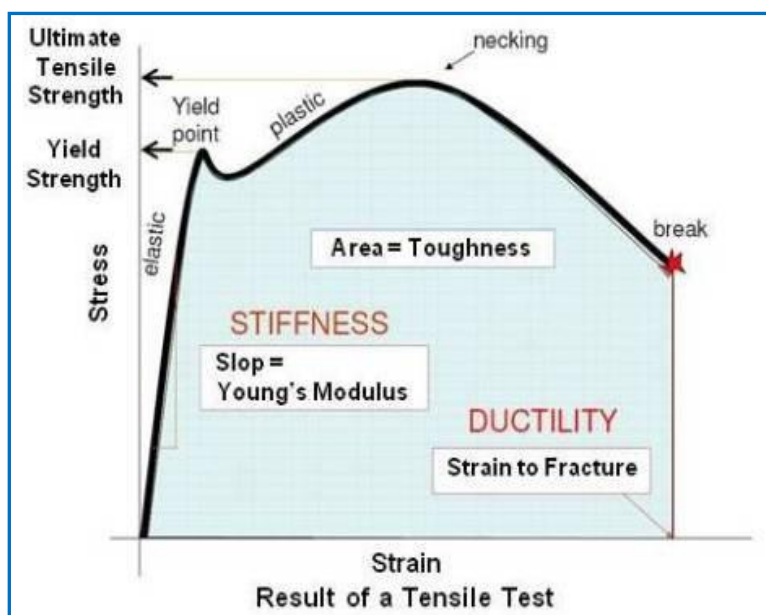
2.2.3 Mechanical strength measurement

2.2.3.1 Dynamic Mechanical Analysis

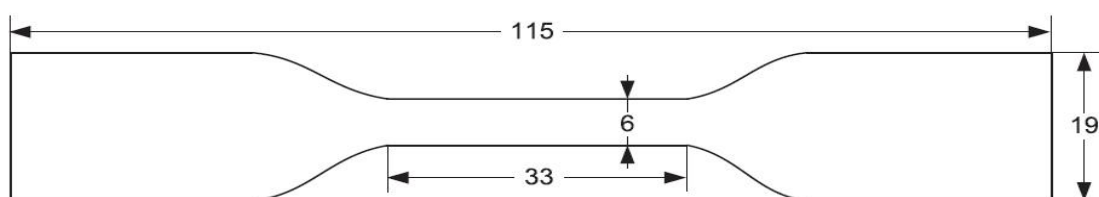
The thermo-mechanical properties of all the PUs and nanocomposite films were measured using a dynamic mechanical analyzer (DMA, TA Instrument model Q-800). Films of 13 mm \times 8 mm \times 0.23 mm (L \times W \times T) dimensions were cut and clamped on the films tension clamp of the pre-calibrated instrument. The samples were annealed at -100° C for 5 minutes and then scanned from -100° C to 50° C at heating rate of 3° C / minute. The storage modulus (E'), loss modulus (E'') and $\tan\delta$ values were measured as function of temperatures at 10Hz frequency with preload force of 0.01N. In some cases, the PU samples were recorded at higher temperature regions $\tan\delta$ vs temperature from -100° C to 200° C and 3° C / minute heating rate was used.

2.2.3.2 Universal Testing Measurement

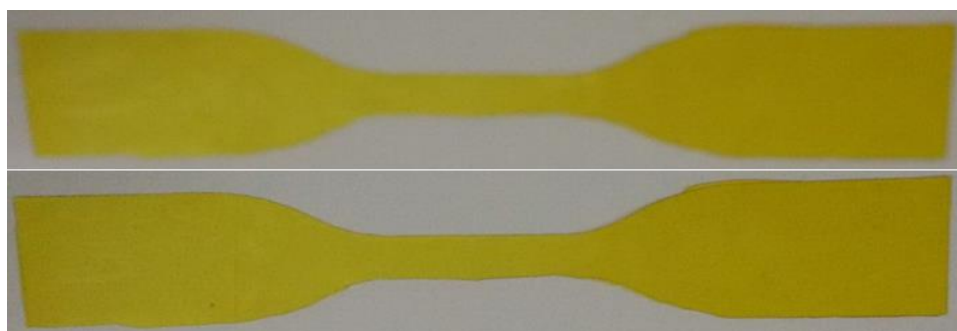
The tensile strength measurements (stress-strain relationship) were carried in a universal testing machine (INSTRON-5965) with 5kN load cell. Dumb-bell specimens were cut following ASTM standard D638 (Type IV specimen). Tensile properties of all the PUs and their nanocomposite films were measured in air atmosphere at room temperature with a crosshead speed 1mm/min. For each sample at least three specimens were tested in the machine to check the reproducibility. The toughness of the polyurethane films, which is the fracture energy per unit volume of the sample, was obtained from the area under the corresponding tensile stress-strain curve.



(A)



(B)



(C)

Figure 2.1. (A) Tensile plots used for analysis of the sample nature (B) ASTM D638-IV used to prepare samples for tensile test measurement (adapted from google images) and (C) Specimen PU film samples.

2.2.4 Microscopic Studies

2.2.4.1. FESEM Study

The cross sectional morphology of PU samples were examined in the Field Emission Scanning Electron Microscope (FESEM, Zeiss Ultra 55 model) instrument operated at 5 kV. The PU films were fractured after dipping into the liquid N₂ to ensure that the fracture side morphology remains intact. The fractured side of the samples was placed vertically in the SEM sample holder and also the surface morphology of all the water dispersible PU (WDPU) and their nanocomposite cured thin film samples were recorded for imaging in the FESEM, gold coated before imaging in FESEM.

2.2.4.2. AFM Study

Atomic Force Microscope (AFM) images of the water dispersible PU (WDPU) film surface were captured in an AFM apparatus (model: Solver Pro M of NT-MDT) working in semi-contact mode. A micro cantilever with a spring constant of 10 N/m was used to scan the samples to determine the surface roughness.

2.2.3.3. TEM Study

A transmission electron microscope (TEM, FEI Tecnai Model No. 2083) operating at 200 kV was used to study the particle morphology of all water dispersible PU (WDPU) and their nanocomposites. The TEM samples were prepared by dropping the appropriately diluted water dispersible PU solution onto the carbon coated copper (200mesh) grid and then scanned for imaging in TEM.

2.2.5. Thermal analysis

2.2.5.1. TG-DTA Study

Thermogravimetric analyses were carried out on a TG-DTA instrument (Netzsch STA 409PC) from 30°C to 800°C with a scanning rate of 10° C / min in the presence of nitrogen gas flow.

2.2.5.2. DSC Analysis

Small amount of PU samples were scanned at a scan rate of 5° C / min on a Mettler-Toledo DSC instrument. Data were recorded from -100 to 40° C in presence of nitrogen atmosphere. Glass transition temperature was identified from the slope change in the thermograms. The DSC was calibrated with indium and zinc before the scan of PU samples.

2.2.6. Contact angle measurement

Contact angle was measured with the G10 (Kruss) system (Hamburg, Germany) using the sessile drop method to evaluate the hydrophobic nature of the films obtained from water dispersible PU (WDPU). Thin films of samples were used for this measurement.

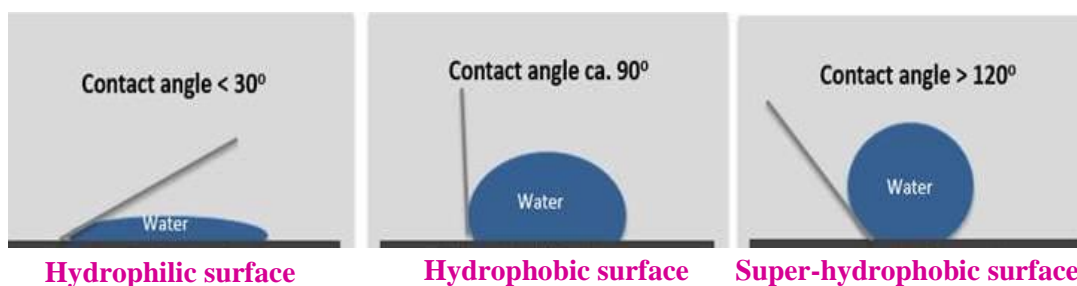


Figure 2.2. The nature of the film surfaces classified as three categories based on contact angle values (adapted from google images)

2.2.7. Particle size analysis

The polydispersity and the particle size of the water dispersible PU (WDPU) and their nanocomposite samples were measured using a light scattering based Zetasizer (Nano-S90, Malvern) instrument. The WDPUs were diluted with water before measurements.

2.2.8. Antibacterial activity

The antibacterial activity of WDPU/TiO₂-SiO₂ nanocomposite films was investigated by a zone inhibition method. The 6 mm diameter circular discs were punched from the nanocomposite film samples for the antibacterial study. *Staphylococcus aureus* (gram-positive) and *Escherichia coli* (gram-negative) bacteria were used as the model microorganisms. Using a spread plate method, 1mL log phase bacterial culture was spread on a nutrient agar plate. The composite film in disc forms was gently placed on the inoculated plates and was then incubated at 37° C for 16 hrs. Zones of inhibition were determined by measuring the clear area formed around each the composite film sample.

2.2.9. Hydroxyl value Measurement

Take three iodine flasks and keep one of these for blank determination. Weigh out accurately 5-8 gm. of HTPB in to the other two flasks. Pipette out 20 mL of the acetylating agent to each of three clean and dry 250 mL glass stopper iodine flasks. Stopper the flasks and swirl until the sample was

completely dissolved. Place all three flasks onto a steam bath at 98-100° C for one hour under reflux. At the end of this time, we added 10 mL of distilled water added to each flask and continue heating for fifteen minutes with stirring. Cool the flasks, rinse the condensers with 2×20 mL water. Add 1mL of phenolphthalein indicator to each flask and titrate with 1N sodium hydroxide solution. The endpoint is reached when the color just turns pinkish orange from the original pale yellowish color.¹⁻⁴

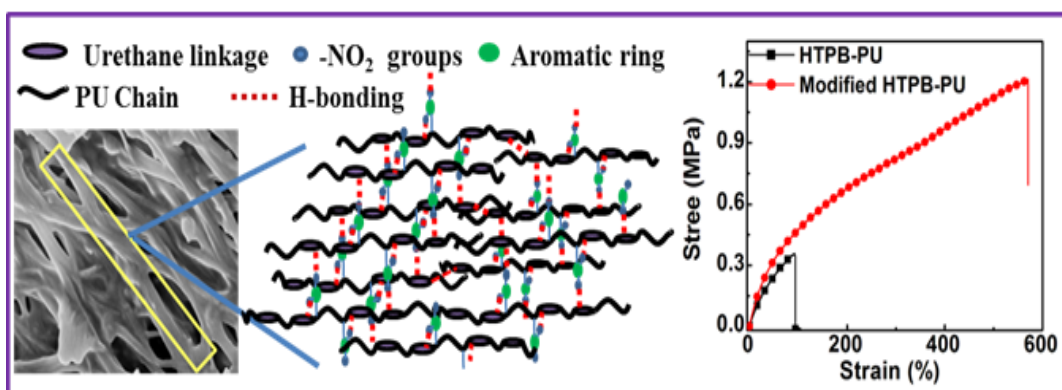
$$\text{-OH Value} = \frac{\text{Vol. of NaOH for blank titration} - \text{Vol. of NaOH for sample titration}}{\text{Weight of sample}} + \text{Acid value}$$

2.3. REFERENCES:

- (1) Petrovic, Z. S.; Yang, L.; Zlatanic, A.; Zhang, W.; Javni, I. J. *Appl. Poly. Sci*, **2007**, 105, 2717–2727.
- (2) Kong, X.; Narine, S. S. *Biomacromolecules*, **2007**, 8, 2203-2209.
- (3) Sarkar, S.; Adhikari, B. *Eur. Polym. J*, **2001**, 37, 1391–1401.
- (4) Lu, Y.; Larock, R. C. *Biomacromolecules*, **2008**, 9, 3332–3340.

CHAPTER 3

Simultaneous improvement of tensile strength and elongation: An unprecedented observation in case of HTPB polyurethanes



3.1. INTRODUCTION

Hydroxyl terminated polybutadiene (HTPB), an oligomeric viscous liquid with terminal hydroxyl groups, is used as polymeric binder in solid propellants. HTPB based polyurethane (PU) rubber obtained upon reaction with diisocyanates is the main matrix of composite solid propellants.¹⁻⁷ In additions to their use in propellant applications, HTPB based PUs have found applications in several other technologically important areas such as membranes, adhesives, separators, coating, sealants, liner materials, etc.⁸⁻¹² Very recently, HTPB based PUs have been used to develop the polymeric phase change materials on the basis of Diels-Alder linkages.¹³ Recently, Wang et al. studied the kinetics of epoxidation of HTPB with hydrogen peroxide under phase transfer catalysis.¹⁴ Detailed studies of structure-property relationship of these epoxide modified HTPB PUs are required to analyze the effect of epoxidation.

A vast amount of work has been reported in the literature on the HTPB based PUs. A majority of these reports studied structure-property relationship of this segmented PU.¹⁵⁻²⁴ A considerable amount of effort has been made toward the studies of thermal stability, effect of aging, susceptibility toward oxygen, and especially the mechanical stability.²⁵⁻³¹ Several types of diisocyanate structures have been used to elucidate the structure-property phenomenon of the PUs.³² A careful analysis of the literature reports brings a general observation that most of the researchers made efforts to improve the tensile properties of HTPB based PUs. Co-polyurethanes synthesized from HTPB lignin with various diisocyanates displayed improvement in tensile strength compared to HTPB-PUs up to 3 wt % lignin incorporation in the diols mixture. Further increase in lignin content in the lignin-HTPB copolyurethane decreases the tensile strength of the materials owing to the high hydroxyl value of lignin.³³ Several authors have used chemical modification approaches to modify the mechanical properties of PUs.³⁴ Very recently, chemical modification strategies have been used to improve the mechanical properties of lignin based polyurethane. Lewis acid treatment of lignin enhances the concentration and reactivity of hydroxyl groups available to react with diisocyanate monomers which results in better integration of lignin into the urethane network; hence, the mechanical properties improve significantly.³⁵ PUs obtained from glycidylazide polymer (GAP), an alternative energetic binder to HTPB for rocket propellants, displayed tunable tensile properties depending upon the amount of residual dimethyl sulfoxide solvent which was used to synthesize the GAP prepolymer.³⁶ Zhang et al. reported simultaneous improvement of tensile strength, Young's modulus, and elongation at break in the case of a polyurethane hybrid obtained from functionalized modified hexa methylene diisocyanatetrimer and dihydroxyl propyl-terminated siloxane oligomers.³⁷ The effects of hydrogen

bonding on the structure-property relationship especially on the mechanical properties of HTPB based PUs have been discussed by several authors in the literature.^{15,18,20,21,38}

Although the efforts made by several authors in the literature to enhance strength and elongation are highly appreciated, there is a tremendous challenge to produce HTPB based PUs where both strength and elongation increases simultaneously since this will be very useful for propellant formulation and many other advanced applications. Keeping this objective as our aim, we hypothesized that if hydrogen bonding interactions can be introduced between the hard and soft segments of HTPB-PU which is otherwise absent then we might see a segmental mixing between the hard and soft segments. With this idea, we search for a diol monomer, which can facilitate the hydrogen bond formation between hard and soft segments. We found out that terminally functionalized HTPB, which we have reported earlier, has hydrogen bond forming nitro functionalities in the HTPB backbone³⁹ and therefore, we felt that this modified HTPB can be an ideal choice as diol monomer for the current aim. This modified HTPB was obtained by attaching dinitrobenzene (DNB) groups at the terminal carbon atoms of HTPB, and this is called HTPB-DNB.

With this idea and readily available appropriate diol monomer (HTPB-DNB) in our stock, we have prepared PUs from HTPBDNB based diols with various diisocyanates and studied their mechanical and thermal behaviours. We have also made efforts to understand the segmental mixing phenomenon using small angle X-ray scattering (SAXS), wide-angle X-ray diffraction (WAXD), spectroscopic, and morphological techniques. All the results of HTPB-DNB-PUs are compared with the PUs, which were obtained from the reactions of native HTPB diol and various diisocyanates using identical polymerization conditions as in the case of HTPB-DNB-PUs.

3.2. SYNTHESIS

3.2.1. Synthesis of HTPB-DNB

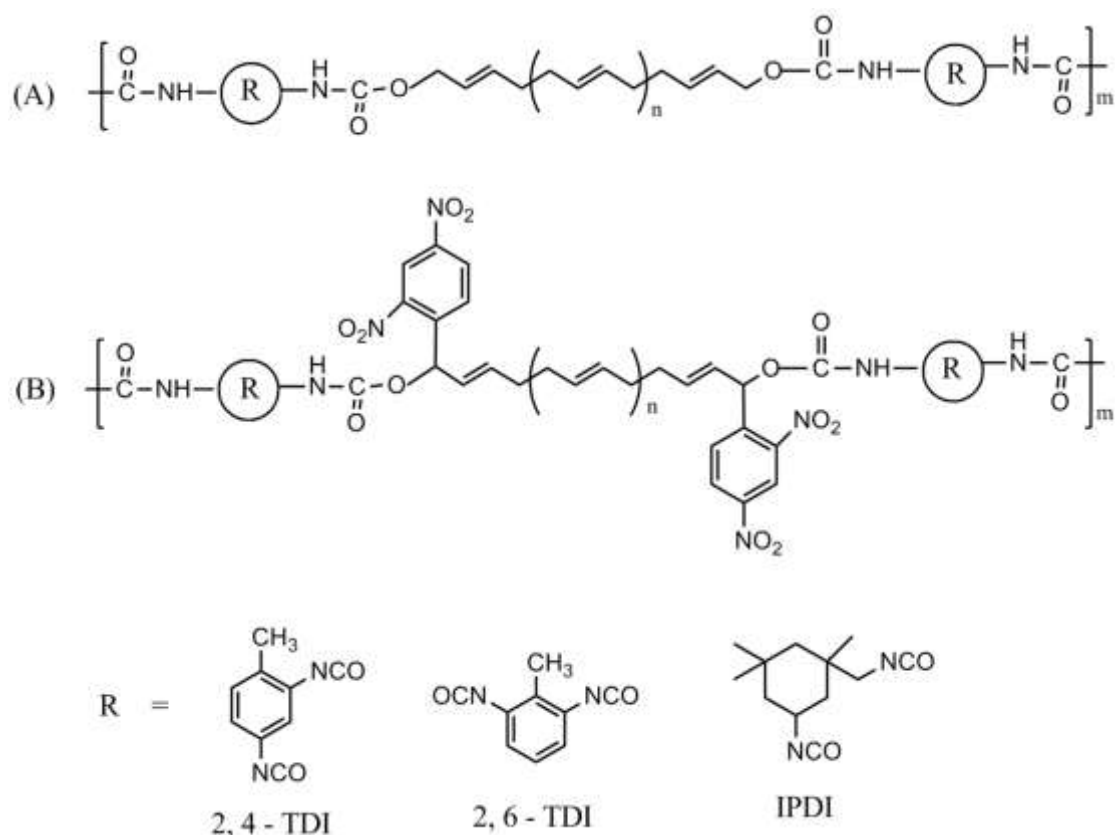
The terminated carbon atom functionalization was carried out by attaching the DNCB molecules covalently using our previously developed method.^{39,40} Briefly, the procedure for the synthesis of HTPB-DNB is as follows: 3.345 g HTPB (0.062 mol, considering 54 as a repeating unit) was taken in a three neck round-bottom flask and dissolved in 10 mL of distilled dichloromethane. After complete dissolution of HTPB in dichloromethane, 0.223 gm (0.01 mol) of NaH was added in the presence of purging nitrogen gas. After 30 min, 0.205 gm (0.001 mol) of 1-chloro-2, 4-dinitrobenzene was added to the reaction mixture. The stirring was continued for another 3 h in presence of nitrogen gas followed by overnight stirring. After the reaction, the product was washed

with hexane and methanol repeatedly to obtain the HTPB-DNB. The resultant product has the following physical characteristics: $M_n = 5600$, PDI = 2.53, viscosity at 27° C = 3826 cP, hydroxyl value = 42.35 mg KOH/g and HTPB-DNB was dried in vacuum oven at 70° C for one day before use.

3.2.2. Synthesis of Polyurethane

A 3.936 g portion of HTPB was dissolved in 10 mL of CHCl_3 in a three-neck round-bottom flask. One neck of the flask was fitted with a guard tube, one neck was used for pouring reactants and through the other neck, and nitrogen gas was purged to maintain the inert atmosphere. We calculated the number of moles of hydroxyl groups using the hydroxyl value of HTPB and the calculated hydroxyl moles obtained was 0.0031 mol. To keep the stoichiometric balance between the diols and diisocyanates, we have taken exactly 0.0031 mol. diisocyanates. The weight taken for 2,4-TDI and 2,6-TDI were 0.539 g and IPDI was 0.688 g. All these weights are equal to 0.0031 mol. We carried out three different reactions of HTPB with three different diisocyanates maintaining exactly equal stoichiometry between the diol and diisocyanate functionalities. Diisocyanate was added to the HTPB solution in the flask, and 0.1 mL of DBTDL was added to the reaction mixture. The reaction mixture was stirred for 3 h in the presence of nitrogen atmosphere, and a homogeneous solution was obtained. Completion of the polyurethane formation was determined by FTIR spectroscopy following an isocyanate peak at 2270 cm^{-1} which disappears after 3 h. Hence, formation of polyurethane was confirmed. A portion of the viscous polyurethane (PU) mixture was poured into the glass Petri dish which was previous coated with silicone releasing agent to obtain the PU sheet. The PU mixture in the glass Petri dish was kept in an oven at 70° C for 5 days for curing of polymer. After 5 days, free-standing cured PU film (sheet) was obtained. We have made PU from three different diisocyanates, and in all cases, reaction and curing conditions were identical.

A similar method as that described above was followed for the preparation of HTPB-DNB-PUs. A 4 g portion of HTPB-DNB was taken which had 0.0034 mol. of diol functional groups as calculated from the hydroxyl value, and hence, 0.0034 mol. diisocyanates were used for the preparation of PUs. The all other reaction conditions and curing time and temperature were kept similar as they were in the case of HTPB-PU. The chemical structures of both types of PUs are shown in Scheme 3.1.



Scheme 3.1. Chemical structures of polyurethanes (A) HTPB-PU and (B) HTPB-DNB-PU

3.3. CHARECTERIZATION TECHNIQUES

All the information about the materials used in this study and the characterization techniques which include spectroscopic characterization by Fourier transform infrared spectroscopy (FT-IR) and solid state NMR, X-ray diffractions (SWAXD), Field emission scanning electron microscopy (FE-SEM), thermogravimetric analysis (TGA), differential scanning coloremtry (DSC), dynamic mechanical analysis (DMA) and universal testing measurement (UTM) analysis studies for all the polyurethane polymer samples are discussed in the Chapter 2.

3.4. RESULTS AND DISCUSSION

3.4.1. Synthesis and Spectroscopic Studies of Polyurethanes

Polyurethanes (PUs) of HTPB and modified HTPB (HTPB-DNB) were prepared using three different diisocyanates (2,4 -TDI, 2,6-TDI, and IPDI) and these PUs were cured for 5 days at 70° C to

obtained free-standing films. We have maintained the -NCO/-OH mole ratio equal to one in all the PUs synthesis. The moles of -OH functionality has been calculated from the hydroxyl values of HTPB and HTPB-DNB.^{33,41} It is to be noted that all the reaction conditions and curing conditions for the preparation of PUs were exactly identical. We have monitored the progress of reaction by recording the IR spectra of the product after 3 h of reaction and before curing of PU. The disappearance of hydroxyl and isocyanate peaks at 3386 and 2270 cm^{-1} , respectively, and appearance of -N-H peak of urethane linkage at around 3286 cm^{-1} (3278 cm^{-1} in the case of HTPB-DNB-PU) confirm the formation of PUs (Figure 3.1). FT-IR spectra of diol monomers (HTPB and HTPB-DNB) and PUs along with the DNCB frequencies are shown in Figure 3.1. The figure clearly indicates the formation of PUs as proved from the sharp -N-H peak observed at around 3280 cm^{-1} .²⁸ The sharper and lower frequency -N-H peak in the case of HTPB-DNB-PU (3278 cm^{-1}) compared to HTPB-PU (3286 cm^{-1}) attributes that perhaps more free -N-H groups are available in the former PU than the later. This also confirmed from the fact that the carbonyl peak appears at 1716 cm^{-1} in the case of HTPB-DNB-PU; whereas, it is at 1710 cm^{-1} in the case of HTPB-PU. These free -N-H groups actually participate in the hydrogen bonding with -NO₂ groups of DNB, which are hanging in the backbone of HTPB-DNB-PU. From the figure, it is clearly seen that the symmetric and asymmetric stretching of -NO₂ (at 1545 and 1354 cm^{-1} ; see the DNCB spectrum in the figure) are shifted toward the lower wavenumbers (1536 and 1340 cm^{-1}) and significantly broaden in case of HTPB-DNB-PU. Hence, the above results indicate that the hanging DNB in the PU backbone yield extra hydrogen bonding in the PU, and we believe this will be reflected in their properties, which will be discussed in the following section.

All the PU samples were further characterized by recording ¹³C solid state NMR (¹³C CP-MAS) to confirm the additional interactions between the -NO₂ functionalities of DNB with the -N-H of the urethane linkage of the PU backbone in the case of PUs obtained from HTPB-DNB diols. Figure 3.2 shows the representative ¹³C solid-state NMR spectra of various PUs.

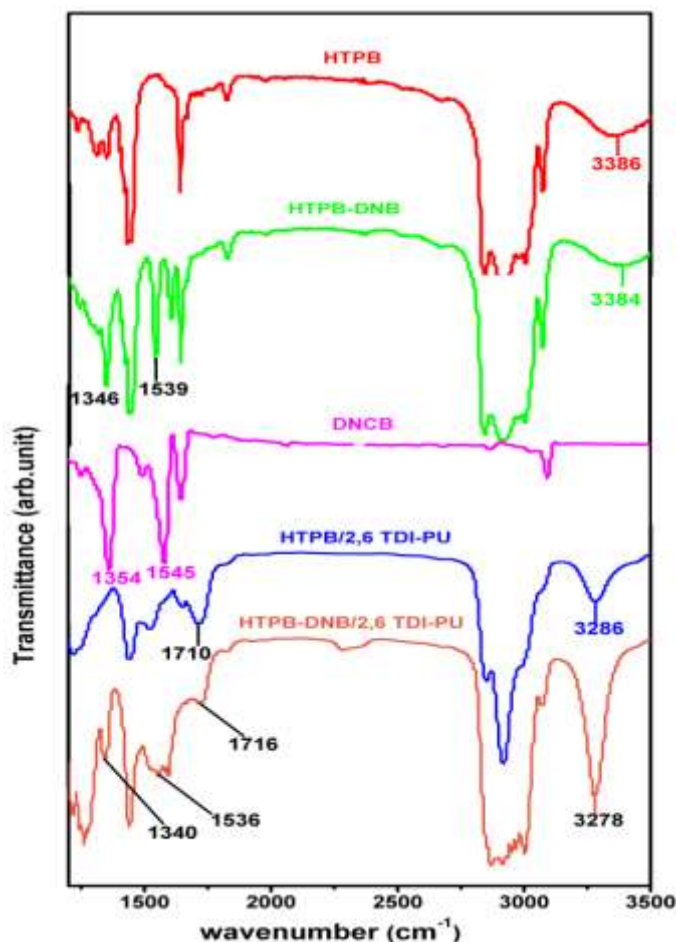


Figure 3.1. FT-IR spectra of HTPB, HTPB-DNB, DNCB, HTPB/2,6-TDI-PU and HTPB-DNB/2,6-TDI-PU.

As expected, all the PUs mostly displays the peaks due to HTPB carbons. The saturated carbon signals appear between 20 and 50 ppm. The 1, 2-unsaturated carbon atom signals come at 112 and 142 ppm, and 1,4-unsaturated multiple peaks are seen around at 130 ppm.^{31,41} In the case of HTPB-DNB-PUs, we noticed two additional peaks at 134 and 155 ppm (shown by arrow marks in the figure). The peak at 134 ppm is due to aromatic carbons of DNB. However, the peak at 155 ppm which is seen only in the case of HTPB-DNB-PU samples and completely absent in HTPB-PUs may be due to the carbonyl carbons of urethanes. Actually, in all the PUs, carbonyl carbons are present; however, their signals appear only in the case of HTPB-DNB-PUs, which can be attributed to the fact that in these cases due to the interactions between the -NO_2 of DNB and urethane -N-H the carbonyl carbon becomes accessible to be detected by NMR signals. Otherwise, these carbons are buried inside

the PU chains and hence, do not respond to NMR frequency. Once again, NMR study clearly indicates the interactions between the DNB and PUs backbone when HTPB-DNB is used as a diol.

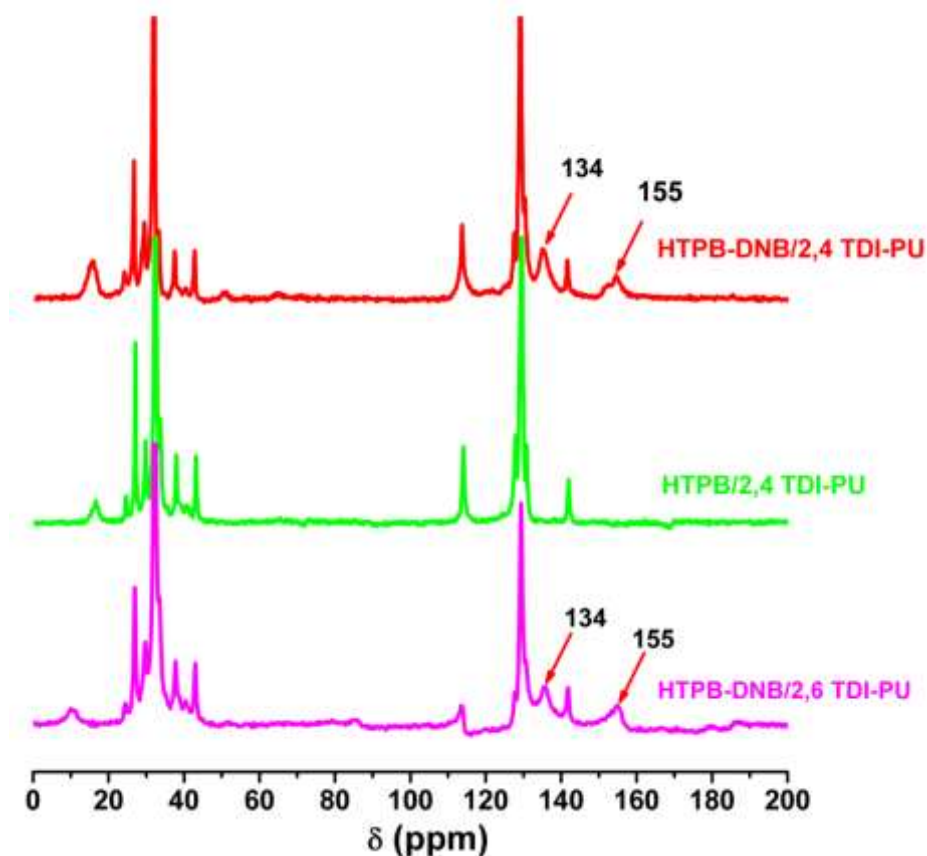


Figure 3.2. ^{13}C solid state (^{13}C CP-MAS) spectra of PUs as indicated in the figure.

3.4.2. Tensile properties

Increase in the cross-linking density in the cured PUs is found to be the reason behind the increase of σ_b , toughness, and E, etc.^{22,35,43} We have calculated the effective cross-linking (N), in all the samples and listed in Table 3.1. The N values of PUs are determined from the E values (Table 3.1) which were calculated from Figure 3.3 (stress-strain plots).

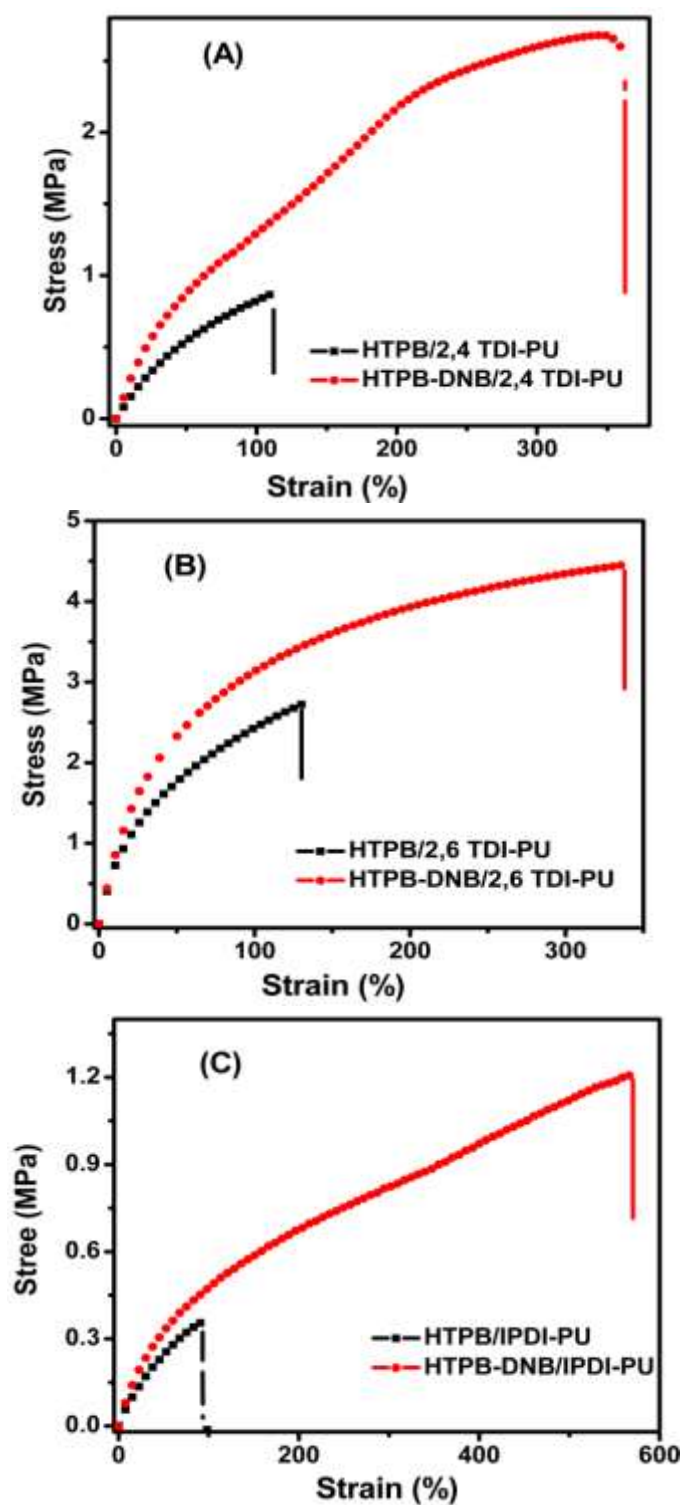


Figure 3.3. Stress-Strain plots of HTPB and HTPB-DNB polyurethanes with various diisocyanates; (A) 2,4-TDI, (B) 2,6 TDI and (C) IPDI

Table 3.1. Various mechanical data obtained from tensile study.

<i>PU polymer</i>	<i>Tensile strength</i> (σ_b , MPa)	<i>Elongation of break</i> (ϵ_b , %)	<i>Toughness</i> (MPa)	<i>Young modulus</i> (E , MPa)	<i>Effective crosslinking</i> (N , m^{-3})
HTPB/2,4-TDI	0.88	111.88	60.54	0.012	114.95×10^{22}
HTPB-DNB/2,4-TDI	2.68	345.47	660.50	0.021	208.06×10^{22}
HTPB/2,6-TDI	2.71	130.01	240.44	0.046	582.29×10^{22}
HTPB-DNB/2,6-TDI	4.46	337.62	1151.78	0.058	720.09×10^{22}
HTPB/IPDI-PU	0.36	91.22	20.24	0.006	57.65×10^{22}
HTPB-DNB/IPDI	1.21	570.26	440.03	0.007	86.12×10^{22}

As per the rubber elasticity theory,³⁵ the number of network stands for unit volume (N , effective cross-linking density) can be estimated from the relation $E = 3NK_B T$, where E is the Young's modulus obtained from the stress-strain plot, K_B the Boltzmann constant, and T is the absolute temperature in kelvin. N values listed in Table 3.1 clearly indicate that effective cross-linking is more in the case of HTPB-DNB-PU than HTPB-PU for all diisocyanates. Here also we see the dependence of isocyanate structures on N values. Therefore, the increase in σ_b , toughness, and E can be explained as a result of increased cross-linking in the case of HTPB-DNB-PU.

However there are two questions which remain unanswered; these are (I) how the cross-linking is more in case of HTPB-DNB-PU compared to HTPB-PU despite the fact that in both the cases -NCO/-OH ratio is equal to one and most importantly (II) why elongation at break (ϵ_b) is higher for HTPB-DNB-PU than HTPB-PU. The increases in N values (cross-linking) should decrease the ϵ_b values, but instead we observed increases in ϵ_b . This contradictory result is bit puzzling, hence the above two questions need to be answered to understand the simultaneous increase of both σ_b and ϵ_b despite the value of -NCO/-OH mole ratio kept as one. To answer these questions, we propose the schematic model as shown in Figure 3.4. The dinitrobenzene molecules randomly present in the PU network in case of PU obtained from HTPB-DNB. The nitro functionalities form hydrogen bonding with the urethane linkages of the PU backbone. In the PU network, all the hydrogen bonding due to -NO₂ functionalities will create an extra supramolecular hydrogen-bonding network in the PU matrix. This extra network because of DNB functionalities enhances the cross-linking density (Table 3.1) despite the $r = 1$. Also, because this extra network is extended throughout the PU matrix, it acts as a bridge between the chains which increases the ϵ_b value. The presence of extra hydrogen bonding

between the -NO_2 functionalities and urethane backbone is discussed in an earlier section using FT-IR and ^{13}C solid-state NMR. To probe further detailed insight of these observations, we have carried out X-ray diffraction and morphological studies, which are discussed in the next sections.

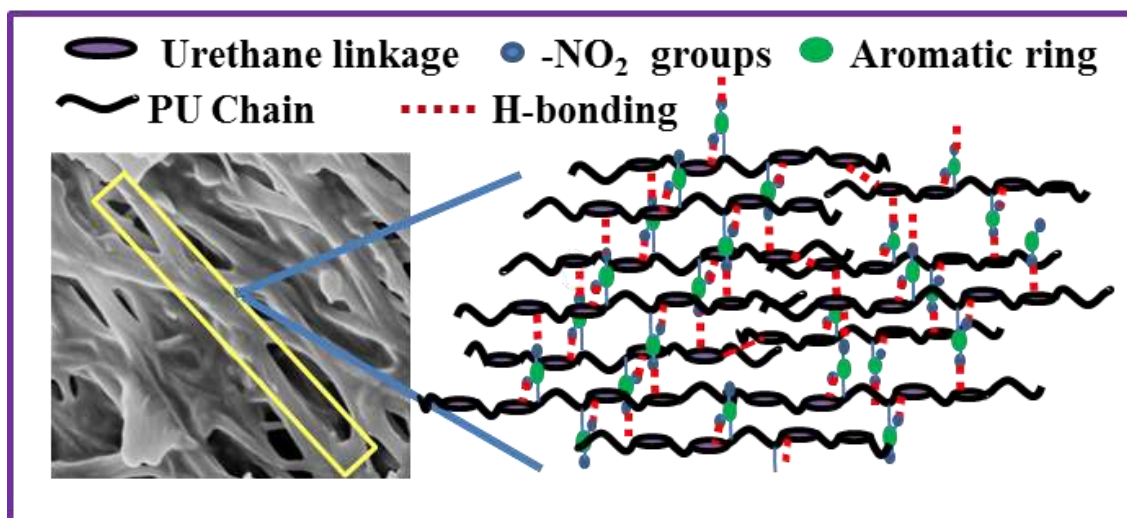


Figure 3.4. Schematic representations of HTPB-DNB-PU showing “fibrous-assembly” structure. The microscopic image is the magnified cross section morphology of this PU obtained from the FESEM imaging.

3.4.3. X-ray studies

All the PU samples are studied using both SAXS and WAXD techniques. SAXS plots in the q range $0.2\text{--}0.7\text{ \AA}^{-1}$ of representative PUs are shown in Figure 3.5. All the PUs displays a broad peak at $q \approx 0.58\text{ \AA}^{-1}$. The respective d -values are mentioned in the figure. It is to be noted that the peak position moves to the lower angle very nominally in the case of HTPB-DNB-PUs; however, the peak intensities of these PUs are relatively stronger than the HTPB-PUs. These results indicate that the phase separation pattern (segmental mixing) between the hard segment (HS) and soft segment (SS) in these two types of PUs are not similar.

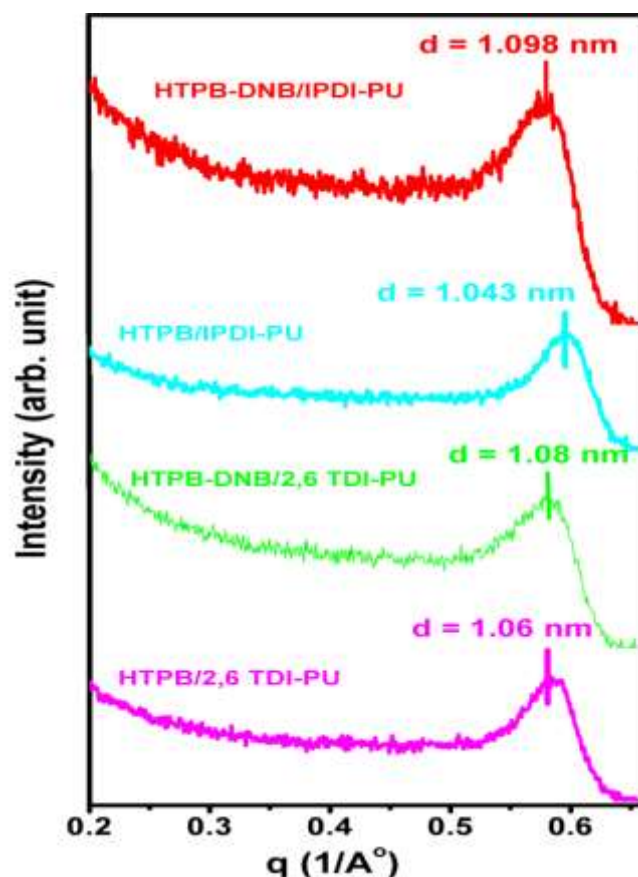


Figure 3.5. SAXS plots of PUs obtained from HTPB and HTPB-DNB with different diisocyanates

To understand the HS-SS phase pattern (segmental mixing) more critically, we have analysed the SAXS data, which were collected from the lower angle measurements using Porod's method, and all the Porod plots are shown in the Figure 3.6. In all the cases, we observed positive deviation of Porod's behavior, which attributes segmental mixing between hard and soft segments. However, it must be noted that deviations are relatively higher (red lines in the figure) in the case of HTPB-DNB-PUs compared to HTPB-PUs. This clearly indicates a higher degree of segmental mixing between the hard and soft segments in the former. This is because of very strong favorable hydrogen bonding interactions between the DNB (which is present in the soft segment) and the urethane linkage as proved from the spectroscopic studies described earlier. With a schematic presentation, Figure 3.4 demonstrates these interactions, which are extended throughout the polymer matrix. Also, it is to be noted that the deviations in the Porod's plots (Figure 3.6) depends upon the type of diisocyanates used to make PUs.

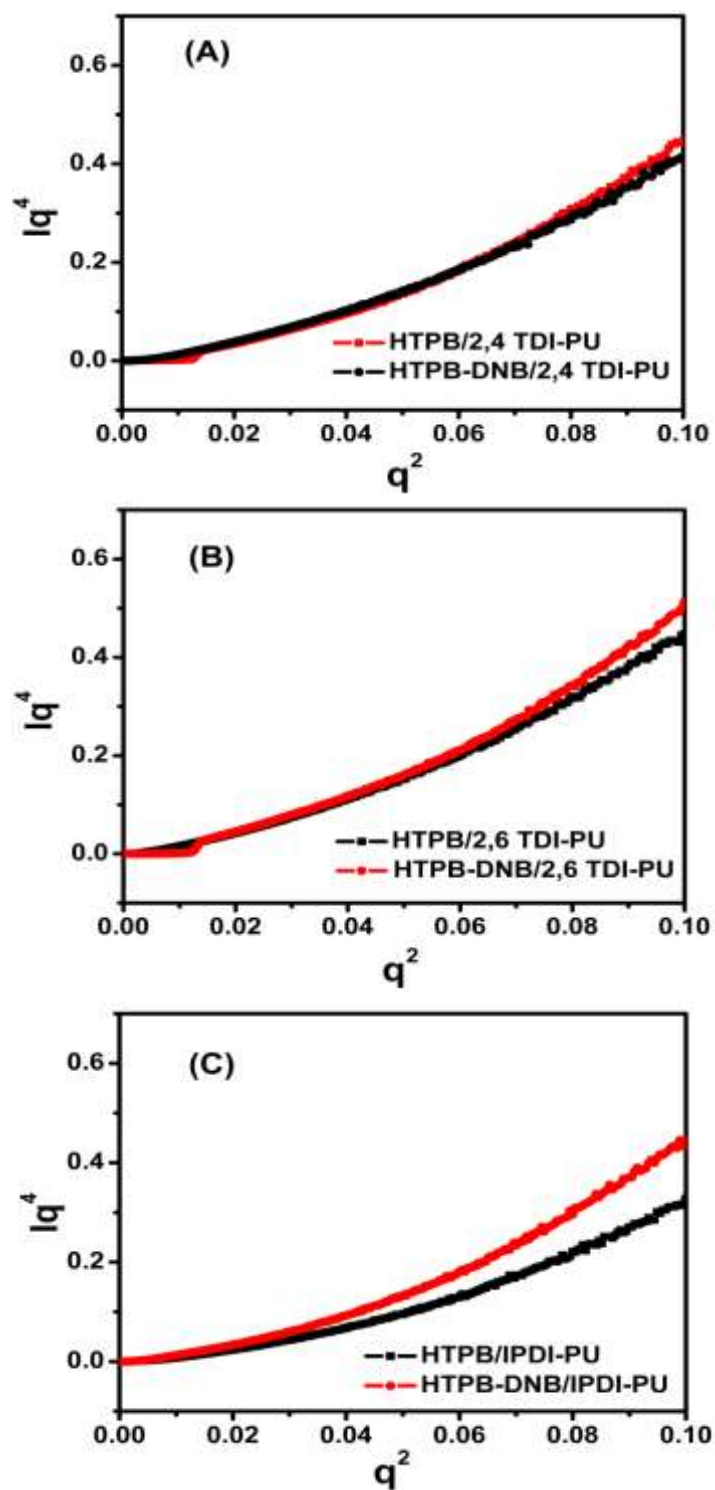


Figure 3.6. Porod plots of PUs obtained from HTPB and HTPB-DNB using different diisocyanates; (A) 2,4-TDI (B) 2,6-TDI and (C) IPDI.

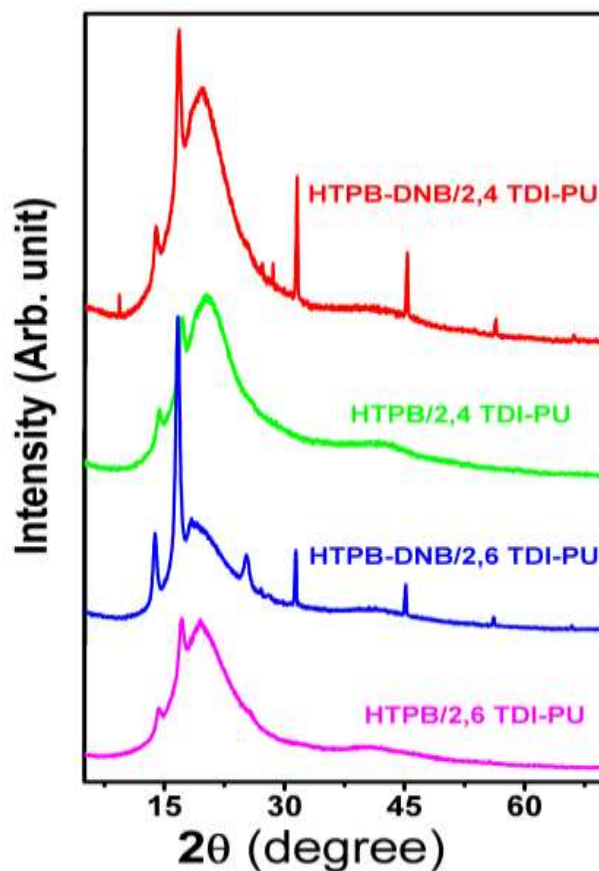


Figure 3.7. WAXD patterns of PUs obtained from HTPB and HTPB-DNB using various diisocyanates

The WAXD patterns of representative PUs are shown in Figure 3.7. HTPB-PUs display amorphous character with only two low intense peaks at $2\theta = 13.65^\circ$ and 16.57° in their amorphous halos. However, HTPB-DNB-PUs show very sharp crystalline peaks at $2\theta = 3.15^\circ$, 16.51° , 31.32° , 45.03° , and 56.50° . Hence, from these results, it is clear that the packing natures in these two cases are not similar. The higher segmental mixing probably allows the HTPB-DNB-PUs to pack in a more ordered way resulting strong crystalline peaks. It can be argued that the crystalline peaks are owing to DNB molecules. However, the amount of DNB present in the PUs would be very less which is not enough to show the diffraction peaks. These peaks are due to strong interactions between the soft segment and polyurethane linkage backbone, which is present throughout the PU as, described in Figure 3.4.

3.4.4. Morphological study

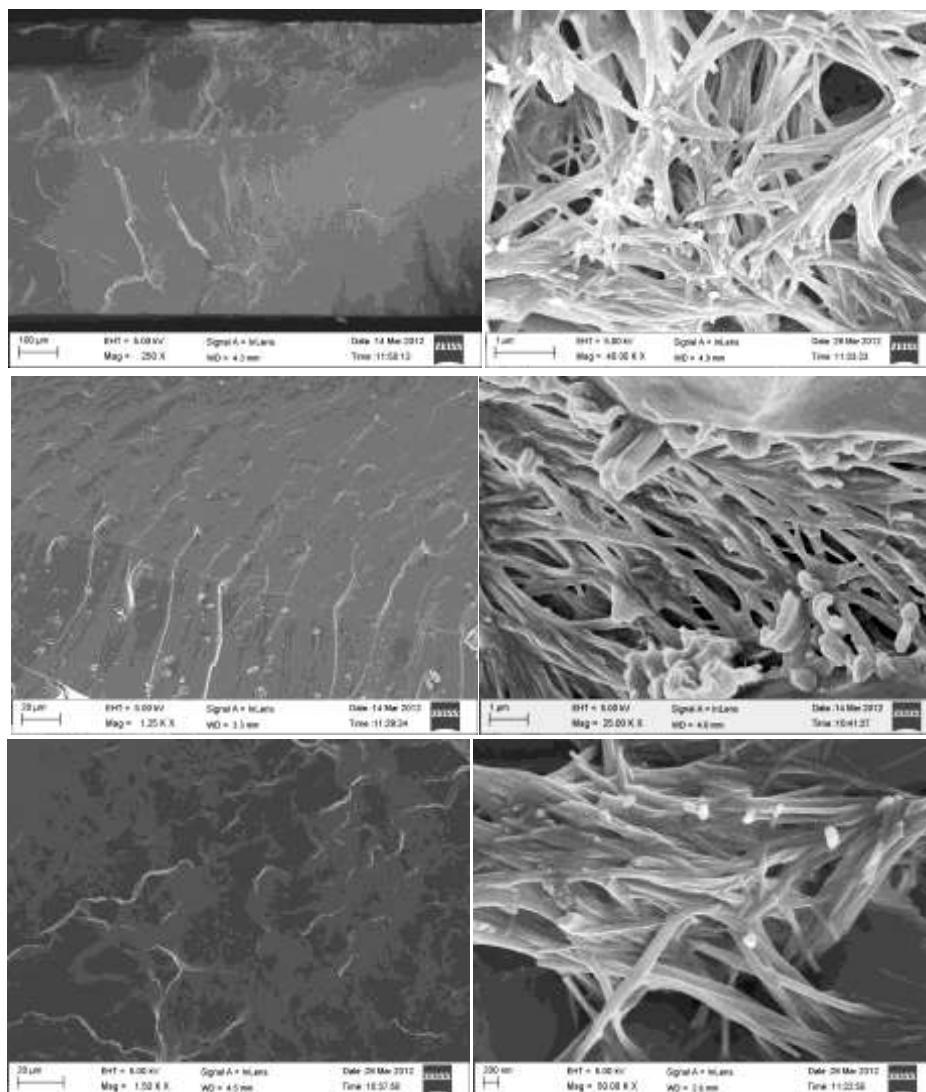


Figure 3.8. FESEM micrographs of frozen fracture cross-section of PUs. HTPB-PUs (left panel) and HTPB-DNB-PUs (right panel). 1st row: 2, 4 TDI, 2nd row 2, 6 TDI and 3rd row IPDI

The superior mechanical properties of modified HTPB-PUs (HTPB-DNB-PUs) compared to HTPBPUs as described earlier is the manifestation of strong hydrogen bonding interactions between the $-\text{NO}_2$ of DNB of soft segment with the PU backbone which results in higher order segmental mixing and more crystalline character in the former as described in the previous section. We also

Investigate, analysed, and compared the morphological outcomes of these two PUs by imaging the frozen fracture cross-section of PU films. The FESEM images are shown in Figure 3.8. The morphological features of two types of PUs are greatly different. We observed micro to nano meter thick long fibers which are crossed and entangled with each other resulting in a fibrous-assembly type morphology in the case of HTPB-DNB-PUs whereas HTPB-PUs are almost featureless. The fibrous-assembly morphology is observed for all types of diisocyanates used here to make PUs. We believe this significant difference in morphology is responsible for significant improvement in the tensile properties in case of HTPB-DNB-PUs. The origin of morphological difference is the segmental mixing pattern, which is significantly high in DNB samples owing to the presence of strong hydrogen bonding interactions between the -NO_2 functionalities and the urethane linkages.

3.4.5. Thermal Study

The measurement of glass transition temperature (T_g) of segmented PUs can give insights of the segmental mixing and microphase separation. We have utilized differential scanning calorimetry (DSC) and dynamic mechanical analyses (DMA) techniques to determine the T_g s. Figures 3.9 and Figure 3.10 show the DSC thermograms and DMA ($\tan \delta$ vs temperature) plots, respectively. Both DSC and DMA detect the T_g for soft segment at ~ -70 and $\sim -60^\circ \text{C}$, respectively for all the samples.⁴⁴ There is very little dependency of T_g values on diisocyanates structure as seen in DSC and DMA plots. Therefore, we can say the modification of HTPB backbone with DNB does not alter the soft segment T_g . This result is expected since the T_g of the soft segments is generally do not alter due to segmental mixing in microphase separated PUs. The T_g due to HS is expected to appear above ambient temperature. All the HTPB-DNB-PUs display HS T_g above 100°C (Figure 3.10B) and show the diisocyanate structure dependency. However, HTPB-PUs do not show any HS T_g as seen in Figure 3.10A. This once again prove the fact that in the case of HTPB-DNB-PUs the greater degree of segmental mixing takes place between the HS and SS owing to the strong supramolecular hydrogen bonding interactions between the -NO_2 of DNB and urethane backbone. Hence, thermal study is in agreement with all other characterizations about the segmental mixing of micro-phases.

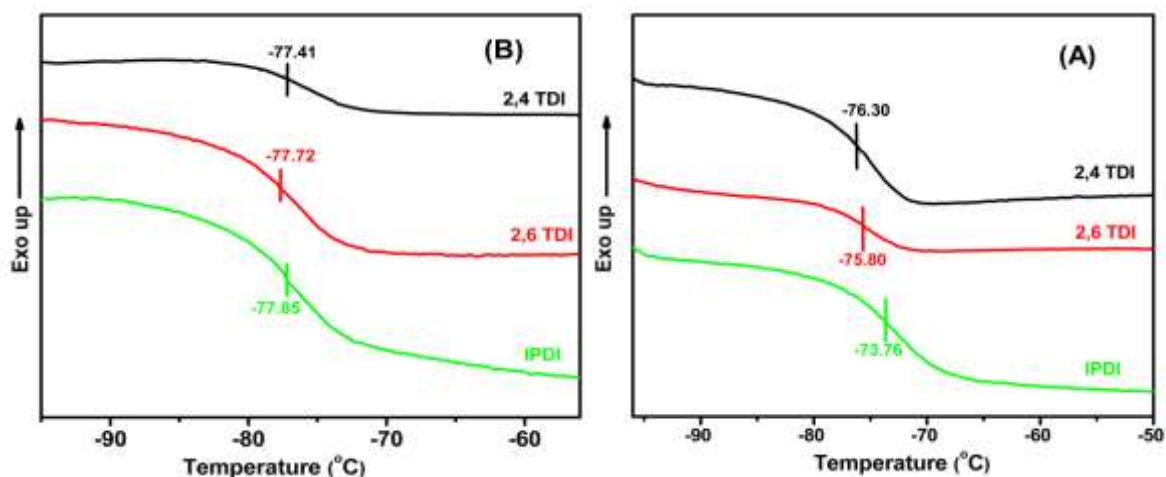


Figure 3.9. DSC Thermograms of PUs (A) HTPB, (B) HTPB-DNB Vertical line indicates the T_g values.

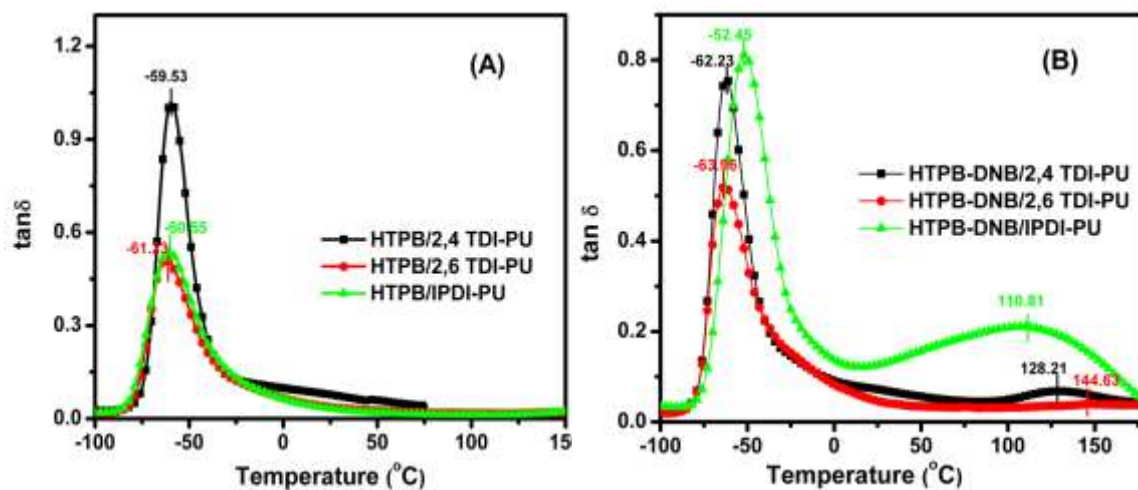


Figure 3.10. $\tan \delta$ vs temperature plots of PUs obtained from DMA study (A) HTPB, (B) HTPB-DNB. T_g values are shown by vertical lines in the figure.

3.5. CONCLUSION

Free standing PU films obtained from modified HTPB (HTPB-DNB) with varieties of diisocyanates have been studied to evaluate the effects of terminal functionalization of the HTPB backbone on the structure-property relationship of the PUs. The current study clearly demonstrated that the modification of the terminal carbon atoms with appropriate functionalities (in this case with dinitrobenzene) can induce an extra hydrogen bonding supramolecular network which in turn enhanced the segmental mixing between the hard-soft segments and yielded partial crystalline character in the PUs. As a result of these, the PUs displayed significantly higher mechanical properties compared to native HTPB-PUs. Most importantly, the modified HTPB-PUs showed simultaneous enhancement of both tensile strength and elongation at break. This simultaneous increase of both mechanical properties is an unprecedented observation in the PU literature and hence opens up a new possibility to make mechanically strong elastomeric PU.

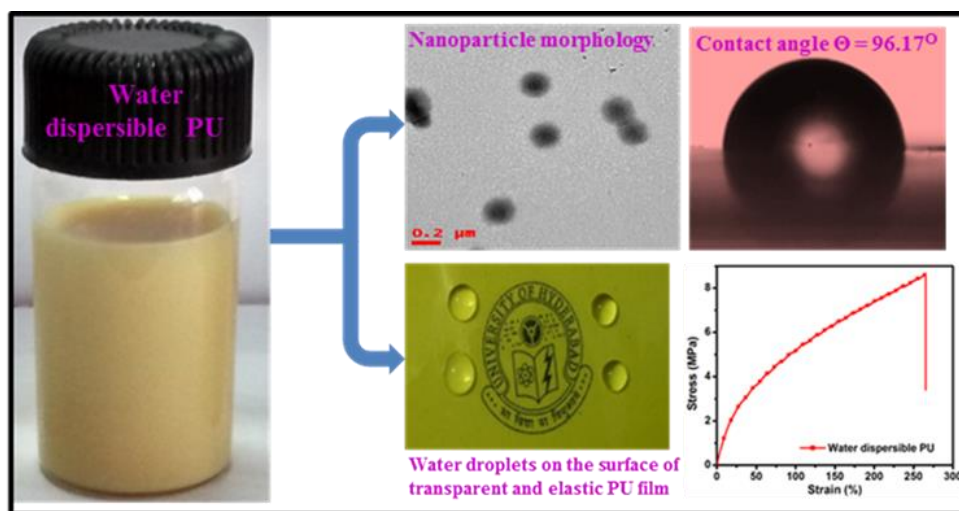
3.6. REFERENCES

- (1) Bunyan, P.; Cunliffe, A. V.; Davis A, Kirby F. A. *Polym. Degrad. Stab.* **1993**, *40*, 239-250.
- (2) Urbanski, T. *Chemistry and Technology of Explosives*, Pergamon Press, New York, 1984.
- (3) Subramanian, K. *J. Polym. Sci. Part-A; Polymer Chem.* **1999**, *37*, 4090-4099.
- (4) Kit, B.; Evered, D. S. *Rocket Propellant Handbook*, New York, 1960.
- (5) Muthiah, R. M.; Manjari, R.; Krishnamoorthy, V. N.; Gupta, B. R. *Polym. Eng. Sci.* **1991**, *31*, 61.
- (6) Krishnan, P. S. G.; Ayyaswamy, K.; Nayak, S. K. *J. Macromol. Sci. Part A: Pure and Appl. Chem.* **2013**, *50*, 128-138.
- (7) Cho, B-S.; Noh, S-T. *J. Appl. Polym. Sci.* **2011**, *121*, 3560-3568.
- (8) Gupta, T.; Pradhan, N. C.; Adhikari, B. *Bull. Mater. Sci.* **2002**, *25*, 533-536.
- (9) Yang, J. M.; Lin, H. T. *J. Membr. Sci.* **2001**, *187*, 159-169.
- (10) Chen, S. H.; Yu, K. C.; Hough, S. L.; Lai, J. Y. *J. Membr. Sci.* **2000**, *173*, 99-106.
- (11) Yang, J. M.; Lin, H. T.; Lai, W. C. *J. Membr. Sci.* **2002**, *208*, 105-117.
- (12) Sarkar, S.; Adhikari, B. *Polym. Degrad. Stabi.* **2001**, *73*, 169-175.
- (13) Swanson, J. P.; Rozvadovsky, S.; Seppala, J. E.; Mackay M. E.; Jensen, R. E.; Costanzo, P. J. *Macromolecules*, **2010**, *43*, 6135-6141.
- (14) Wang, Q.; Zhang, X.; Wang, L.; Mi, Z. *Ind. Eng. Chem. Res.* **2009**, *48*, 1364-1371.
- (15) Manjari, R.; Joseph, V. C.; Pandureng, P.; Sriram, T. *J. Appl. Polym. Sci.* **1993**, *48*, 271-278.
- (16) Huang, S. L.; Chang, P.; Tsai, M.; Chang, H. *Sep. Purif. Technol.* **2007**, *56*, 63-70.
- (17) Hocaoglu, O.; Ozbelge, T.; Fikret, P.; Ozkar, S. *J. Appl. Polym. Sci.* **2001**, *79*, 959-964.
- (18) Tien, Y. I.; Wei, K. H. *Polymer* **2001**, *42*, 3213-3221.
- (19) Gupta, T.; Debasish, D.; Adhikari, B. *Polym Int.* **2003**, *52*, 938-948.
- (20) Huang, S.; Lai, J. *J. Appl. Polym. Sci.* **1997**, *64*, 1235-1245.
- (21) Huang, S.; Lai, J-Y. *Eur. Polym. J.* **1997**, *33*, 1563-1567.
- (22) Sekkar, V.; Bhagawan, S. S.; Prabhakaran, N.; Rao, M. R.; Ninan, K. N. *Polymer* **2000**, *41*, 6773-6786.
- (23) Alibeik, S.; Rizkalla, A. S.; Mequanint, K. *Eur. Polym. J.* **2007**, *43*, 1415-1427.
- (24) Zawadzki, S. F.; Akcelrud, L. *Polym. Int.* **1997**, *42*, 422-428.
- (25) Bohn, M. A.; Elsner, P. *Propellants, Explosives, Pyrotechnics.* **1999**, *24*, 199-205.
- (26) Mothe, C. G.; De, A. C. R. *Thermochim. Acta.* **2000**, *357*, 321-325.

- (27) Luciene, D.V.; Thiago, C.; Milton, F. D.; Marta F. K. T.; Luis, C. R. *Mater.Res.* **2011**, *14*, 372-375.
- (28) Nagle, D. J.; Celina, M.; Rintoul, L.; Fredericks, P. M. *Polym. Degrd. Stabi.* **2007**, *92*, 1446-1454.
- (29) Mowery, D. M.; Assink, R. A.; *Polymer*, **2005**, *46*, 10919-10924.
- (30) Vieira, E. F. S.; Cestari, A. R.; Zawadzki, S. F.; *J. Therm. Anal. Calori.* **2004**, *75*, 501-506.
- (31) Harris, D. J.; Assink, R. A.; Celina, M. *Macromolecules*, **2001**, *34*, 6695-6700.
- (32) Sekkar, V.; Gopalakrishnan, S.; Devi, K. A. *Eur. Polym. J.* **2003**, *39*, 1281-1290.
- (33) Sarkar, S.; Adhikari, B. *Eur. Polym. J.* **2001**, *37*, 1391-1401.
- (34) Santerre, J. P.; Brash, J. L. *Ind. Eng. Chem. Res.* **1997**, *36*, 1352-1359.
- (35) Chung, H.; Washburn, N. R. *ACS Appl. Mater. Interfaces* **2012**, *4*, 2840-2846.
- (36) Bui, V. T.; Ahad, E.; Rheume, D.; Whitehead, R. *Ind. Eng. Chem. Res.* **1997**, *36*, 2219-2224.
- (37) Zhang, Q.; Hu, J.; Gong, S. *J. Appl. Polym. Sci.* **2011**, *122*, 3064-3070.
- (38) Amrollahi, M.; Sadeghi, G. M. M.; Kashcooli, Y. *Materials and Design* 2011, *32*, 3933-3941.
- (39) Shankar, R. M.; Roy, T. K.; Jana, T. *J. Appl. Polym. Sci.* **2009**, *114*, 732-741.
- (40) Shankar, R. M.; Roy, T. K.; Jana, T. *Bull. Mater. Sci.* **2011**, *34*, 745-754.
- (41) Lu, Y.; Larock, R. C. *Biomacromolecules*. **2008**, *9*, 3332-3340.
- (42) Gooch, J. W.; Dong, H.; Schork, F. J. *J. Appl. Polym. Sci.* **2000**, *76*, 105-114.
- (43) Rubinstein, M.; Colby, R. H. In *Polymer Physics*; Oxford University Press: New York, 2003.
- (44) Chen, T. K.; Chui, J. Y.; Shieh, T. S. *Macromolecules* **1997**, *30*, 5068-5074.

CHAPTER 4

Hydrophobic, water dispersible polyurethane: Role of polybutadiene diol structure



4.1. INTRODUCTION

Demands for coating and adhesives materials, which are free of any kind of organic solvents, are rapidly growing due to environmental considerations owing to the fact that these materials can be formulated from aqueous medium and method of preparation is considered a green approach.¹⁻⁵ Polyurethane (PU)-based coating materials are often used owing to their several significant advantages compared to other polymeric coating materials.^{6,7} Therefore, there is a great deal of challenges and interests involved in the development of water-dispersible PU (WDPU) coating materials as a next generation green coating materials. The most important and simple advantage of WDPUs that one can think of is that even their film can be prepared readily by simply evaporating water at ambient temperature. Among other advantages, the most significant one is that the viscosity of dispersed particles does not strongly dependent upon the molecular weight of PU and hence processing a formulation is rather straightforward.^{8,9} And one more advantage compared to solvent-borne PU is that WDPU is generally less expensive since no cost is involved because of the solvent. Because of these numerous advantages, aqueous PU dispersion, or WDPU, is an important class of materials and hence can be used in various fields such as textile, coatings, fiber sizings, and manufacture of adhesives.¹⁰⁻¹⁵ As a result, there is a huge scope of developing and studying the new class of WDPUs.

Aqueous PUs are commonly prepared with incorporation of ionic groups into the polymer backbone. The WDPUs are mostly ionic because usually it contains -COOH groups, which are incorporated by coreacting with appropriate monomer into the polymer backbone, and these -COOH groups can be neutralized with triethylamine. This can result in a polymeric backbone, which forms a colloidal system in aqueous medium.

Hydroxyl-terminated polybutadiene (HTPB) is a diol oligomeric viscous liquid, which finds many applications, especially as a binder in solid rocket propellant.¹⁶⁻¹⁸ There are several methods, published by us and other groups, that modify the HTPB backbone with varieties of functionality to enhance the physical properties like energy output¹⁹⁻²¹ and thermal and mechanical strength of resulting PU obtained from HTPB and diisocyanate polymerization. Recently, we demonstrated that attachment of dinitrobenzene (DNB) to the terminal position of HTPB, called HTPB-DNB, has improved the physical properties, especially tensile properties, significantly owing to the formation of supra molecular hydrogen bonding network fibrillar structure.²²

Having obtained good properties of HTPB by modifying the backbone, we plan to utilize this new diol (called HTPB-DNB) to make PU-based materials for coating applications with an aim to

achieve a thermal and mechanically strong coating. Also the presence of extra -NO₂ functional groups and phenyl rings might help us in improving the hydrophobic characteristics of the final resulting PU materials. Therefore, we prepared water dispersible PU by using HTPB and HTPB-DNB as the diol with an aim to achieve hydrophobic, water-dispersible, and mechanically strong coating material.

We have also studied the effect of a hard segment of synthesized PUs, which is controlled by the diol content in the chain, on the physical properties of WDPU coating material. Several characterizations, for example, transmission electron microscopy (TEM), Fourier transform infrared (FT-IR) spectroscopy, thermogravimetric analysis (TGA), dynamic mechanical analysis (DMA), tensile strength, contact angle, and atomic force microscopy (AFM), are carried out to prove the claim we make in this article.

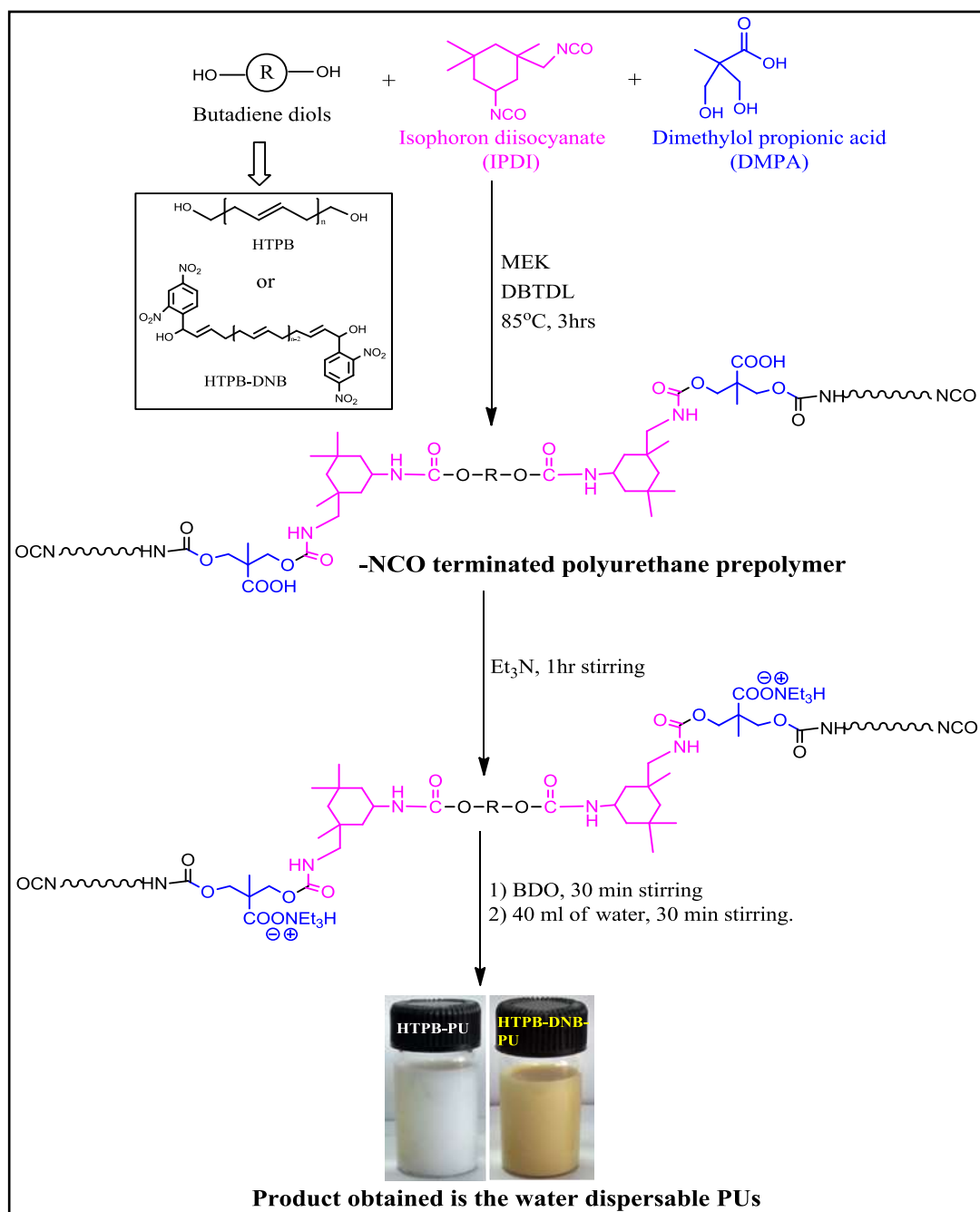
4.2. SYNTHESIS

4.2.1. Preparation of Water Dispersible Polyurethanes

The reaction protocol for the synthesis of WDPU is shown in Scheme 4.1 and the detailed reaction recipes (molar composition of the reactants) are presented in Table 4.1. The butadiene diol (HTPB or HTPB-DNB) and DMPA were taken into a three-neck flask, which is equipped with a mechanical stirrer, nitrogen inlet, condenser, and thermometer. The mixture was stirred in a constant temperature oil bath at 85° C. IPDI and a catalytic amount (20 µL) of DBTDL were added into the reaction mixture after 20 min. of stirring. The reaction was continued by stirring at 85° C in the presence of N₂ atmosphere for another 3 h. With progress of reaction, a viscous liquid was formed, indicating the formation of polymer. We added 3-5 mL of MEK at about 2 h during the reaction progress so as to prevent the viscosity development due to formation of polymer. After 3 h of reaction, -NCO-terminated polyurethane (PU) prepolymer was formed which was confirmed by the presence of urethane linkage and -NCO peak frequencies in the IR spectra of the prepolymer sample. The whole reaction mixture containing -NCO-terminated PU prepolymer was cooled down to room temperature. Then TEA (1.2 equiv of DMPA) was added to the prepolymer to neutralize the carboxylic acid group present in the -NCO terminated PU prepolymer because of DMPA and 1 h stirring was continued. These prepolymer further chain extended by adding a required quantity of butane diol (BDO) (see the Table 4.1), and stirring was continued for about 30 min or until the complete disappearance of -NCO peak frequency at 2270 cm⁻¹ in the IR spectra was observed. The resultant product was dispersed in about 40 mL of water with vigorous stirring, which resulted in the milky water dispersion of PUs. The measured solid content is about 15% (w/v). The molar composition and hence the hard segment (HS)

variation are tabulated in the Table 4.1. The HS was varied 28-40% in both cases and achieved by altering the relative composition of the monomers as shown in Table 4.1.

Scheme 4.1. Synthesis of Water-Dispersible polyurethanes^a



^a PUs obtained from HTPB are white in color and PUs obtained from HTPB-DNB are light yellow in color.

Table 4.1. Reaction mixture compositions for the synthesis of WDPU^a

Entry ^b	Mols of -NCO (IPDI)	Mols of -OH ^c (HTPB)	Mols of -OH ^d (HTPB-DNB)	Mols of -OH ^e (DMPA)	Mols of -OH ^f (BDO)	Hard segment (Wt%) ^g
HTPB-PU30	0.0320	0.0184	—	0.0120	0.0016	29.52
HTPB-PU32	0.0358	0.0184	—	0.0144	0.0032	32.40
HTPB-PU35	0.0400	0.0184	—	0.0160	0.0056	35.31
HTPB-PU38	0.0440	0.0184	—	0.0170	0.008	37.75
HTPB-PU41	0.0460	0.0184	—	0.0190	0.010	40.76
HTPB-DNB-PU29	0.0320	—	0.0184	0.0120	0.0016	28.44
HTPB-DNB-PU32	0.0358	—	0.0184	0.0144	0.0032	31.86
HTPB-DNB-PU35	0.0400	—	0.0184	0.0160	0.0056	34.59
HTPB-DNB-PU37	0.0440	—	0.0184	0.0170	0.008	37.06
HTPB-DNB-PU40	0.0460	—	0.0184	0.0190	0.010	40.11

^a Hard segment contents were varied from ~28% to 41% by adjusting the monomers composition. The molar ratio of -NCO and -OH was kept constant at 1:1 in the case of all the compositions. ^b Samples are identified as XXX-PU-YY, where XXX is the type of diol (either HTPB or HTPBDNB and YY is calculated hard segment (wt%) content. ^c Hydroxyl mole ratio of HTPB calculated from hydroxyl value. ^d Hydroxyl mole ratio of HTPB-DNB calculated from hydroxyl value. ^e Hydroxyl mole ratio of DMPA. ^f Hydroxyl mole ratio of BDO. ^g Hard segment content (wt%) = $[(W_{IPDI} + W_{DMPA} + W_{BDO} + W_{TEA})]/[(W_{HTPB \text{ OR } HTPB-DNB} + W_{IPDI} + W_{DMPA} + W_{BDO} + W_{TEA})]$

4.2.2. Preparations of PU Films from Water-Dispersible PU (WDPU)

The WDPUs were poured into a glass plate and dried at room temperature for 24 h. After that, the glass plate with the sample was kept at 70° C inside an oven for 2 days. Then we obtained transparent, elastic films. The thicknesses of the film were about 150 μm. The films were stored in the desiccator for further characterization.

4.3. CHARECTERIZATION TECHNIQUES

All the information about the materials used in this study and the experimental methods, characterization techniques which include spectroscopic characterization by fourier transform infrared spectroscopy (FT-IR) and proton NMR, transmission electron microscopy (TEM), particle size

analyser (PSA), thermogravimetric analysis (TGA), differential scanning calorimetry (DSC), dynamic mechanical analysis (DMA), contact angle measurement (CA), atomic force microscopy (AFM) and universal testing measurement (UTM) analysis studies for all the polyurethane polymer samples are discussed in the Chapter 2.

4.4. RESULTS AND DISCUSSION

4.4.1. Synthesis of Water Dispersible PUs

Although there are many reports on water-dispersible PUs, until now there are no reports on modified HTPB-based water-dispersed PUs. We have prepared a series of WDPU using HTPB and HTPB-DNB as diols, IPDI as a diisocyanate, and BDO as a chain extender. The HTPB-DNB was obtained from HTPB by forming a chemical attachment of DNB molecules at the terminal position by following a procedure as described by us previously.¹⁹ Dimethylol propionic acid (DMPA) has also been used as a diol source in the PU synthesis (Scheme 4.1). DMPA is a diol with carboxylic acid functionality and hence it creates ionic portion (carboxylic) into the PU chain, which might help in getting the water solubility of the PU. The synthesized series of polyurethanes have various hard segment contents, which have been achieved by altering the weight ratio of DMPA, BDO, and IPDI (Table 4.1). The calculation of hard segment values is shown in Table 4.1 and for all the cases, we maintained the -NCO/-OH ratio constant, which is equal to 1. Hard segment (HS) content is varied from 28% to 40% and we observed the formation of very good dispersions with long stability of dispersion in this HS range only. The moles of -OH functionality were calculated from the hydroxyl values of HTPB and HTPB-DNB. As can be seen from Scheme 4.1, we have used an extra diol source by using a reactant called DMPA, which helped us to prepare water-dispersible PUs owing to the presence of ionic (carboxylic) group in the DMPA. In this water-dispersed PU synthesis, DMPA incorporates -COOH functionality in the PU backbone and also reacts with the -NCO to form PUs. The -COOH groups are neutralized with triethylamine, the resulting polymer is in ionic form and as a result it is easily dispersed in water. To obtain stable water dispersed PU, a minimum amount of DMPA is required so that dispersed polymer can store for a longer time and therefore we have optimized the reaction composition as well. We have monitored the progress of the reaction by recording the IR spectra and observed the complete disappearance of -NCO peak at 2270 cm^{-1} , and only after did we add water to synthesized PU to obtain water dispersion of PU. The reaction scheme and the compositions are presented in Scheme 4.1 and Table 4.1, respectively. A good water

dispersion is obtained upon completion of reaction for all the compositions (Table 4.1) synthesized here as shown in Scheme 4.1

4.4.2. FT-IR Study

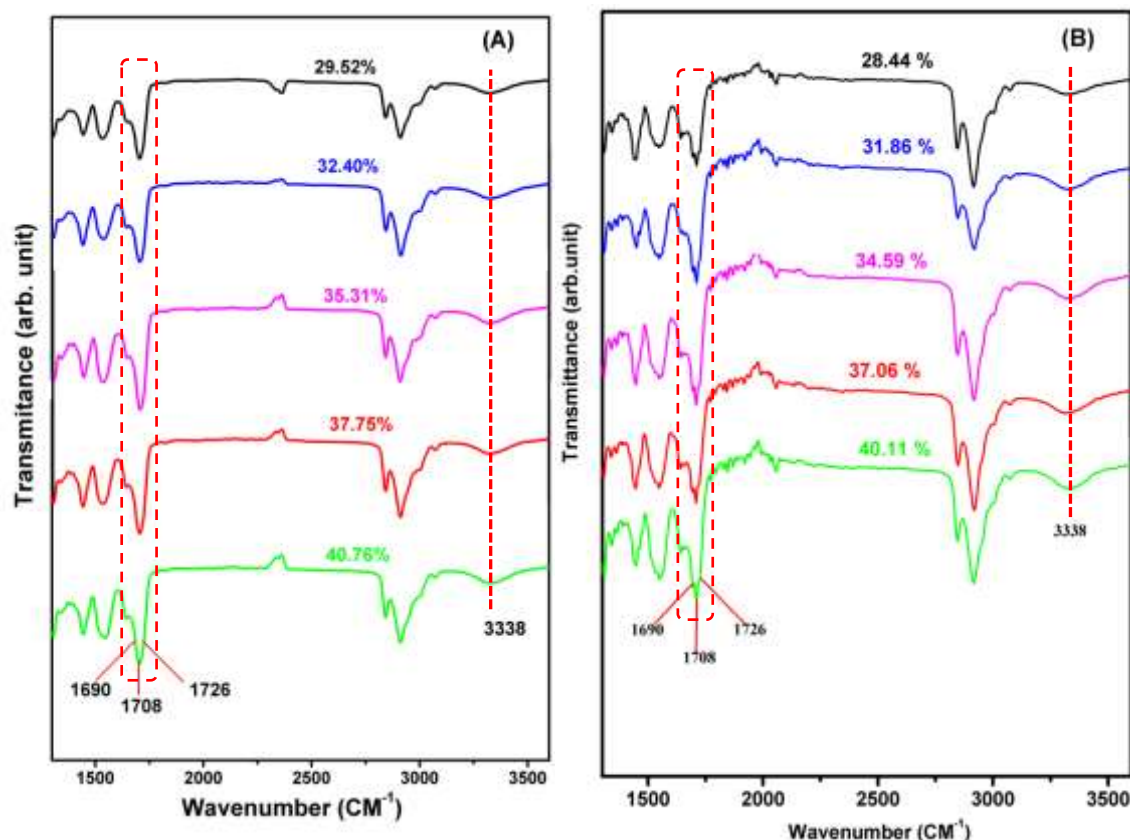


Figure 4.1. FT-IR spectra of (A) HTPB-PUs and (B) HTPB-DNB-PUs with different hard segment content as indicated in the figure.

FT-IR analysis was carried out to verify the progress of the reaction during the polymer synthesis and also to do the structural analysis of the resulting polymer. The absorption peak of the -NCO group at 2270 cm⁻¹ decreases during the reaction and completely disappeared after completion of the reaction. Only after this -NCO peak disappeared, water was added with vigorous stirring to obtain water-dispersed polyurethanes (WDPUs). The polyurethane structure is proved by noting the absorption band at around 3338 cm⁻¹ (-N-H stretching) as shown in Figure 4.1.

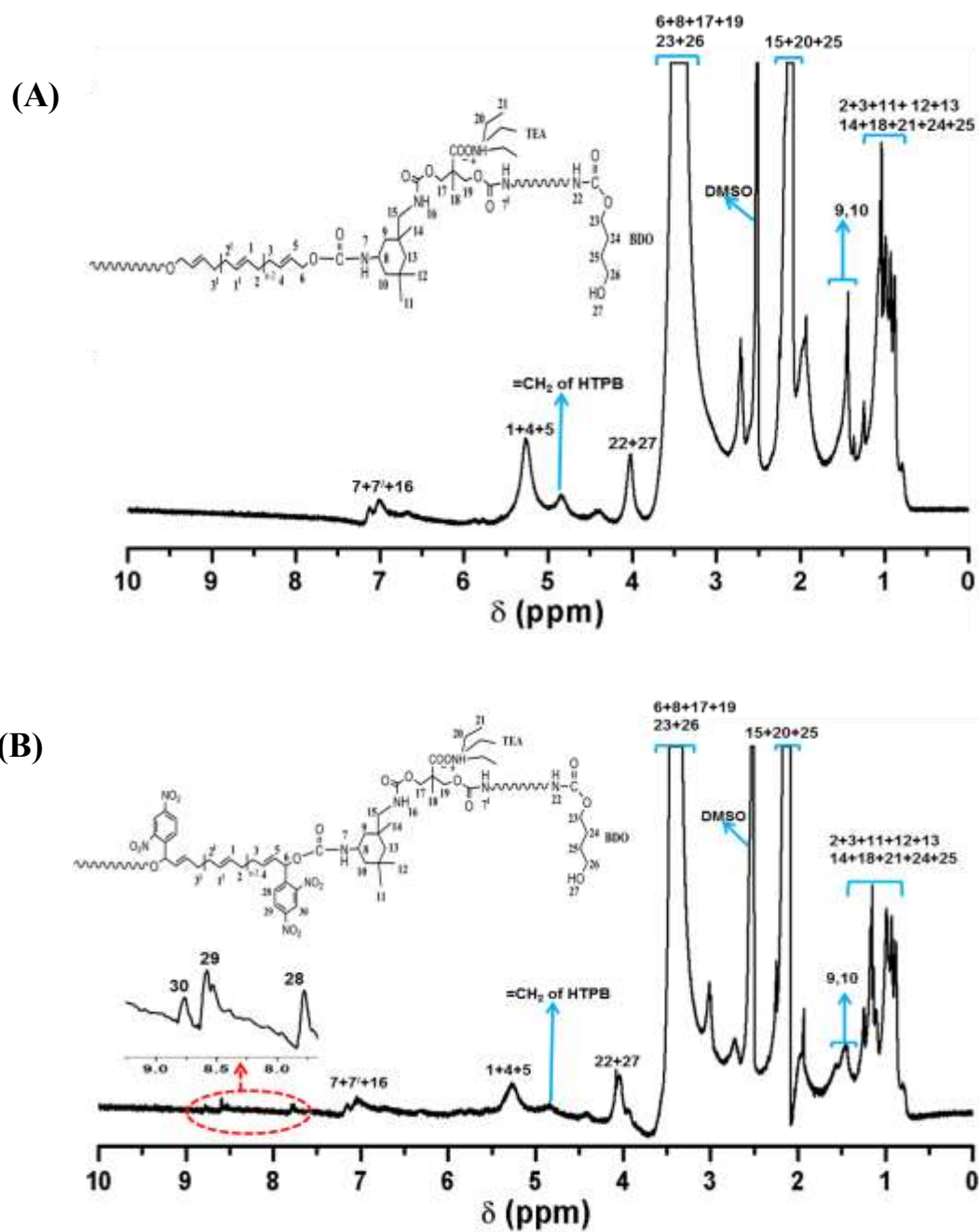


Figure 4.2. ^1H NMR spectra of water dispersible PUs (A) HTPB-PU and (B) HTPB-DNB-PU. $\text{DMSO-}d_6$ was used as a NMR solvent. The chemical structure of PUs and the peak assignments are shown in the figure.

This peak intensity increases with increasing hard segment, indicating the formation of more –CO-NH linkages. Three bands observed at around 1726, 1708, and 1690 cm^{-1} are the vibrating frequencies of the carbonyl region. The peak at 1726 was assigned to the free –C=O stretching, whereas the peak at 1708 cm^{-1} is due to hydrogen-bonded –C=O stretching. These peaks frequencies are consistent with earlier reports on water-dispersible polyurethanes synthesized from soybean oil, which was used as a soft segment.²³ A small absorption band at around 1690 cm^{-1} is due to the formation of urea linkages, which may be the reaction of some of the unreacted isocyanates with water while making water dispersion. The intensity of the bands attributed to free and hydrogen-bonded urethane carbonyls (1726 and 1708 cm^{-1}) increases with increasing hard segment content of PU because of the increasing formation of urethanes bonds.

Figure 4.2 shows the proton NMR spectra of WDPUs and the peak assignments. The chemical shifts obtained are matching very well with the expected structure. The presence of DNB moieties in the case of HTPB-DNB-PU is clearly visible in the spectra (inset of Figure 4.2 B) and hence confirms the structure of synthesized PUs.

4.4.3. Stability and Morphological Studies of Synthesized PU Dispersions

As described in the Experimental Section and Scheme 4.1, our current reaction conditions and methodology ensure the formation of PU with ionic structure into its backbone. Therefore, it is expected that this PU structure should yield homogeneous water dispersion when dispersed in aqueous medium. With this objective in mind, we have prepared water dispersions of all PU samples (both HTPB-PU and HTPB-DNB-PU) with about 15% (by weight) of polymers in water. Figure 4.3 shows the pictures of water dispersions of PU with various hard segment (HS) contents for both HTPB-PU and HTPB-DNB-PU after storing at different time intervals. As can be seen from the figure, the dispersions are highly stable for a very long time, even beyond 1 year. The light yellowish color of the HTPB-DNB-PU dispersion is due to the color of DNB functionalities in the modified PU backbone. We have also noticed that all the dispersions are very stable in a regular laboratory environment.

To see that our reaction conditions result in water dispersions as shown in Figure 4.3, we have carried out a TEM experiment and presented the TEM images in Figure 4.4. As can be seen from the figure, all the PU samples possess particle (nanoparticle) morphology, attributing to the formation of particles of PU which are dispersed in the aqueous medium. We have also measured the particle size using a light-scattering based particle size analyzer (PSA) and the results are shown in Figure 4.5. Table 4.2 lists the stability data of these water dispersible PUs (WDPUs) and compares the particle

size obtained from TEM study with PSA measurements. These data are in good agreement, except that in some cases the size obtained from the PSA measurement is slightly bigger than the TEM, owing to the fact that in the former, hydrodynamic radius is measured, whereas in the latter, the dried particles are imaged. The particle size of WDPU ranges from ~ 130 to 270 nm.







	HTPB-PU _s (%HS)			HTPB-DNB-PU _s (%HS)		
	29.52	35.31	40.76	28.44	34.59	40.11
Just prepared						
After 3months						
After 10months						

Figure 4.3. Photographs of water dispersible PUs of different hard segment contents at various storing time intervals.

In both cases (HTPB-PUs and HTPB-DNB-PUs), the particle size decreases with increasing HS ratio. Both TEM and PSA measurements display similar trends in the particle size variation with changing HS ratio. Although we could not ascertain the exact reason for this, the decreasing particle size with increasing HS may be due to the more rigid structure of higher HS containing PUs. Table 4.2 and Figure 4.5 data clearly show that the polydispersity of all the WDPU samples are very narrow and PDI decreases with increasing HS content. The control over the particle size of the water-dispersible PUs is very important since it plays a key role for particular applications. For example, dispersions of relatively larger particles are preferred in surface coatings for rapid drying, and smaller particle sizes are desirable when deep penetration of the dispersion into a substrate is essential.²⁴ HTPB-DNB-PUs shows slightly bigger particle size than HTPB-PUs may be due to steric factor arising from the terminal-functionalized DNB moiety. It is also noticed from TEM images that most of these particles are spherical in shape and result in very stable dispersion as shown in Figure 4.4.

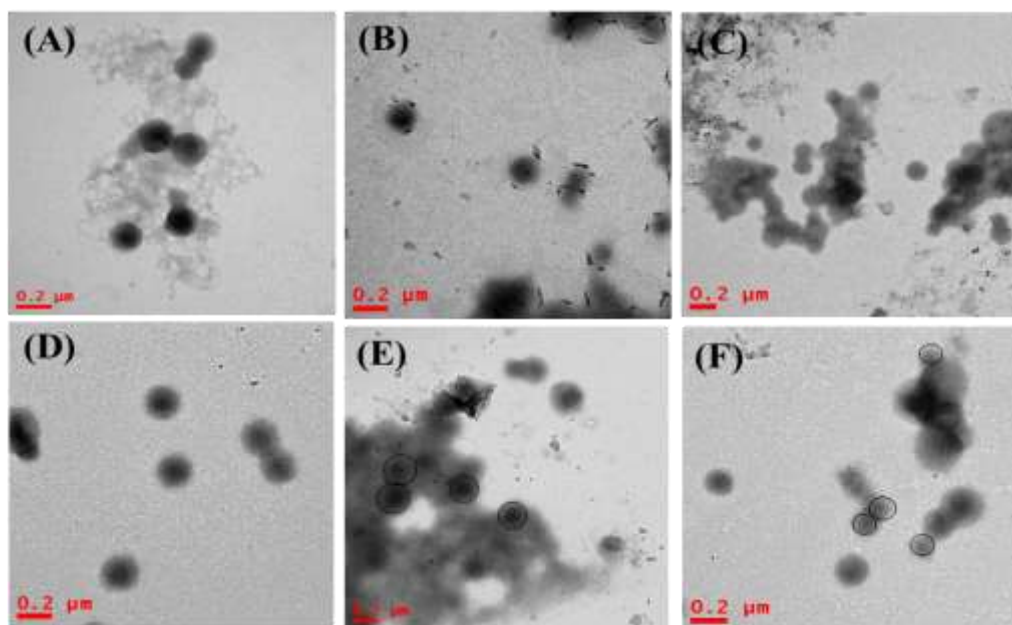


Figure 4.4. TEM images of all water dispersed PUs with varying hard segments ratio: HTPB-PUs (A-C); (A) 29.52%, (B) 35.31%, (C) 40.76% and HTPB-DNB-PUs (D-F); (D) 28.44%, (E) 34.59%, (F) 40.11%. Note that all the images have identical scale bar.

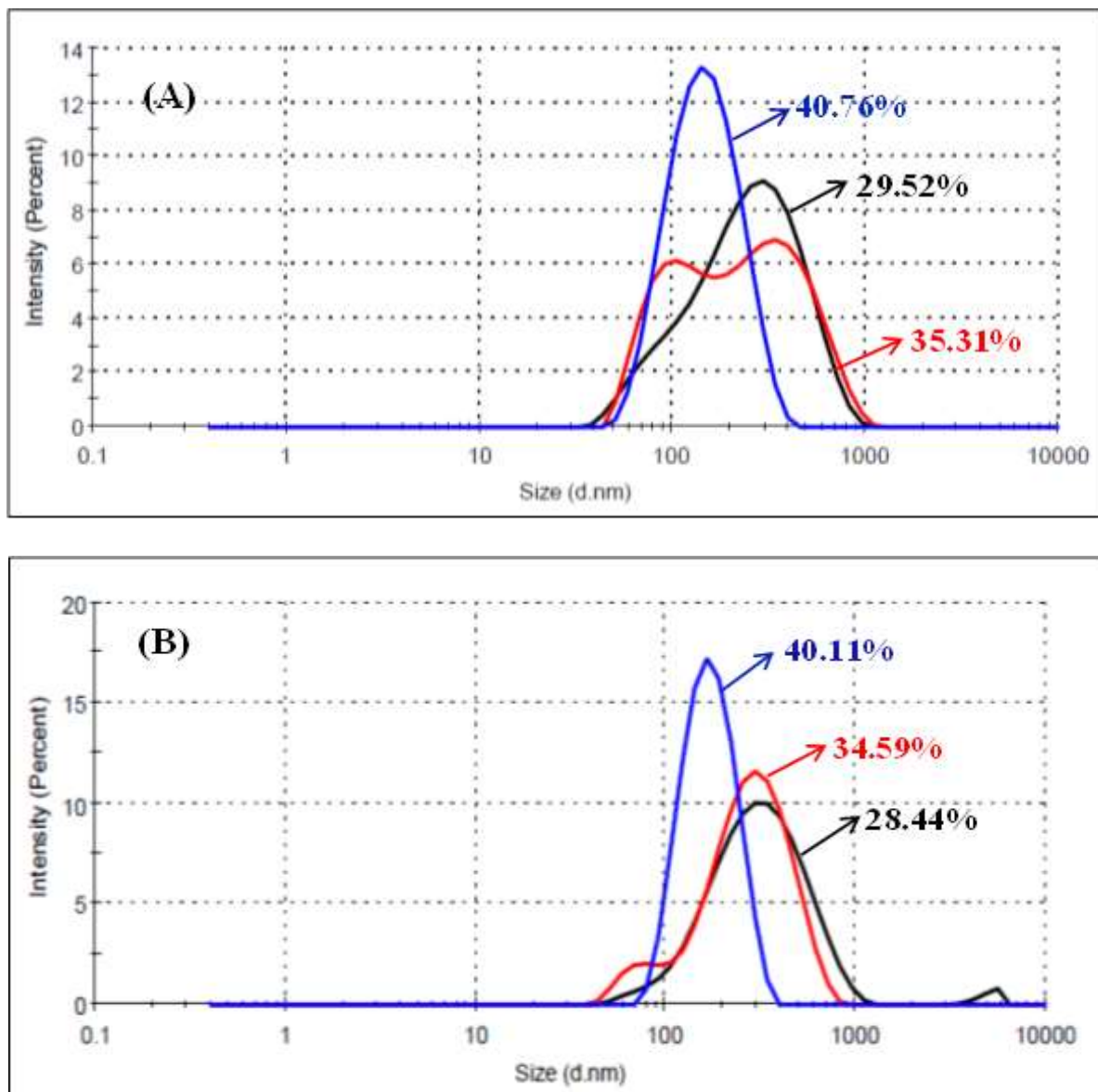


Figure 4.5. Particle size and the size distribution plots (obtained from Zetasizer measurements) of WDPU samples: (A) HTPB-PU and (B) HTPB-DNB-PU. The hard segment content of the samples is indicated in the figure.

Table 4.2. Particle size, stability of WDPUs samples obtained by using HTPB and HTPB-DNB diols

Entry	Hard Segment (wt %)	Stability (months)	Particle size ^a (nm)	PDI ^a	Particle size ^b (nm)
HTPB-PU30	29.52	>12	193	0.28	195
HTPB-PU35	35.31	>12	170	0.30	160
HTPB-PU41	40.76	>12	129	0.16	125
HTPB-DNB-PU29	28.44	>12	269	0.26	200
HTPB-DNB-PU35	34.59	>12	218	0.24	170
HTPB-DNB-PU40	40.11	>12	158	0.09	140

^a Particle size and PDI from Zetasizer measurement and ^b Particle size from TEM analysis

4.4.4. Preparation of Film from WDPUs and Their Characterizations

After confirming that our synthetic protocol of PUs produces water-dispersible PUs, we need to confirm that these PUs can produce stable films so that these WDPUs can be used as coating material. To make the film, we have cured the sample inside the oven at 70° C for 2 days. Freestanding elastic films were obtained from all the WDPUs samples and these films were subjected to several characterizations such as TGA, DMA, tensile properties, contact angle measurement, and AFM studies. The next section will evaluate these results with an objective to find out the various properties of WDPUs films and their suitability as coating materials.

4.4.5. Thermogravimetric Analysis

The TGA curves of all the cured PU films obtained from HTPB and HTPB-DNB with different hard segment contents are shown in Figure 4.6. Thermal stability of the PUs primarily depends upon the polyols and isocyanate structures. Generally, water-dispersed PUs show less thermal stability because of the presence of labile urethane and urea linkages of PU polymers.^{25,26} Figure 4.6 clearly shows that the PUs undergo thermal degradation in more than one stage. The thermal degradation of PU films started at around 230-240° C and were followed by another weight loss at around 350-400° C. These degradations observed at different temperature ranges can be attributed to the decomposition of the labile urethane urea bonds. Also it is important to note that with increasing hard segment content (inset of Figure 4.6), thermal degradation increases because of increasing number of urethane urea bonds. Table 4.3 data compares the thermal degradation between the HTPB-PUs and HTPB-DNB-PUs. It is evident from Table 4.3 data that thermal stabilities of

HTPB-DNB-PUs are slightly higher than HTPB-PUs irrespective of their hard segment content and this may be due to the presence of extra cross-linking owing to hydrogen-bonded supramolecular assembly in the case of HTPB-DNB-PUs.

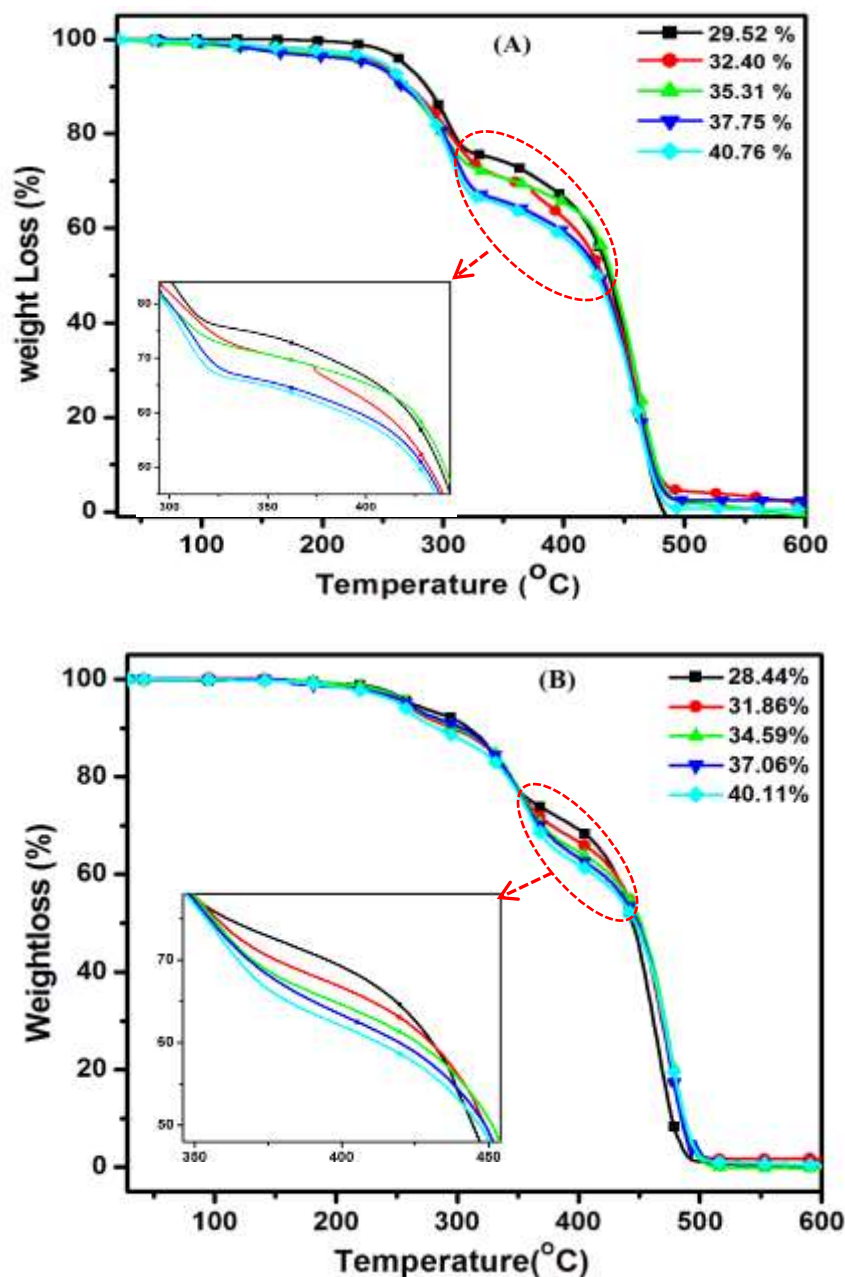


Figure 4.6. TGA plots of (A) HTPB-PUs and (B) HTPB-DNB-PUs after curing the water dispersible PUs at 70°C for two days. Inset: Magnified portion of the TGA plots to show the changes in thermal stability with increasing hard segment contents of PUs.

Table 4.3. Comparison of thermal stability of films obtained from WDPUs of HTPB-PUs and HTPB-DNB-PUs.

Entry	HS (%)	T_{10}^a	T_{40}^b	T_{max}^c
HTPB-PUs	29.52	285.67	421.88	479.81
	40.76	270.71	385.90	485.78
HTPB-DNB-PUs	28.44	306.63	430.86	493.27
	40.11	284.18	409.91	505.24

^aTemperature at which 10% weight loss occurs, ^bTemperature at which 40% weight loss occurs and

^cTemperature at which maximum weight loss occurs

4.4.6. Tensile Properties of PU

Stress-strain behaviours of all the water-dispersed PUs obtained from two (HTPB and HTPBDNB) different diols are shown in Figure 4.7. Table 4.4 lists the tensile strength (σ_b) and elongation at break (ϵ_b) obtained from stress-strain plots of PUs (Figure 4.7) and used for estimation of the mechanical strength of the resulting PUs. We have also determined the toughness and young modulus (E) of PU samples from Figure 4.7 plots and included in Table 4.4. The toughness values are calculated by integrating the area under stress-strain plot. Young modulus (E) values are calculated from the slope of the linear portion of the stress-strain plot where Hooks law is maintained. Figure 4.7 (C and D) and Table 4.4 data clearly demonstrated that HTPB-DNB-PUs have higher tensile properties (both yield stress and yield strain) than HTPB-PUs. It is also to be noted that HS content significantly influences the tensile properties. Yield stress increases with increasing HS content whereas yield strain decreases with increasing HS in both types of PUs as observed in Figure 4.7 (A and B). The toughness and Young modulus obtained from stress-strain profile also greatly influenced by the choice of types of diol and HS content. The reasons behind such tensile properties have been explained by us in a recent article based on our observation in which we demonstrated that in the case of HTPB-DNB-PUs, extra supramolecular hydrogen bonding between the $-\text{NO}_2$ of terminal-functionalized DNB moiety and urethane linkage of $-\text{N}-\text{H}$ enhances the amount of cross-linking in the chains which in turn changes the morphology and crystalline nature of PUs, allowing more interactions between the hard and soft segment of PU. As a result of these, there is a significant enhancement in the tensile properties of HTPB-DNB-PUs compared to HTPB-PUs.²²

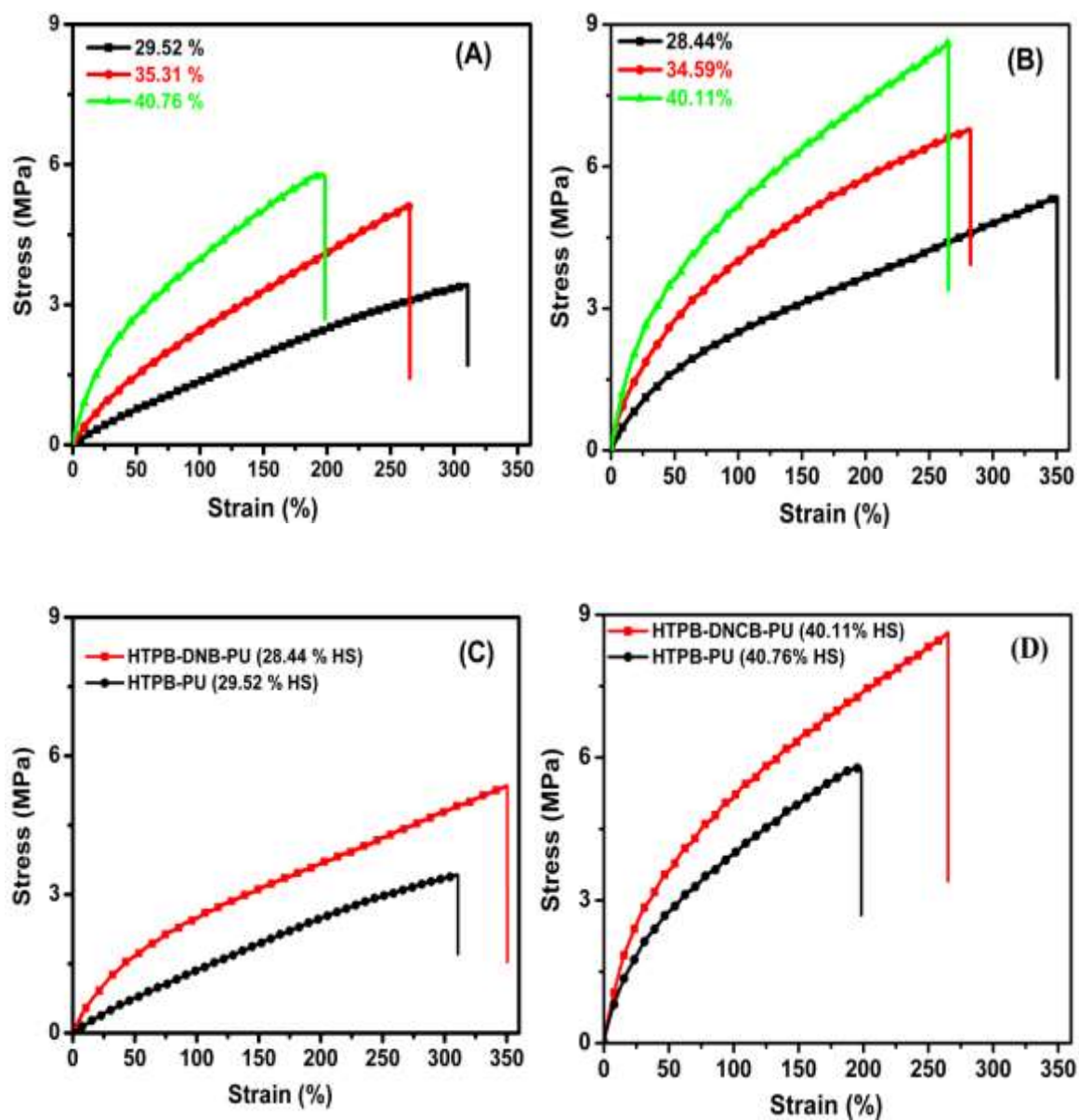


Figure 4.7. Tensile properties of WDPUs films with increasing HS content (A) HTPB-PU (B) HTPB-DNB-PU. Comparison of tensile properties of both types of PUs for similar HS content (C and D)

We believe a similar situation in this case and therefore we have calculated the effective cross-linking (N) of all the WDSPU films and listed them in Table 4.4. The N values of PUs are determined from the Young modulus (E) values (Table 4.4) which were calculated from Figure 4.7 (stress-strain plots). As per the rubber elasticity theory,^{22,27} the number of network stands for unit volume (N, effective cross-linking density) can be estimated from the relation $E = 3NK_B T$, where E is the Young modulus obtained from the stress-strain plot, K_B the Boltzmann constant, and T the absolute temperature in Kelvin. N values listed in Table 4.4 clearly indicate that effective cross-linking increases with increasing HS content and more in the case of HTPB-DNB-PUs because of the presence of $-NO_2$ functional groups in HTPB-DNB and hence the interaction as discussed before.

Table 4.4. Mechanical properties of films obtained after curing the water dispersible PUs.

Entry	Tensile strength (MPa)	Yield strain (%)	Toughness (MPa)	Young modulus (MPa)	Effective crosslinking ($N/M^3 \times 10^{22}$)	Storage modulus ^a (MPa)	T_g^b (°C)	T_g^c (°C)
HTPB-PU30	3.42	310	597.34	0.010	79.74	2997	-61	-78
HTPB-PU35	5.10	262	772.23	0.0155	123.60	3039	-60	-77
HTPB-PU41	5.77	198	469.44	0.0158	125.59	3309	-57	-76
HTPB-DNB-PU29	5.31	350	1144.34	0.0146	116.42	3285	-61	-79
HTPB-DNB-PU35	6.83	282	1356.05	0.0179	142.60	3392	-60	-78
HTPB-DNB-PU40	8.59	264	1492.05	0.0265	211.30	3562	-56	-77

^a measured at -100° C, ^b obtained from $\tan\delta$ vs. temperature plot of DMA study, ^c measured from DSC thermograms.

4.4.7. Thermal Transitions and Modulus of PUs

Figure 4.8 shows the storage modulus (E'), loss modulus (E''), and $\tan \delta$ plots as a function of temperature for all the films of HTPB-PUs and HTPB-DNB-PUs with different hard segment contents; the important data collected from these plots are summarized in Table 4.4.

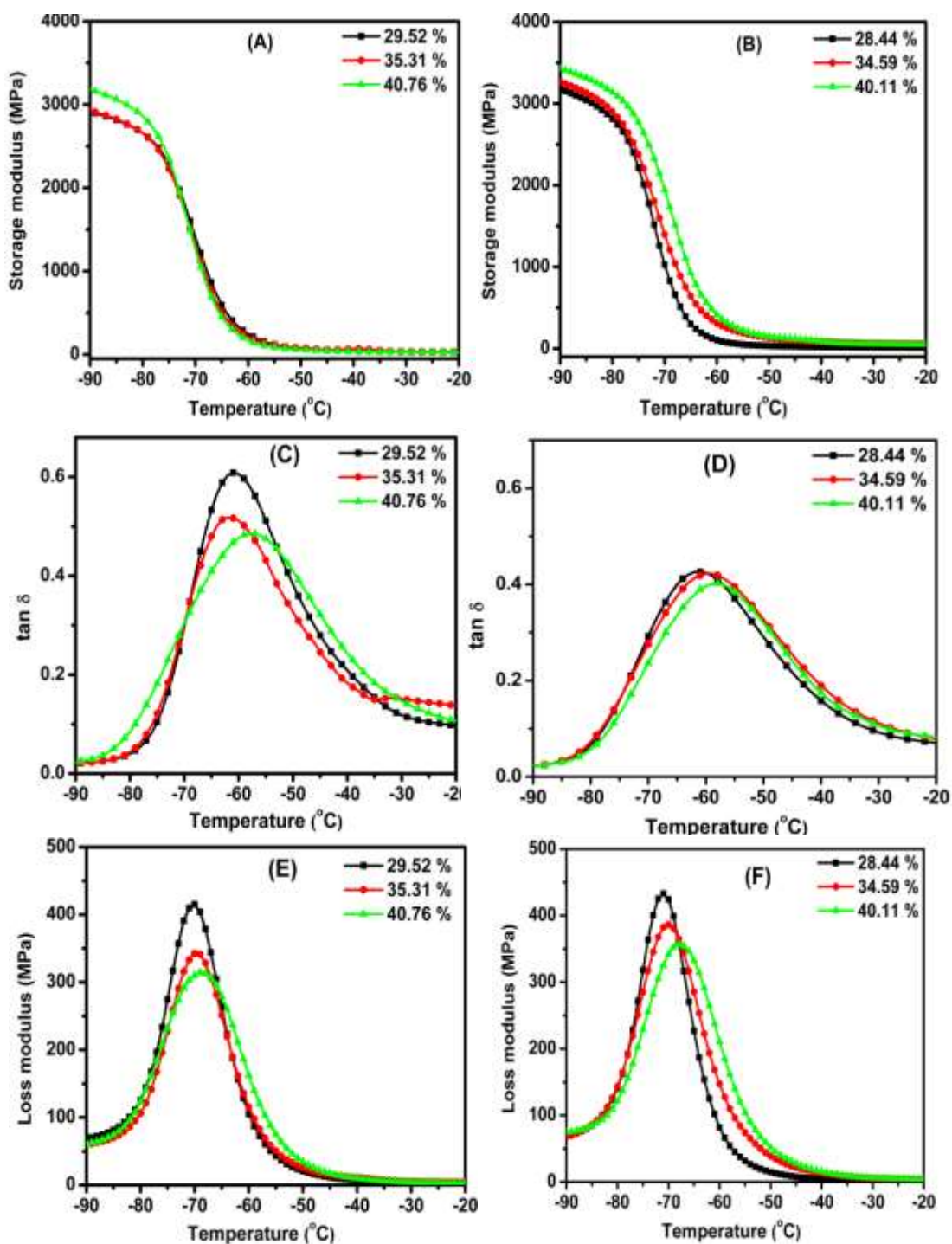


Figure 4.8. DMA plots of HTPB-PUs (A, C and E) and HTPB-DNB-PUs (B, D and F) of various hard segment contents as indicated in the figure

The results obtained from DMA studies Figure 4.8 (A and B) clearly showed that HTPB-DNB-PUs are mechanically stronger than HTPB-PUs and strength (modulus) increases with increasing HS contents. This observation is in agreement with the tensile measurement data as presented in an earlier section. From Figure 4.8 and Table 4.4 data, it is also clear that all the PUs films are elastic in nature with glass transition temperature (T_g) values around -60°C as listed in Table 4.4. The T_g value does not alter much with change in the HS content, there is a very small decrease in T_g values with increasing HS content in both sets of PUs. The little variation between the T_g values obtained from $\tan \delta$ vs temperature and E'' vs temperature plots is expected as it has been reported by several authors earlier. In summary, our DMA study proves that the obtained PU films are having high mechanical strength with subambient temperature T_g and thus resulting in rubbery PU films, which is one of the important characteristics a coating material should have.

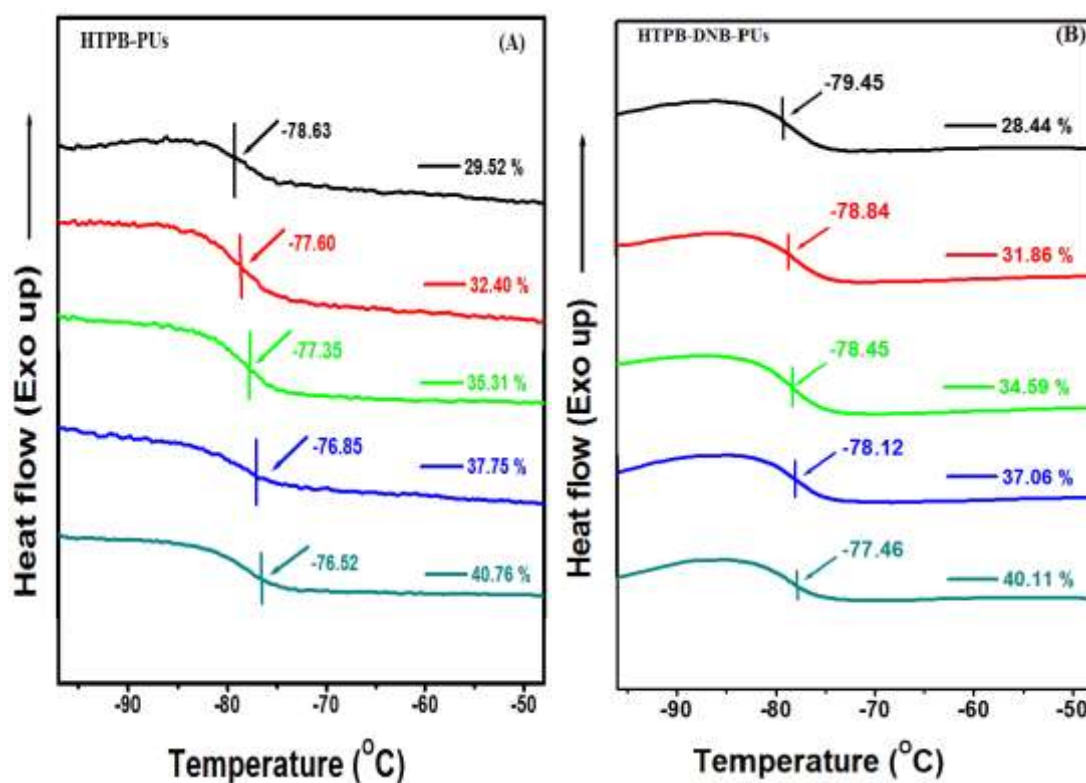


Figure 4.9. DSC plots of (A) HTPB-PUs and (B) HTPB-DNB-PUs of variable HS contents as indicates in the figure.

To reconfirm the T_g values and rubbery nature of our PU films, we also carried out differential scanning calorimetry experiment to measure the T_g values and the results are presented in Figure 4.9 and the data listed in Table 4.4. The results clearly indicate that T_g is in the subambient range at around -70°C , suggesting the elastic rubbery nature of our PU films and also the results tallied with the DMA results discussed in the previous section. The small difference (around 10°C) in T_g values between the DSC and DMA is because of the difference in measurement techniques. It is also noted that T_g values of HTPB-DNB-PUs are a little lower than HTPB-PUs (obtained both in DMA and DSC results) is because of the extra interaction between the $-\text{NO}_2$ group and urethane $-\text{N}-\text{H}$ group in the case of HTPB-DNB-PUs. Although there is not much significant variation in T_g values with increasing HS content, there is a definite trend in decreasing T_g with increasing HS content.

4.4.8. Surface Hydrophobicity of PU Films

In an earlier section, we proved that the PU films obtained from WDPUs of HTPB and HTPB-DNB upon curing display very good thermal, mechanical, and elastic properties. Therefore, we can think of using these WDPUs as coating material since these dispersions form good films readily and these films exhibit required the properties to qualify as a coating material. However, it would also be interesting and useful if these films of WDPUs have hydrophobic character. To determine their hydrophobicity, we have measured the surface water contact angle of all PU films and the results are shown in Figure 4.10 and data tabulated in Table 4.5.

Wettability is a fundamental property of the solid surface, which is governed by both surface energy and the geometrical arrangement or microstructure of the surface and this can be determined by measuring water contact angle.^{28–32} Wettability is the surface property of the films and this is used for measuring the hydrophobicity of the film surface. We measured the contact angle for all the WDPU film samples using distilled water. The results shown in Figure 4.10 and Table 4.5 clearly indicate that the contact angle increases with increasing hard segment content of PUs in both (HTPB and HTPB-DNB) cases. Contact angle crosses 90° in the case of higher HS sample, suggesting reasonably high hydrophobic surface in these samples. Even lower HS content samples have values very close to 90° , resulting in the hydrophobic nature of the resulting PU films of WDPUs for both HTPB and HTPB-DNB cases. Also it must be noted that contact angle values of all the HTPB-DNB-PU films are slightly higher than those of the corresponding HTPB-PU films (Table 4.5) and this may be due to morphological (microstructural) differences between these two groups of samples arising because of extra hydrogen bonding interactions in the case of HTPB-DNB-PU samples as described earlier.²²

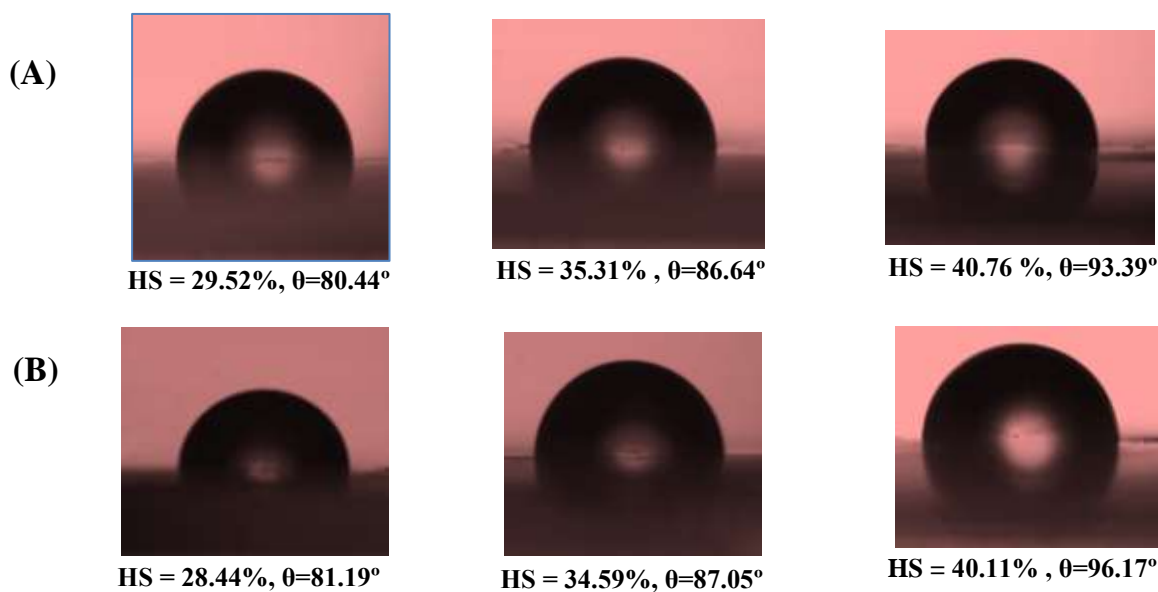


Figure 4.10. Images of water contact angles of various HS content PUs: (A) HTPB-PUs (B) HTPB-DNB-PUs

Table 4.5. Contact angles and surface roughness of PU films obtained by curing WDPUs of HTPB and HTPB-DNB.

Entry	Hard Segment (wt %)	Contact angle (degree)	Roughness (R_q) (nm)
HTPB-PU30	29.52	80.44	5.50
HTPB-PU35	35.31	86.64	9.63
HTPB-PU41	40.76	93.39	14.74
HTPB-DNB-PU29	28.44	81.19	4.88
HTPB-DNB-PU35	34.59	87.05	7.74
HTPB-DNB-PU40	40.11	96.17	15.48

To understand the origin of the hydrophobic nature of these PU films, we checked the films surface structure by scanning in AFM and the surface topography (along with 3D view) are shown in Figure 4.11. The surface roughness values are measured and listed in Table 4.5. Figure 4.11 topographic images and measured roughness (Table 4.5) clearly indicate that, with increasing HS content of PU backbone, the film roughness increases, which is probably the reason for increasing contact angle with increasing, resulting in hydrophobic surfaces.^{33–36} It should be noted that the roughness values differ slightly from HTPB-PUs to HTPB-DNB-PUs which may be the reason behind the variations of their contact angles.

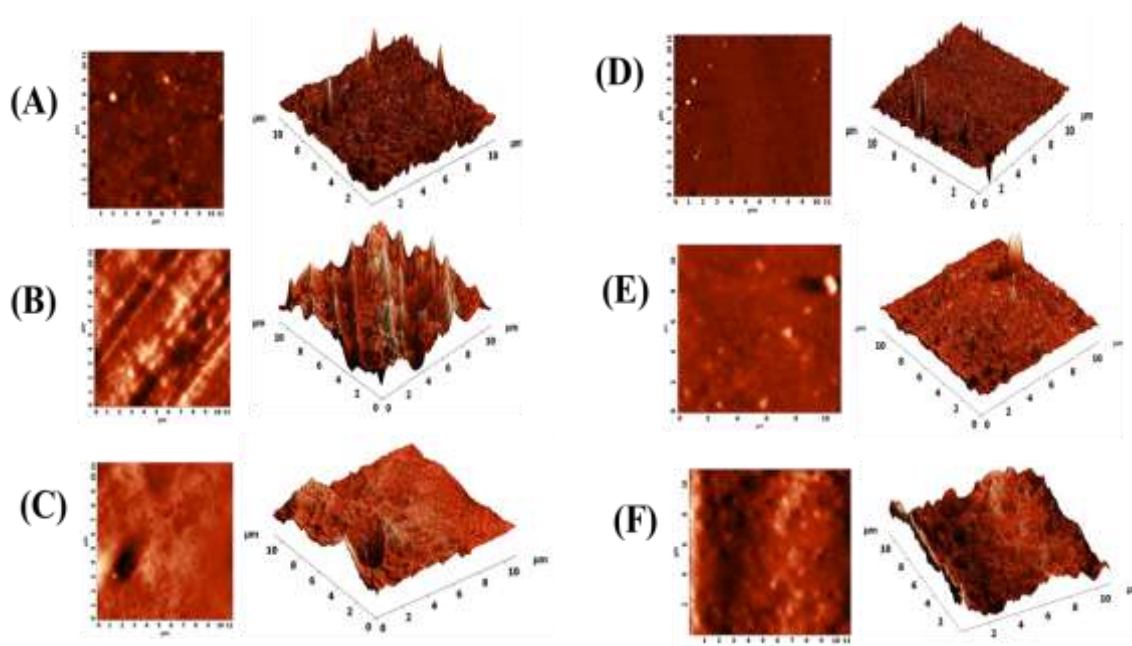


Figure 4.11. AFM images of various hard segment content PU films surface: HTPB-PUs [(A) HS=29.52%, (B) HS=35.31%, (C) HS=40.76%] and HTPB-DNB-PUs [(D) HS=28.44%, (E) HS=34.59%, (F) HS=40.11%]. 3D views of all the AFM images are also shown in the right side of each image.

4.5. CONCLUSION

We have developed a novel method for the synthesis of water dispersible PUs from butadiene diols with an objective for their use in coating. Synthesized WDPUs have been characterized by checking storage stability and morphological features, and these characterizations suggested the long-term stability and nanoparticle morphology of the WDPUs. The films obtained from these WDPUs showed very high thermal stability, mechanical stability and elastic behaviour. We have varied the hard segment contents in the PU backbone and studied the effect of hard segments on the properties, and it has been discovered that hard segment influences all of the above measured properties to a great extent; for example, higher hard segment resulted in a hydrophobic surface which has a contact angle $>90^\circ$. The results obtained in this study suggested that the water dispersible PUs synthesized in this study can be used as hydrophobic coating material. In addition, we also compared all the above mentioned physical properties in regard to the diol structure and found that the terminal-modified HTPB with a hydrogen-bonding functional group displayed better properties compared to unmodified HTPB.

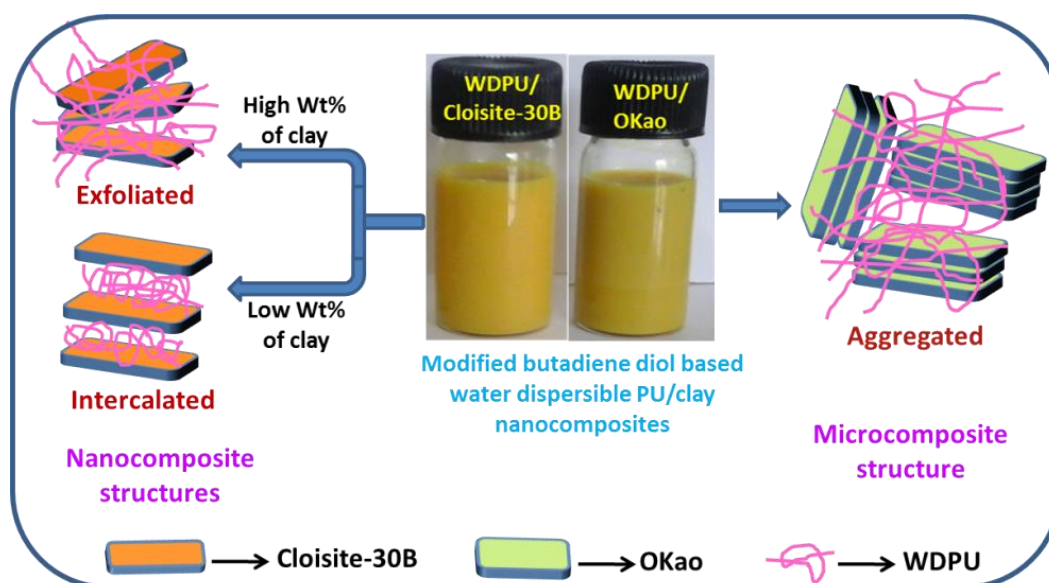
4.6 REFERENCES

- (1) Coutinho, F. M. B.; Delpech, M. C.; Alves, L. S. *J. Appl. Polym. Sci.* **2001**, 80, 566.
- (2) Kim, B. K.; Yang, J. S.; Yoo, S. M.; Lee, J. S. *Colloid Polym. Sci.* **2003**, 281, 461.
- (3) Wen, T. C.; Wu, M. S. *Macromolecules* **1999**, 32, 2712.
- (4) Kim, B. S.; Kim, B. K. *J. Appl. Polym. Sci.* **2005**, 97, 1961.
- (5) Yang, C. H.; Li, Y. J.; Wen, T. C. *Ind. Eng. Chem. Res.* **1997**, 36, 1614.
- (6) Chattopadhyay, D. K.; Sreedhar, B.; Raju, K. V. S. N. *Ind. Eng. Chem. Res.* **2005**, 44, 1772.
- (7) Schutzius, T. S.; Bayer, I. S.; Qin, J.; Waldroup, D.; Megaridis, C. M. *ACS Appl. Mater. Interfaces*, **2013**, 5, 13419.
- (8) Sugano, S.; Chinwanitcharoen, C.; Kanoh, S.; Yamada, T.; Hayashi, S.; Tada, K. *Macromol. Symp.* **2006**, 239, 51.
- (9) Barrere, M.; Landfester, K. *Macromolecules* **2003**, 36, 5119.
- (10) Agirre, A.; Heras-Alarcon, C.; Wang, T.; Keddie, J. L.; Asua, J. M. *ACS Appl. Mater. Interfaces*, **2010**, 2, 443.
- (11) Delpech, M. C.; Coutinho, F. M.B. *Polymer Testing*, **2000**, 19, 939.
- (12) Kobayashi, S.; Song, J.; Craig Silvis, H.; Macosko, C. W.; Hillmyer, M. A. *Ind. Eng. Chem. Res.* **2011**, 50, 3274.
- (13) Romero, G.; Lopis, I. E.; Zhou, J.; Rojas, E.; Franco, A.; Espinel, C. S.; Fernandez, A. G.; Gao, C.; Donath, E.; Moya, S. E. *Biomacromolecules*, **2010**, 11, 2993.
- (14) Liu, Q.; Singh, A.; Liu, L. *Biomacromolecules*, **2013**, 14, 226.
- (15) Hyungu, I.; Roh, S. C.; Kim, C. K. *Ind. Eng. Chem. Res.* **2011**, 50, 7305.
- (16) Grythe, K. F.; Hansen, F. K.; Walderhaug, H. *J. Phys. Chem. B*, **2004**, 108, 12404.
- (17) Reshmi, S.; Arunan, E.; Nair, R. C. P. *Ind. Eng. Chem. Res.* **2014**, 53, 612.
- (18) Ganesh, K.; Sundarrajan, S.; Kishore, K. *Macromolecules*, **2000**, 33, 326.
- (19) Shankar, R. M.; Roy, T. K.; Jana, T. *J. Appl. Polym. Sci.* **2009**, 114, 732.
- (20) Shankar, R. M.; Saha, S.; Meera, K. S.; Jana, T. *Bull. Mater. Sci.* **2009**, 32, 507.
- (21) Sankar, R. M.; Roy, T. K.; Jana, T. *Bull. Mater. Sci.* **2011**, 34, 745.
- (22) Malkappa, K.; Jana, T. *Ind. Eng. Chem. Re.* **2013**, 52, 12887.
- (23) Lu, Y.; Larock, R. C. *Biomacromolecules*, **2008**, 9, 3332.
- (24) Park, H. S.; Chunga, I. D.; Hartwig, A.; Kim, B. K. *Colloids and Surfaces A: Physico chem. Eng. Aspects*, **2007**, 305, 126.
- (25) Lligadas, G.; Ronda, J. C.; Galia, M.; Cadiz, V. *Biomacromolecules*, **2007**, 8, 686.

- (26) Coutinho, F. M. B.; Delpech, M. C. *Polymer Degradation and Stability*, **2000**, 70, 49.
- (27) Chung, H.; Washburn, N. R. *ACS Appl. Mater. Interfaces*, **2012**, 4, 2840.
- (28) Wu, W.; Zhu, Q.; Qing, F.; Han, C. C. *Langmuir*, **2009**, 25, 17.
- (29) Makal, U.; Uslu, N.; Wynne, K. J. *Langmuir*, **2007**, 23, 209.
- (30) Brassard, J.; Sarkar, D. K.; Perron, J. *Appl. Sci.* **2012**, 2, 453.
- (31) Yang, S.; Wang, L.; Wang, C.; Chen, L.; Chen, S. *Langmuir*, **2010**, 23, 18454.
- (32) Zhang, X.; Shi, F.; Niu, J.; Jiang, Y.; Wang, Z. *J. Mater. Chem*, **2008**, 18, 621.
- (33) Feng, X.; Feng, L.; Jin, M.; Zhai, J.; Jiang, L.; Zhu, D. Reversible Super-hydrophobicity to Super-hydrophilicity Transition of Aligned ZnO Nanorod Films. *J. Am. Chem. Soc.* **2004**, 126, 62.
- (34) Kim, P.; Kreder, M. J.; Alvarenga, J.; Aizenberg, J. *Nano Lett*, **2013**, 13, 1793.
- (35) Otts, D. B.; Cueva-Parra, L. A.; Pandey, R. B.; Urban, M. W. *Langmuir*, **2005**, 21, 4034.
- (36) Deng, X.; Schellenberger, F.; Papadopoulos, P.; Vollmer, D.; Butt, H. *Langmuir*, **2013**, 29, 7847.

CHAPTER 5

Functionalized polybutadiene diol based hydrophobic, water dispersible polyurethane nanocomposite: Role of Organoclays structure



Malkappa, K.; Rao, B. N.; Jana, T. (Communicated to *J. Phys. Chem. C*)

5.1. INTRODUCTION

In recent years, both academic and industrial groups are putting enormous attention towards the development of environmentally friendly water dispersible polyurethane (WDPU) with the aim to eliminate the volatile organic compounds used as solvent in conventional PUs^{1,2} to meet the environmental regulations. The WDPU represents a vital class of coating resins because of major advantages viz nontoxicity, non-flammability, abrasion resistance, durability, excellent adhesion and tenable properties. Hence, WDPU has attracted several applications which include adhesives, coatings for various substrates including textile fabrics, plastic, wood, glass fibers and biomedical and biodegradable materials.³⁻⁹ Regardless of the property which may be inherent of WDPU, there is a continuing need to improve the more and more desired properties which can be tailored to meet the highly diversified demands of WDPU. To do these, many researchers have made the nanocomposites of solvent borne PUs¹⁰⁻¹⁴ but a few researchers have reported the development of nanocomposites of WDPU.¹⁵⁻¹⁷

In addition to environmental concern, it is important to have hydrophobic character of WDPU for the potential use in coating and hence efforts have been made to enhance hydrophobic character along with thermo-mechanical stability of the film obtained from cured WDPU. To achieve this several nanocomposites of WDPU with clays (layered silicates) have been reported so far.¹⁸⁻²² However, nanocomposites of hydroxyl terminated polybutadiene (HTPB) diol based WDPU is not reported in the literature so far. HTPB is a widely used diol source for preparing polyurethane (PU) for numerous applications especially in the solid rocket propellant.²³⁻²⁶

Our research group has modified HTPB with various energetic functionality with the objective of enhancing the various properties especially mechanical properties of HTPB based PUs.²⁷⁻³⁰ One such modification in which 2,4-dinitrobenzene (DNB) molecules are attached in the terminal position of HTPB (we named it as HTPB-DNB) is found to be a good diol precursor for preparing high tensile PU and WDPU as reported by us earlier.^{31,32} In Chapter 4, we have developed the method for syntheses of water dispersible polyurethanes (WDPU) of HTPB and HTPB-DNB with various hard segment content and also observed that the properties of WDPUs obtained from HTPB-DNB are better than HTPB-PUs.³² Although results of our previous study is very encouraging, but still the highest measured contact angle obtained was 96° for cured WDPU films obtained from HTPB-DNB-PU with hard segment (HS) around ~40 wt%. Our aim is to enhance the contact angle further (may be achieve close to 120°) without compromising tensile and other physicochemical characteristic of WDPUs.

One possible way, which can be applied, is that to increase hard segment since we had noticed increase in hydrophobicity with increasing hard segment but our repeated attempts were unsuccessful in preparing stable WDPUs of HTPB-DNB with HS more than 40%. Therefore, the search of other avenues led us to consider in preparing WDPU from the nanocomposites of HTPB-DNB-PU (where HS is 40%) with a hope that contact angle will increase since the silicate layer may bring extra hydrophobicity in the material in addition it will reinforce the mechanical strength.

To our surprise, we could not find any report on the clay composites of HTPB based WDPUs. These absence of literature and our hypothesis (as described above) encourages us to the present study, in which we have prepared and studied WDPU/clay nanocomposites using HTPB-DNB as diol sources for preparing PU and we used two structurally different types of clay. These clays are Cloisite-30B (a montmorillonite type clay with 2:1 smectite structure) and Kaolinite (1:1 illite) clay. The choices of these clays are driven by the abundance, low cost and their structural difference. We would also like to investigate the effect clay structure on the final properties of WDPU nanocomposites.

5.2. SYNTHESIS

5.2.1. Organic modification of Kaolinite clay

Kaolinite (Kao) was organically modified with dimethyl sulfoxide (DMSO) using the procedure as discussed earlier.³³ Briefly, the procedure is as follows: Kao and DMSO were taken into the round bottom flask and sonicated for 2 hrs. to enhance the Kao dispersion. After this, the mixture was stirred for 4 days to complete intercalation of DMSO in the Kao basal planes. Finally, the suspension was filtered and then washed with methanol to remove the excess DMSO. After that, the resultant precipitate was kept in vacuum oven at 100° C for complete drying. The modified Kao was designated as OKao.

5.2.2. *In-situ* preparation of water dispersible polyurethane/clay nanocomposite

Two types clay viz. OKao and Cloisite-30B were used for the preparation of water dispersible polyurethane (WDPU)/clay nanocomposite. An *in-situ* preparation procedure was followed instead of conventional blending process where usually certain weight % of nano fillers are added to the polymer solution. In the current *in-situ* process, desired amount of clay was added to the polymeric diol, i.e. HTPB-DNB. The clay weight fractions were altered from 1% to 5% (by weight) with respected to HTPB-DNB. Require amount of clay (either OKao or Cloisite-30B) and HTPB-DNB were taken in a three-neck flask which was equipped with a mechanical stirrer, nitrogen inlet, condenser and a

thermometer. The mixture was stirred in a constant temperature oil bath at 85° C for 5 h for the intercalation or exfoliation of the clay with the polyol (HTPB-DNB). After 5 hours of stirring, required amount of DMPA (dimethylol propionic acid), IPDI (isophorone diisocyanate) and catalytic amount (20 μ L) of DBTDL (dibutyl tin dilaurate) were added into the reaction mixture. The reaction was continued by stirring at 85° C in presence of N₂ atmosphere for another 3 h MEK (methyl ethyl ketone) 3-5 mL was added at about 2 h during the reaction progress so as to prevent the viscosity development due to formation of polymer. After 3 h of reaction, -NCO terminated polyurethane (PU) prepolymer with clay was formed which was confirmed by the presence of urethane linkage and -NCO peaks frequencies in the IR spectra of the prepolymer sample. The whole reaction mixture, which contains -NCO terminated PU prepolymer and clay was cooled down to room temperature. Then triethyl amine (TEA), (1.2 equivalents of DMPA) was added to the prepolymer/clay reaction mixture to neutralize the carboxylic acid group because of DMPA and further one hour stirring was continued. This prepolymer/clay further chain extended by adding required quantity of BDO and stirring was continued for about 30 minutes or until the complete disappearance of -NCO peak in the IR spectra at 2270 cm⁻¹. The resultant product was dispersed in about 40 ml of water with vigorous stirring which resulted the milky water dispersion of PU/clay nanocomposite. The reaction scheme procedure is shown in Scheme 5.1. The calculated hard segment (HS) content for the PU is 40%. In the current study, we did not alter the HS content; however we altered the type of clay and the clay loading in the WDPU/clay nanocomposites.

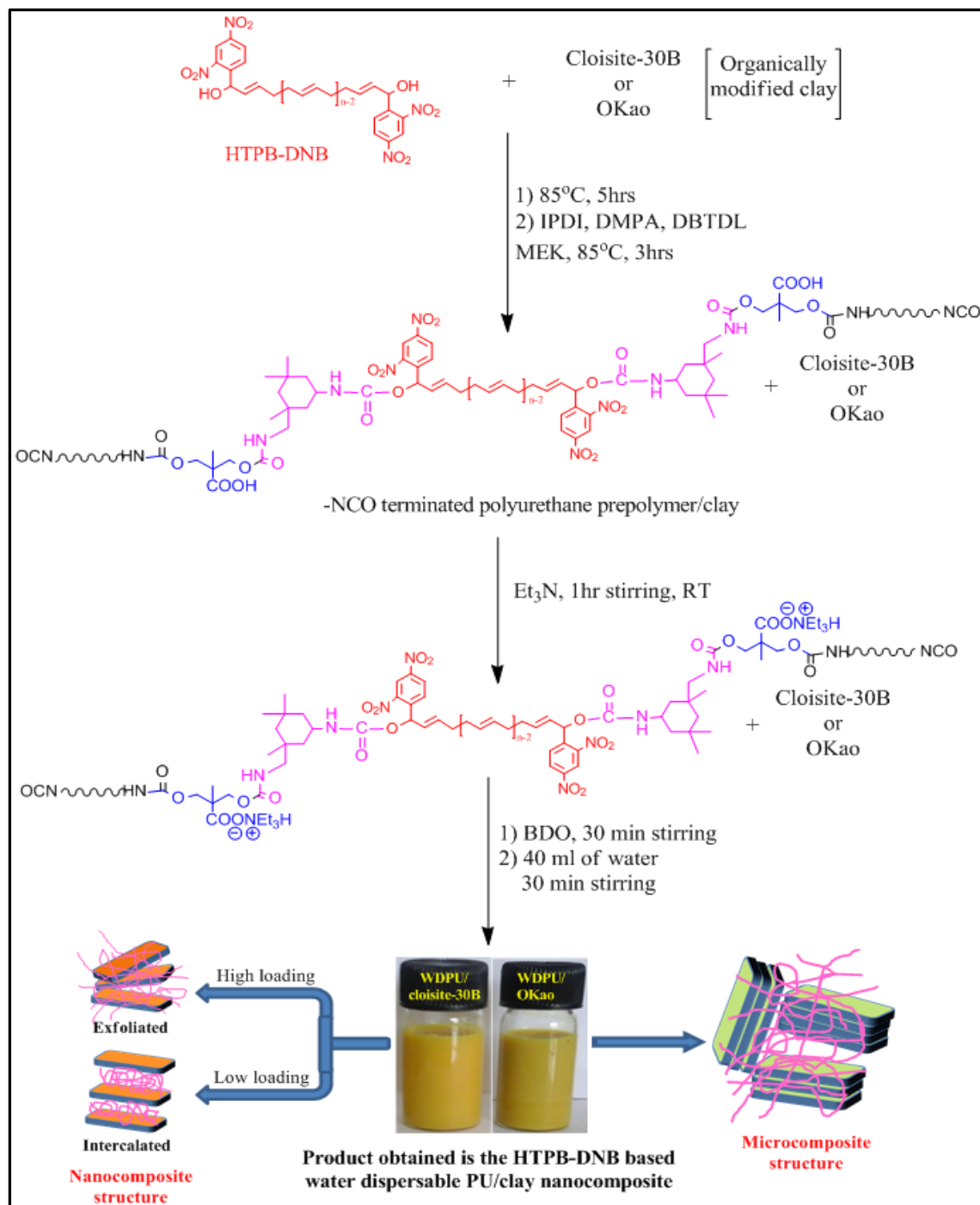
5.2.3. Preparations of PU films from WDPU/clay composites

The WDPU/clay composites were poured in a glass plate and dried at room temperature for 24 hours. After that the glass plate with the sample was kept at 70° C inside a hot air oven for 2 days. Then we pilled off the strong and elastic films from the glass plates. The thicknesses of the films were about 200 μ m. The films were stored in the desiccator for all further characterizations.

5.3. CHARECTERIZATION TECHNIQUES

All the information about the characterization techniques which include spectroscopic characterization by fourier transform infrared spectroscopy (FT-IR) and solid state ¹³C-NMR, X-ray diffractions (WAX), transmission electron microscopy (TEM), particle size analyser (PSA), field emission scanning electron microscope (FE-SEM), thermogravimetric analysis (TGA), differential scanning coloremtry (DSC), dynamic mechanical analysis (DMA), contact angle measurement (CA)

and universal testing measurement (UTM) analysis studies for all the clay nanocomposite polymer samples are discussed in the Chapter 2.



Scheme 5.1. Synthesis of water dispersible polyurethane/clay nanocomposites.

5.4. RESULTS AND DISCUSSION

5.4.1. Preparation of WDPU/clay composite

An *in-situ* method has been developed to prepare HTPB-DNB based WDPU/clay nanocomposites with two types of organically modified clays namely Cloisite-30B and OKao. Our synthetic strategy (as discussed in the experimental section) is such that the resulting PU would be water dispersible. And also our method ensures the formation of particles as we observed in our earlier work (Chapter 4) of preparation of WDPU from HTPB-DNB.³² However, in this work we have incorporated clays in the reaction mixture with an objective to enhance the hydrophobicity and other physicochemical properties of the final cured WDPU films. Therefore, it is important to verify that the resulting WDPU/clay nanocomposites yield water dispersible nanoparticles. Figure 5.1 shows the particle size and size distribution plots obtained from zetasizer measurement for all nanocomposites along with pristine WDPU. The results clearly indicate the formation of particles in the range of 100 to 200 nm with low polydispersity. To check the shape of the particles, we carried out TEM experiments and the representative micrographs are shown in Figure 5.2. All particles in all the cases are spherical in shape. Particle size measured from TEM is little lower than the zetasizer as expected because of the absence of the solvent in the case of TEM technique. Table 5.1 lists the all particle size and PDI for all nanocomposites. It is to be noted that particle size varies with changing clay content in both the clay cases. In case of Cloisite-30B, size increases with increasing clay content. On the other hand size decreases with increasing clay content in case of OKao composites. This variation may be linked to the nanocomposite structure formation which are different in these two clays (will be discussed in the next section). Also it is to be noted that the PDI increases with increasing clay content especially in case Cloisite-30B which is attributing the aggregation/exfoliation at high clay loading which is also apparent from TEM micrograph.

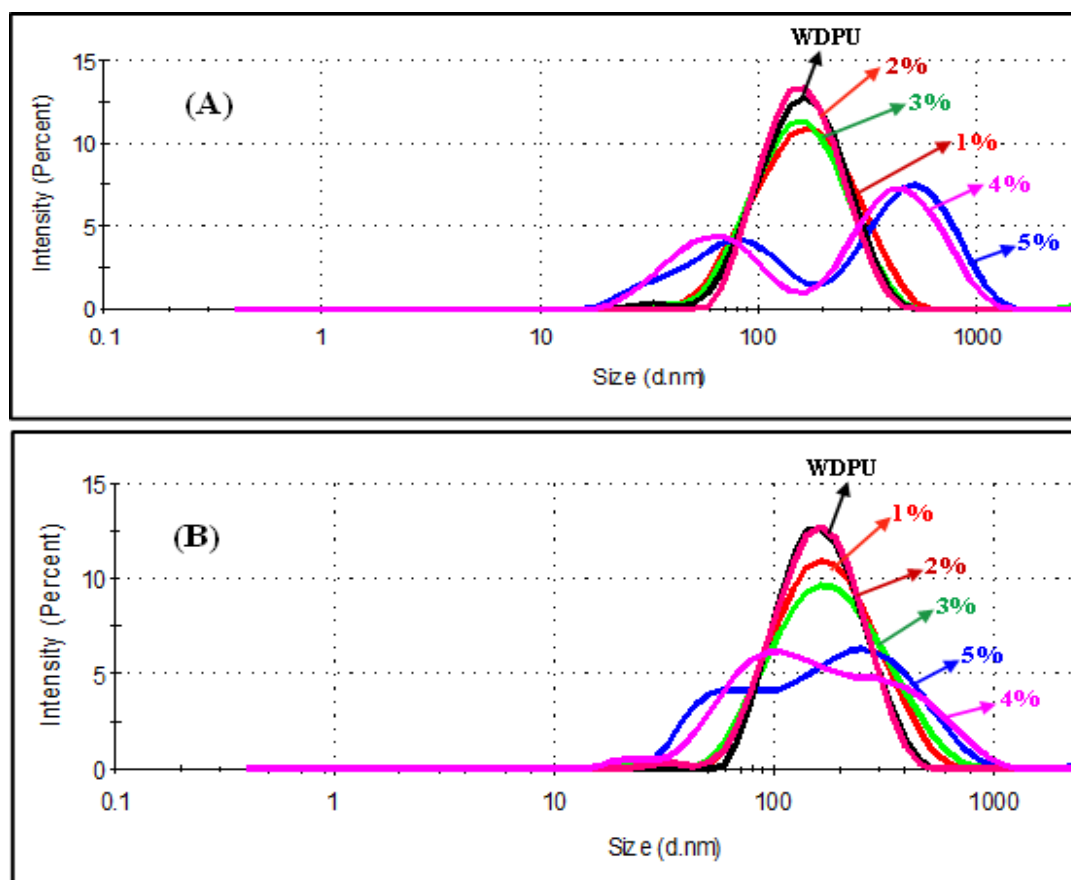


Figure 5.1. Particle size and size distribution plots (obtained from Zetasizer) of HTPB-DNB based WDPU/clay composites with (A) Cloisite-30B and (B) OKao clay. Compositions are indicated in the figure.

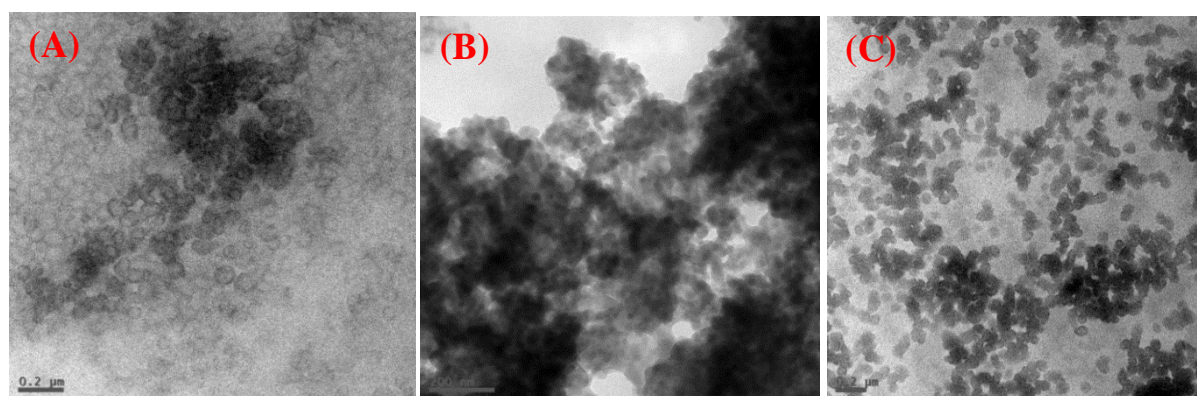


Figure 5.2. TEM images of HTPB-DNB based WDPU: (A) WDPU (control experiment, only HTPB-DNB), (B) WDPU/Cloisite-30B-3% and (C) WDPU/OKao-3%

Table 5.1. Particle size and PDI of nanocomposites as a function of clay content in the nanocomposite.

<i>Sample Identification</i>	<i>Clay (%)</i>	<i>Particle Size^a (nm)</i>	<i>PDI^a</i>
WDPU	0	142	0.166
WDPU/Cloisite-30B	1	145	0.192
	2	150	0.243
	3	151	0.287
	4	153	0.843
	5	167	0.766
WDPU/OKao	1	155	0.220
	2	159	0.237
	3	156	0.254
	4	137	0.469
	5	140	0.481

^a Measured from zetasizer

5.4.2. FT-IR study

IR spectra of WDPU/clay composites with both types of clay are shown in Figure 5.3. The clay contents in the composites were varied from 1% to 5 wt% with respect to polymer weight and all the IR spectra are shown in Figure 5.3. The main functional group in the PU chain are urethane –N-H and carbonyl stretching frequencies. The 2949 and 2867 cm^{-1} peaks are due to the alkane –C-H stretching vibration. The absorption band at around 3326 cm^{-1} for H-bonded -N-H stretching frequency. The carbonyl region of pristine WDPU displays three bands at around 1728, 1708, 1690 cm^{-1} . The peak at 1728 cm^{-1} is assigned to the free –C=O stretching, whereas the peak at 1708 cm^{-1} is due to hydrogen-bonded –C=O stretching and a small absorption band at around 1690 cm^{-1} is due to the formation of urea linkage.³² However, we could observed only one sharp peak at 1703 cm^{-1} in case of Cloisite-30B composite and 1697 cm^{-1} in case of OKao composite instead of three peaks as shown in Figure 5.3. Therefore, it clearly indicates that all carbonyl groups are involved in the formation of hydrogen bond or some other specific interactions with silicate layers of clays. The other characteristic

peaks are 1386 and 1364 cm^{-1} due to -C-N stretching, 1241 cm^{-1} due to ester C-O-C asymmetric stretching vibration, 1174 cm^{-1} due to coupled C-N and C-O stretching vibrations, 1062 cm^{-1} due to ester C-O-C symmetric stretching vibration and 1557 cm^{-1} due to C-H-N vibration of associated secondary urethane groups. In both the clay composites, absorption band appear at around 1020 cm^{-1} to 1030 cm^{-1} corresponding to O-Si-O stretching frequency and the peak intensity gradually increases with increasing clay percentage indicating the incorporation of clay particles in the composite.³³ The peak at 1116 cm^{-1} due to S=O stretching frequency of DMSO is clearly seen in case of OKao composites (Figure 5.3.B) and hence attributed that OKao clay is introduced into polymer matrix.³⁴⁻³⁶

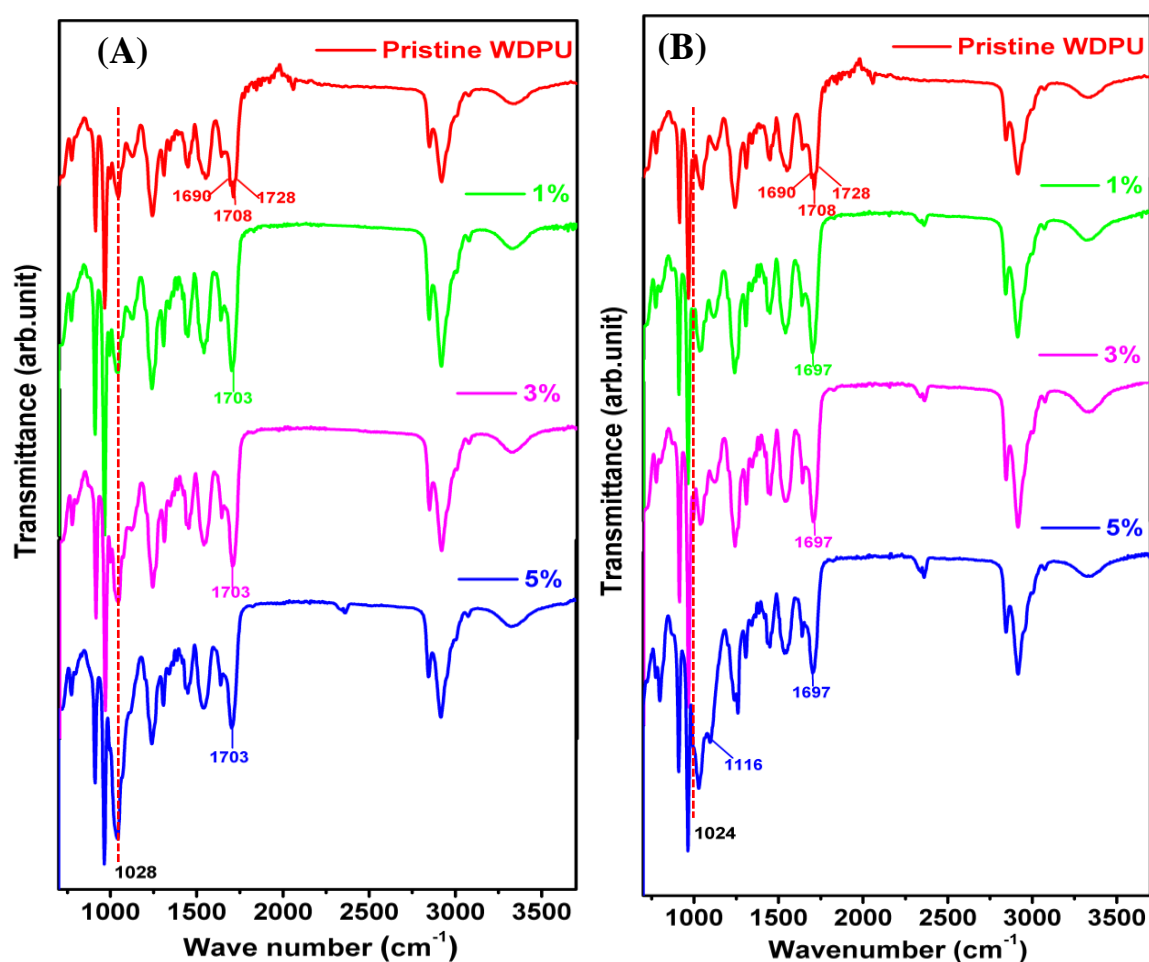


Figure 5.3. IR spectra of HTPB-DNB based WDPU/clay composites with (A) Cloisite-30B (B) OKao clay. The composite compositions are indicated in the figure.

5.4.3. Solid-state NMR study

The pristine WDPU and all the nanocomposites samples were studied by recording ^{13}C solid state NMR and the results are shown in Figure 5.4. A magnified portion of the spectra (δ 100-200 ppm) is only presented here for better clarity of important peaks in the context of discussion. The spectral characteristics are quite similar to our previously reported results and also the spectral fractures of all nanocomposites are almost similar. Multiple peaks are observed at around 20-50 ppm due to saturated carbons of HTPB (not shown here in the figure) and unsaturated HTPB carbon signals are obtained at around 110-145 ppm. The spectral characteristics of clays (Cloisite-30B and OKao) could not be separated since their peaks (δ 43 ppm in case of OKao and δ 32 ppm in case of Cloisite-30B) are merged with the saturated carbon signals of HTPB at around 20-50 ppm. A careful analysis and comparison of nanocomposite spectra with pristine WDPU reveal interesting information. Two important peaks are seen at around 156 and 175 ppm corresponding to carbonyl carbon of urethane and carboxylate, respectively. Both the peaks display marginal shift towards the higher field (lower δ) and decrease in the peak intensity (height) with increasing clay loading in the nanocomposites. These observations indicates that the peak broadening is taking place.³⁷ To understand this changes in the peaks nature, we analyzed these peaks by calculating the full width at half maximum (FWHM) of both the 156 and 175 ppm peaks for all the nanocomposite samples and data are shown in the Figure 5.5. The FWHM value increases with increasing clay loading. The FWHM of δ 156 ppm peak for WDPU/Cloisite-30B-5% is 506 Hz and for WDPU/OKao-5% is 505 Hz whereas it is 450 Hz for pristine WDPU. The difference from pristine WDPU to both clay composites is > 50 Hz and hence it clearly indicates that the broadness of the peak increases with the clay loading in both types of the clay composites. Similarly, the peak at 175 ppm shows significant line broadening of both clay composites. The measured value of FWHM is 639 Hz for pristine WDPU and for WDPU/Cloisite-30B-5% is 997 Hz and for WDPU/OKao-5% is 917 Hz. Here, the difference from pristine WDPU to clay composite PU is ~300 Hz, this means that the broadness of the peak increases in both types of the clay loadings. It is worth to note that the increase in line width is different in two cases indicates the effect of clay structure on the nanocomposite structure. These observations clearly attribute to the presence of interactions between the PU chain and the functional groups of silicate layers in the clay. Therefore, our SS-NMR observations quite clearly agree with our IR observation and prove the formation of WDPU/clay nanocomposites.

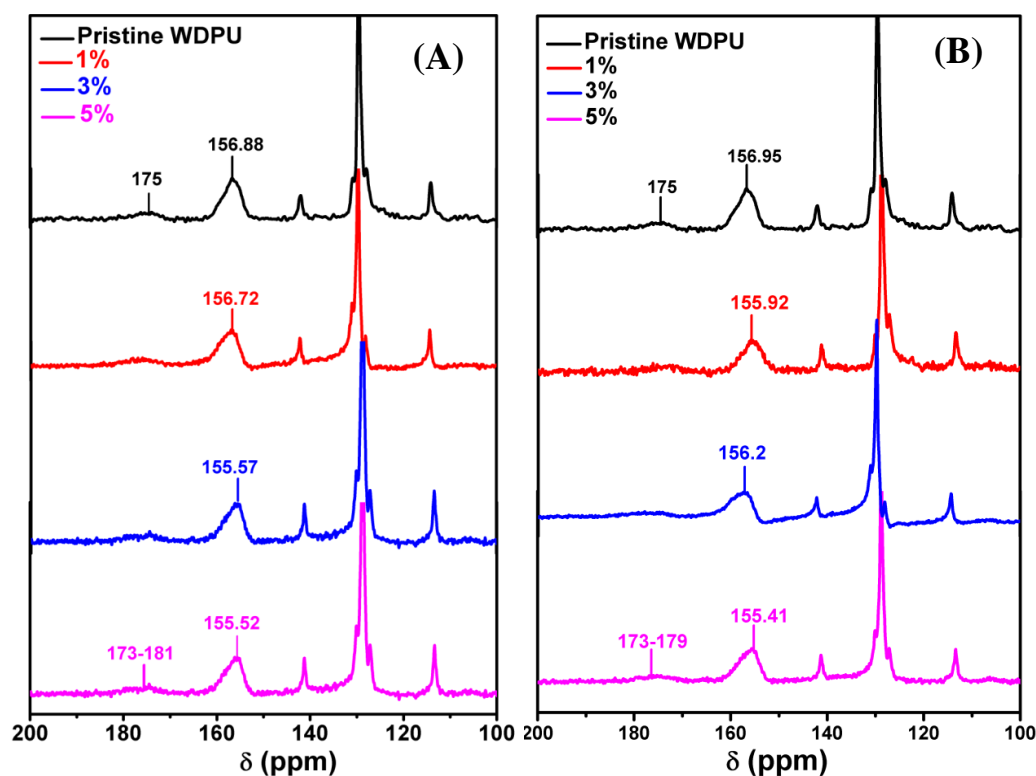


Figure 5.4. ^{13}C Solid state (^{13}C CP-MAS) spectra of HTPB-DNB based WDPU/clay composites with (A) cloisite-30B (B) OKao clay. Weight % of clay in the composite are indicated in the figure.

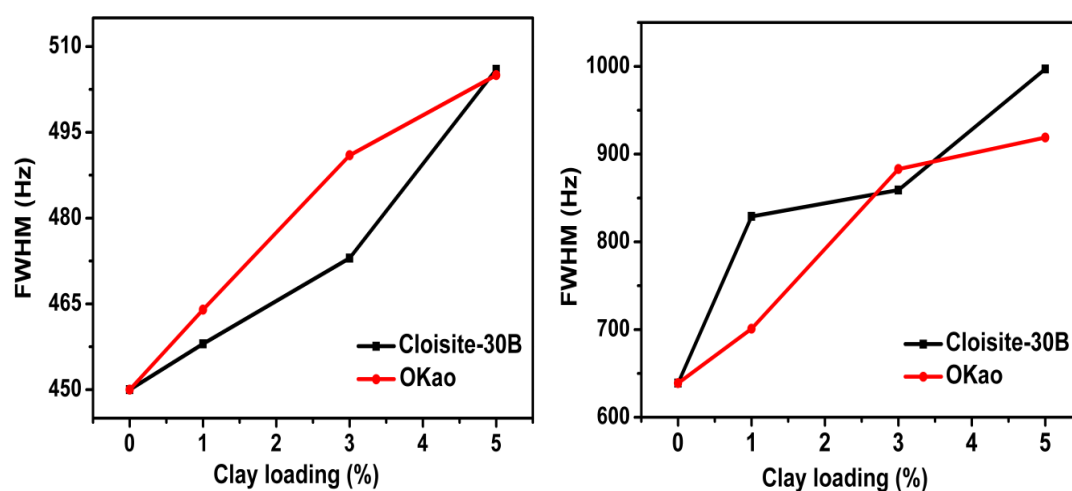


Figure 5.5. Peak broadening presented in terms of FWHM as a function of clay loading for the carbonyl carbon of (A) urethane at $\delta 156$ ppm and (B) carboxylate at $\delta 175$ ppm.

5.4.4. X-ray diffraction study

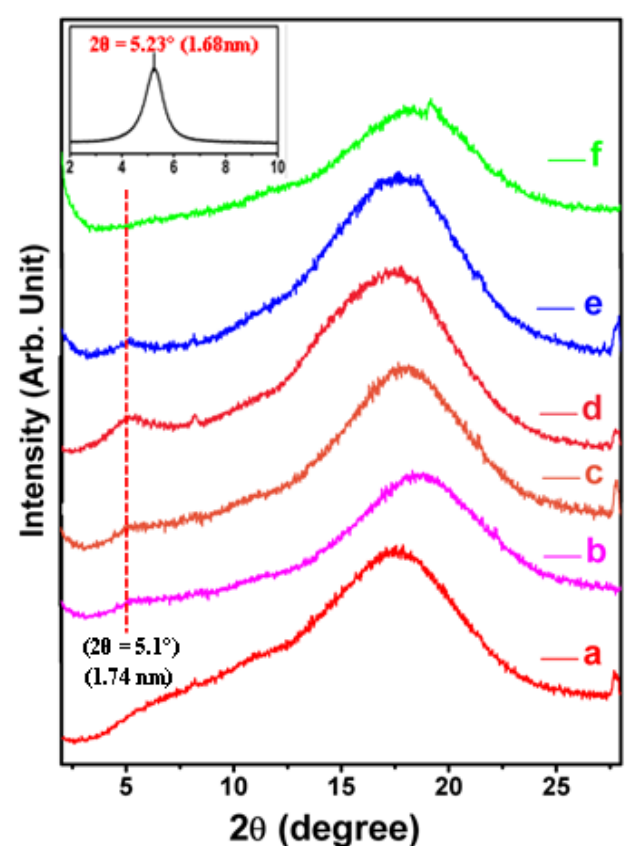


Figure 5.6. WAXD patterns of HTPB-DNB based WDPU/Cloisite-30B clay nanocomposites with loading in wt% (a) 0% (Pristine WDPU) (b) 1% (c) 2% (d) 3% (e) 4% and (f) 5%. Inset: WAXD pattern of Cloisite-30B clay

Wide angle X-ray diffraction (WAXD) patterns of Cloisite-30B clay and all nanocomposites of this clay with WDPU are shown in the Figure 5.6. The characteristic sharp peak of basal plane of Cloisite-30B is observed at $2\theta = 5.23^\circ$ ($d = 1.68$ nm). The nanocomposite samples show the clay loading dependency as observed from the figure. It is clearly seen that with increasing clay content from 1 to 3 wt %, the peak slightly shifted to higher distance and appeared at $2\theta = 5.1^\circ$ ($d = 1.74$ nm) and also the peak intensity increases. But further increase of clay loading such as 4 wt %, the intensity of $2\theta = 5.1$ peak decreases and the peak completely disappeared at 5 wt %.³⁸ This shifting of the peak or in other words increase in basal plane distance in case of clay loading up to 3 wt % attributes the intercalating of clay in the PU matrix. On the otherhand, slowly disappearance of basal plane peaks indicates the formation exfoliated nanostructure when clay loading is greater than equal to 4 wt %. It

has been reported that in case of PU/Cloisite-30B nanocomposites, the electrostatic forces between the clay platelets have tendency to squeeze the PU polymer chains inside the clay layers and subsequently yields to an intercalated structure.³⁹⁻⁴² However in the current study, the PU chains are having ionic (anionic) groups in the back bone; hence when this WDPU chains interact with cationic Cloisite-30B clays, the electrostatic interaction between the clay and the polymer chains overrules the interactions between the clay platelets and therefore it is expected that the clay layers would be exfoliated. However to have this interaction a minimum loading of clay is required and that is why we observed above 4 wt % exfoliated structure and below which intercalated structure where WDPU chains are partially squeezed into clay layers.

WAXD patterns of Kao, OKao and all nanocomposites of WDPUs with OKao are shown in the Figure 5.7. The peak at $2\theta = 12.32^\circ$ ($d = 0.72$ nm) corresponds to the Kao basal planes. The peak shifts to a lower angle $2\theta = 7.79^\circ$ ($d = 1.14$ nm) after modification with DMSO (Figure 5.7A). This means intercalation of DMSO takes place which increases the d-spacing due to the expansion of the interlayer space and this value is agreement with previous reported values.^{33,43-45} Intercalated or exfoliated structure of the nanocomposite are the two most frequently observed structures in case of polymer nanocomposites with OKao. However, in this case we found an unusual and interesting observation. Figure 5.7B shows that with increasing OKao loading in the WDPU/OKao nanocomposite, the basal plane peak at $2\theta = 12.32$ degree ($d = 0.72$ nm) of unmodified Kao appears and increases intensity with increasing clay content. The basal plane peak for OKao at $2\theta = 7.79$ degrees ($d = 1.14$ nm) completely disappears. This indicates that WDPU polymers displaced the modifier (DMSO in this case) completely from the gallery of the OKao clay layers and converts the OKao to Kao. This result is possible due to the strong interactions between anionic WDPU and the positively charged OKao layers. Because of this interaction the DMSO got displaced and clay layers decreases their basal plane gap by interacting with the polymer. As a result the clays are aggregated and this aggregation increases with increasing clay loading into the nanocomposite.⁴⁵ The next section will discuss the implication of this structure on the properties of these nanocomposites.

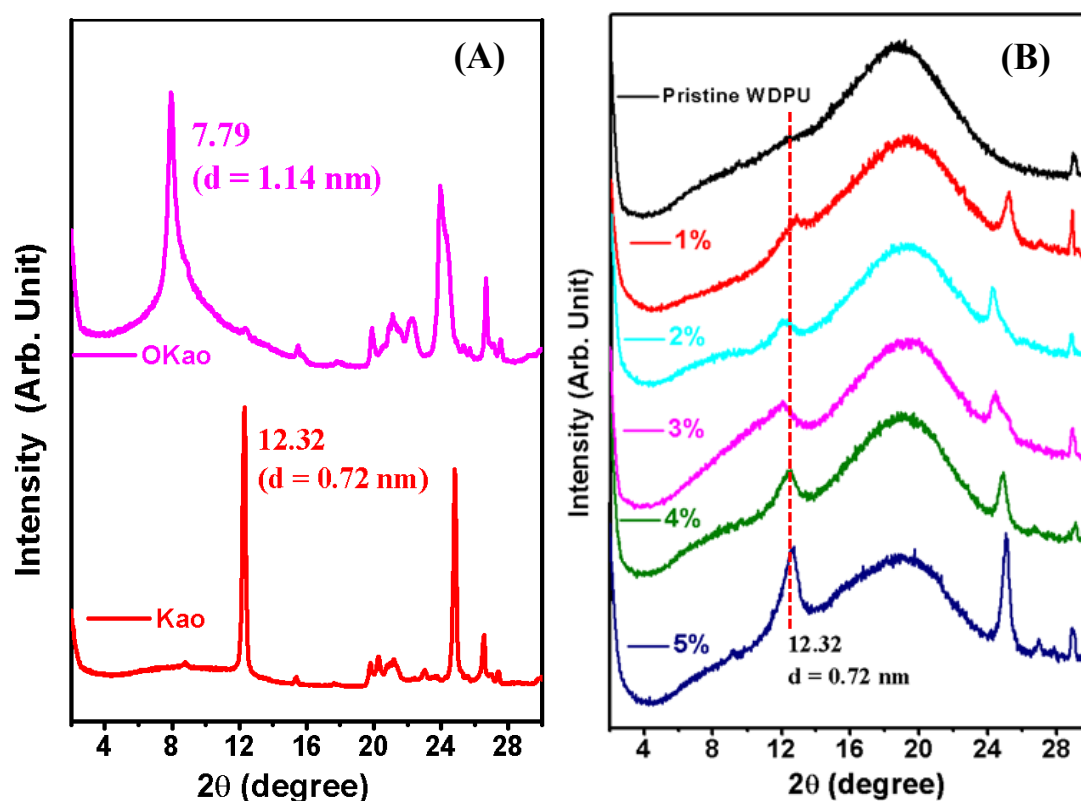


Figure 5.7. WAXD pattern of (A) Kao and OKao (B) all HTPB-DNB-WDPU/OKao nanocomposites and the compositions of nanocomposites are shown in the figure.

5.4.5. Morphology study

To reconfirm the nanocomposite structure as established by the X-ray studies (discussed in the previous section), we have analysed our nanocomposite structures by capturing morphological fractures of samples using TEM and FESEM. TEM images of nanocomposite samples with different weight loading for both clays are shown in Figure 5.8. The intercalated morphology is obtained when Cloisite-30B clay loading is 1 to 3 wt % (Figure 5.8. A, B) and this result is in agreement with the X-ray data discussed in the previous section. Careful analysis of TEM images also revealed that the layer spacing (basal plane distance) of intercalated structure obtained from TEM images (Figure 5.8. A, B) are matching with X-ray distance (Figure 5.6). On the otherhand when Cloisite-30B clay loading is increased to 5 wt %, the structure of the nanocomposite becomes exfoliated as clearly seen from TEM images (Figure 5.8.C) which is again in agreement with X-ray data (Figure 5.6.).^{45,46-48} TEM images of WDPU/OKao nanocomposites with 1, 3 and 5 wt % loading are presented in Figure 5.8.(D to F) and

display aggregated structure which is tallying with X-ray data (Figure 5.7.) The images clearly shows the aggregation of clay plates with thick dark lines like small pieces and on further increase in clay content thick lumps and aggregated spherical morphology is observed (Figure 5.8. F)^{49,50} The above results are very well in agreement with WAXS study (Figure 5.7.)⁴⁵

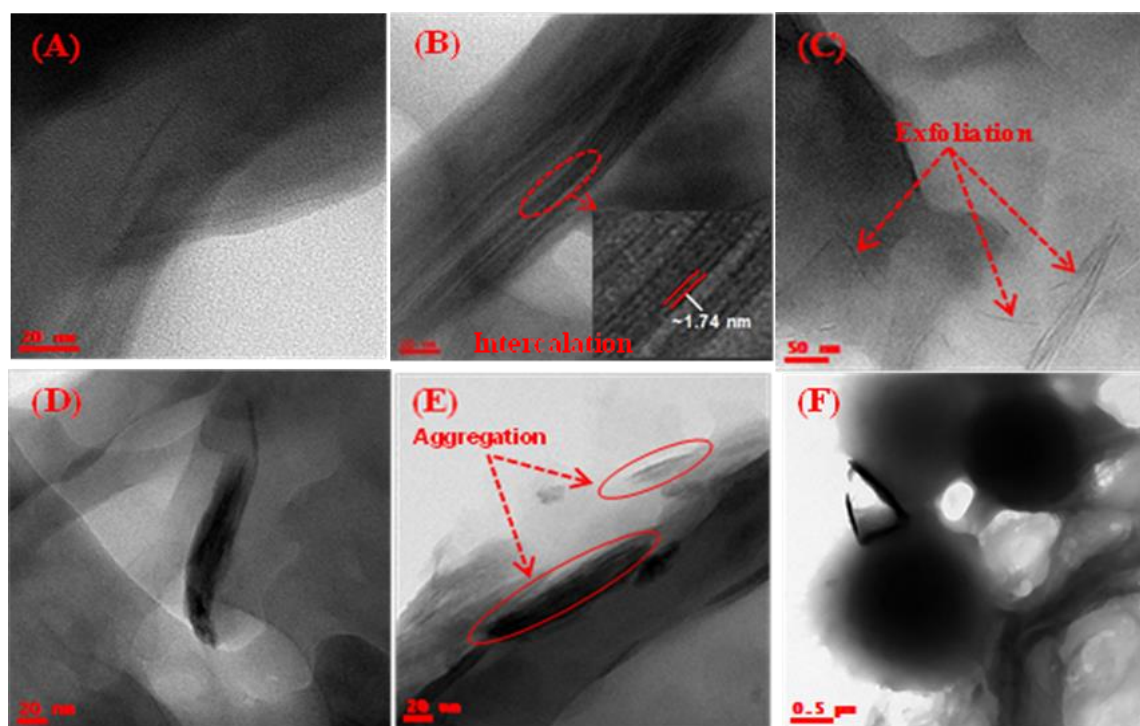


Figure 5.8. TEM micrographs of HTPB-DNB based WDPU/clay composites. (A), (B) and (C) are the Cloisite-30B composites with 1, 3 and 5 wt%, respectively and (D), (E) and (F) are the OKao composites with 1, 3 and 5 wt%, respectively.

The FESEM micrographs of pristine WDPU and the composite PU films are shown in Figure 5.9. The surface of pristine WDPU is much smoother than composite PUs (Figure 5.9A). The surface roughness increases with increasing Cloisite-30B clay loading. However, an aggregated morphology is observed and aggregation size increases with increasing clay content in case of OKao composites. A similar kind of morphology with the OKao composite polymer is reported earlier by several authors in the literature.^{45,51}

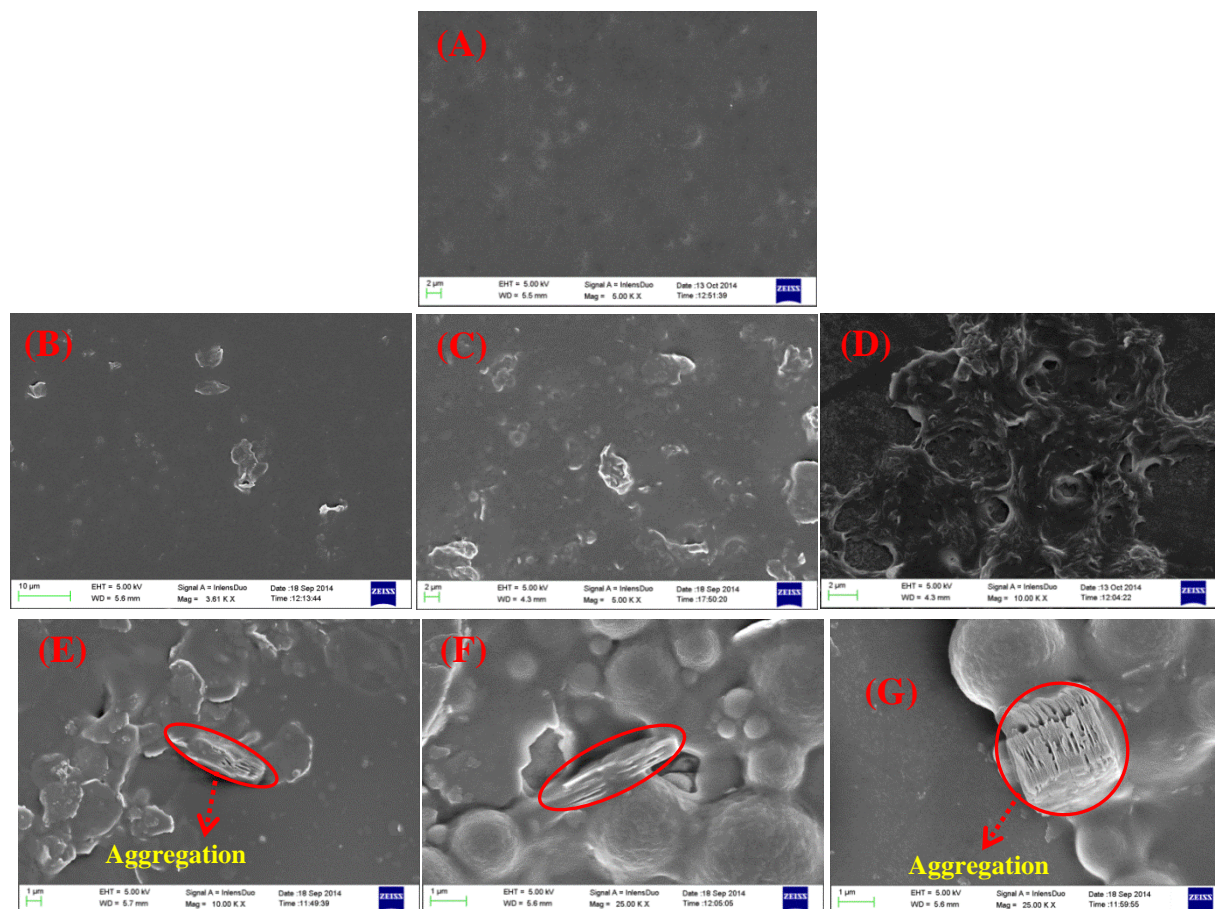


Figure 5.9. FESEM images of HTPB-DNB-WDPU/clay composites; (A) Pristine WDPU (B) WDPU/Cloisite-30B-1% (C) WDPU/Cloisite-30B-3% (D) WDPU/Cloisite-30B-5% (E) WDPU/OKao-1% (F) WDPU/OKao-3% and (G) WDPU/OKao-5%.

5.4.6. Tensile properties

The tensile properties of all the films obtained from WDPU/clay nanocomposites with both types of organoclays and with different wt% loadings are shown in Figure 5.10. to evaluate the strength of all the composite PU films. The tensile strength (σ_b) and elongation at break (ϵ_b) obtained from stress-strain plots of Figure 5.10. are summarised in Table 5.2. Also, we calculated the toughness and young modulus (E) from the stress-strain profile and included in Table 5.2. The method of calculation for toughness and E has been discussed elsewhere. From Figure 5.10 (A), it is clearly observed that the stress-strain properties are changing with varying (1 to 5 wt %) clay loading of WDPU/clay nanocomposites because of changing structure of the composite. We observed intercalated structure up to 3 wt % loading of Cloisite-30B and in this wt% loading, elongation

decreases slightly and stress increases minimally. However after > 4 wt % of clay (Closite-30B) loading, a significant decrease in elongation and dramatic increase in stress are observed which is the result of exfoliated structure as proved from X-ray and microscopy studies. Table 5.2 data also ascertain our above observations. On the otherhand, the tensile properties in case of nanocomposites of OKao display different nature with increasing clay loading. There is a little change in elongation when loading of OKao is only 1%, but after that dramatic sharp decrease in elongation and significant increases in strength are observed. This can be attributed to the formation of aggregated structure, as discussed in this X-ray and morphology data in previous section, which increases further with increasing clay content. Therefore from the above discussion it can be concluded that both the nature of clay and loading of clay influence the mechanical strength of WDPU/clay composite owing to the formation of different nanocomposite structure.

From the Figure 5.10., we observed that the nature of the film changing from elastomer to plastic by altering clay loading in both types of nanocomposite of WDPUs. For example, the pristine WDPU film was elastomeric having an elongation of more than 300% and at higher clay loading PU films having plastic property because of sharp decreasing elongation and increasing strength.^{51,53} In addition, all the nanocomposites effective crosslinking (N) are calculated from Figure 5.10. and listed in Table 5.2. The N values are determined from the E values of Table 5.2. The rubber elasticity theory,⁵⁴ in which the number of network stands for unit volume (N, effective crosslinking density) can be estimated from the relation $E = 3NK_B T$, where the E is the young modulus obtained from the stress-strain plots, K_B the Boltzmann constant and T is the absolute temperature in kelvin. It clearly indicates that effective crosslinking is increasing with increasing wt % of clay content for both types of clay nanocomposites of WDPUs and more in case of higher wt% clay. It is well known that increases in crosslinking increases the stress and make the film more like a rigid plastic.

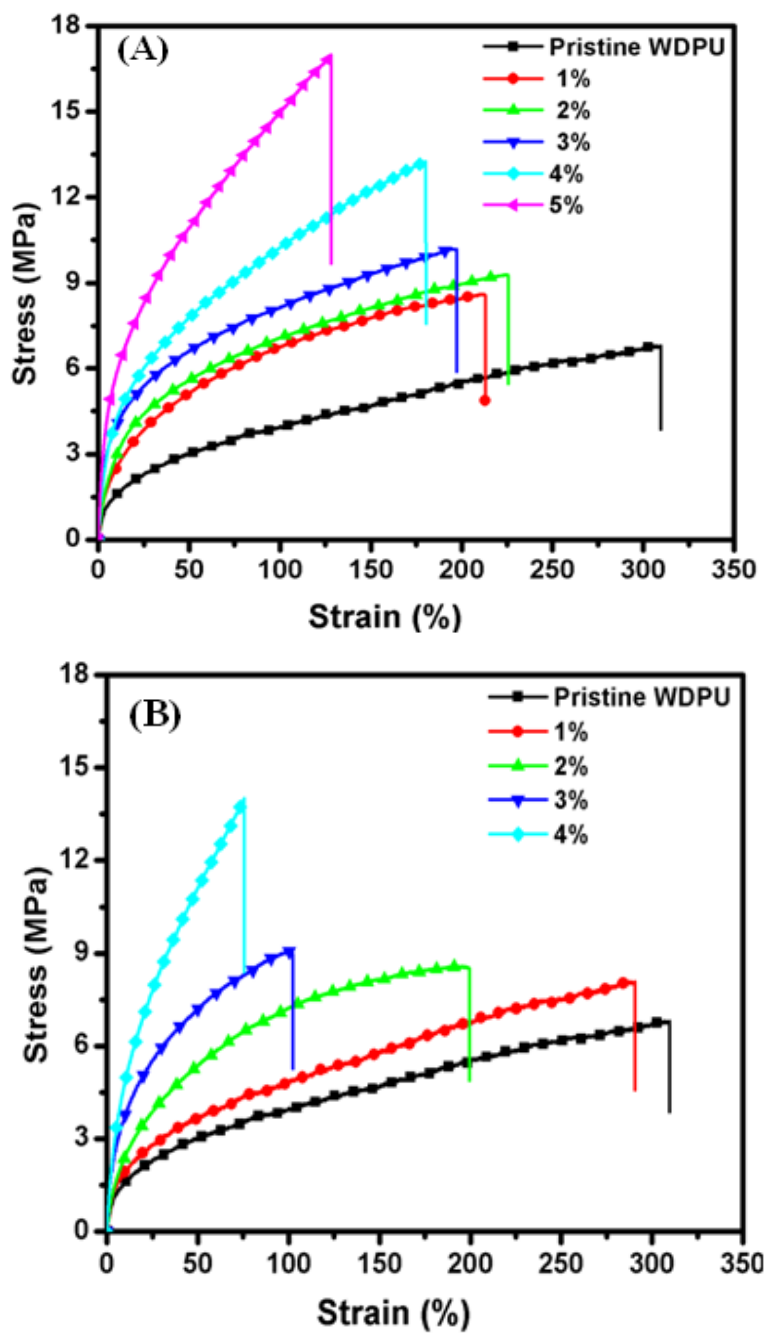


Figure 5.10. Stress-strain profiles of WDPU/clay nanocomposite with different clays; (A) Cloisite-30B (B) OKao. The amount of clay loading in the nanocomposites is indicated in the figure.

Table 5.2. Various tensile data obtained from stress-strain profiles of all WDPU/clay nanocomposite films.

<i>Sample Identification</i>	<i>Modified Clay (%)</i>	<i>Tensile strength (MPa)</i>	<i>Yield strain (%)</i>	<i>Toughness (MPa)</i>	<i>Young modulus (MPa)</i>	<i>Effective crosslinking (N/M³) × 10²²</i>
<i>Pristine WDPU</i>	0	6.76	307.57	1434.28	0.325	2591
<i>WDPU/Cloisite-30B</i>	1	8.53	211.62	1362.05	0.527	4202
	2	9.26	225.21	1523.66	0.517	4441
	3	10.21	196.38	1564.34	1.102	8787
	4	13.23	177.60	1683.93	1.074	9362
	5	17.10	127.35	1490.44	1.434	11435
<i>WDPU/OKao</i>	1	8.02	290.57	1600.10	0.405	3229
	2	8.51	198.64	1302.88	0.457	3644
	3	9.12	101.09	689.13	0.951	7583
	4	13.92	74.95	686.32	1.031	8939

5.4.7. Thermal stability

The thermal stabilities of the pristine WDPU and nanocomposite films containing 1 to 5 wt % of clays were recorded in presence of nitrogen flow and the TGA traces are shown in Figure 5.11. It is clear from the TGA data that the thermal stability of PU film has increased slightly after nanocomposite formations and also increases with the increasing clay loading in both the cases of Cloisite-30B and OKao composites. This improvement in thermal stability of nanocomposite at all the temperature ranges is due to the uniform dispersion of the silicate layers in the PU matrix. Generally, the water dispersible PUs displays poor thermal stability because of the presence of labile urethane and urea linkages. In previous Chapter (Chapter 4), we have explained that the thermal degradation of water dispersible PUs with different percentage of hard segment content.³² We observed that in both nanocomposites, the thermal degradation started at around 230°C. Increase in thermal stability in nanocomposites is because of the chain motions of polymer molecules in the silicate layers were barred and limited, and also silicate layers act as a barrier for polymer chain from the temperature^{55,56} It is also observed that the nanocomposites which are obtained from Cloisite-30B display higher thermal stability than WDPU/OKao nanocomposites. This is due to the higher degree of dispersion in the case of former, which resists the polymer chains.

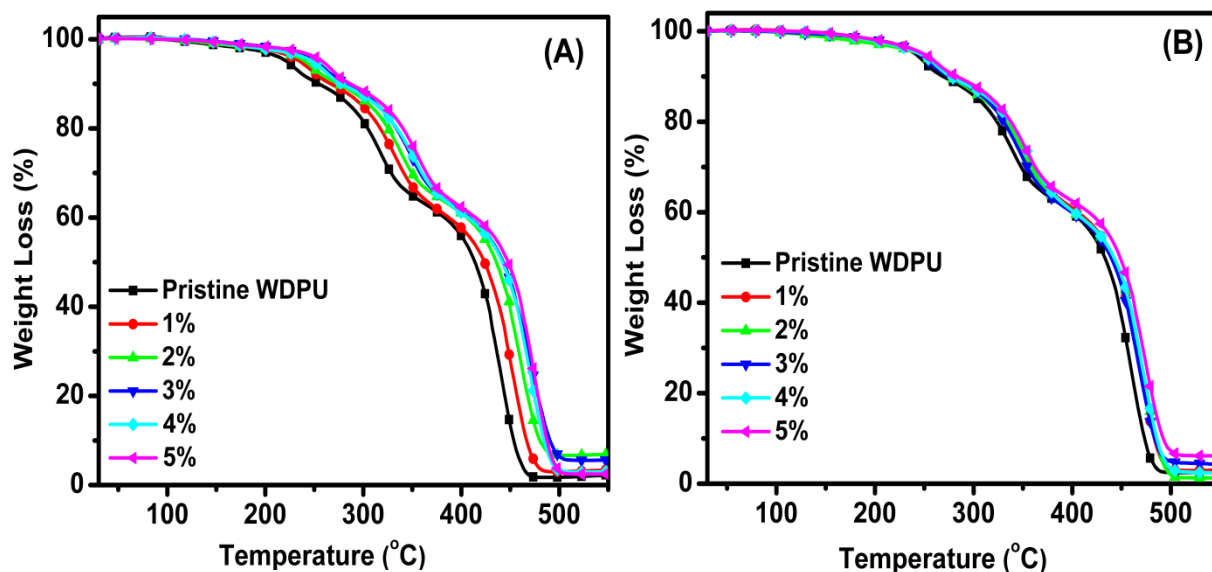


Figure 5.11. TGA curves of HTPB-DNB based WDPU/clay composites; (A) WDPU/Cloisite-30B (B) WDPU/OKao with different wt% as indicated in figure.

5.4.8. Thermal transitions

A dynamical mechanical analyzer (DMA) was used to study the thermal transitions of nanocomposites. Figure 5.12 shows the storage modulus (E'), loss modulus (E''), and $\tan\delta$ plots as a function of temperature for all the films of WDPU/clay nanocomposites with different types of clays and varying clay loading, and the important data collected from these plots are summarized in Table 5.3. From the E' vs. temperature plots (Figure 5.12 A and D), it is observed that the modulus increases with increasing clay loading in both the cases indicating the mechanical reinforcement of the nanocomposite by the silicate layers of the clay owing to the large surface area of nanoclay. However, it is also to be noted that the increase in modulus with increasing clay loading is more significant in case of nanocomposites of Cloisite-30B than OKao. This result is in agreement with the tensile data. The reason for such observation may be due to the formation of intercalated and exfoliated structures in case of Cloisite-30B nanocomposites in which clay layers are homogeneously dispersed than the aggregated structure observed in case of OKao nanocomposites.

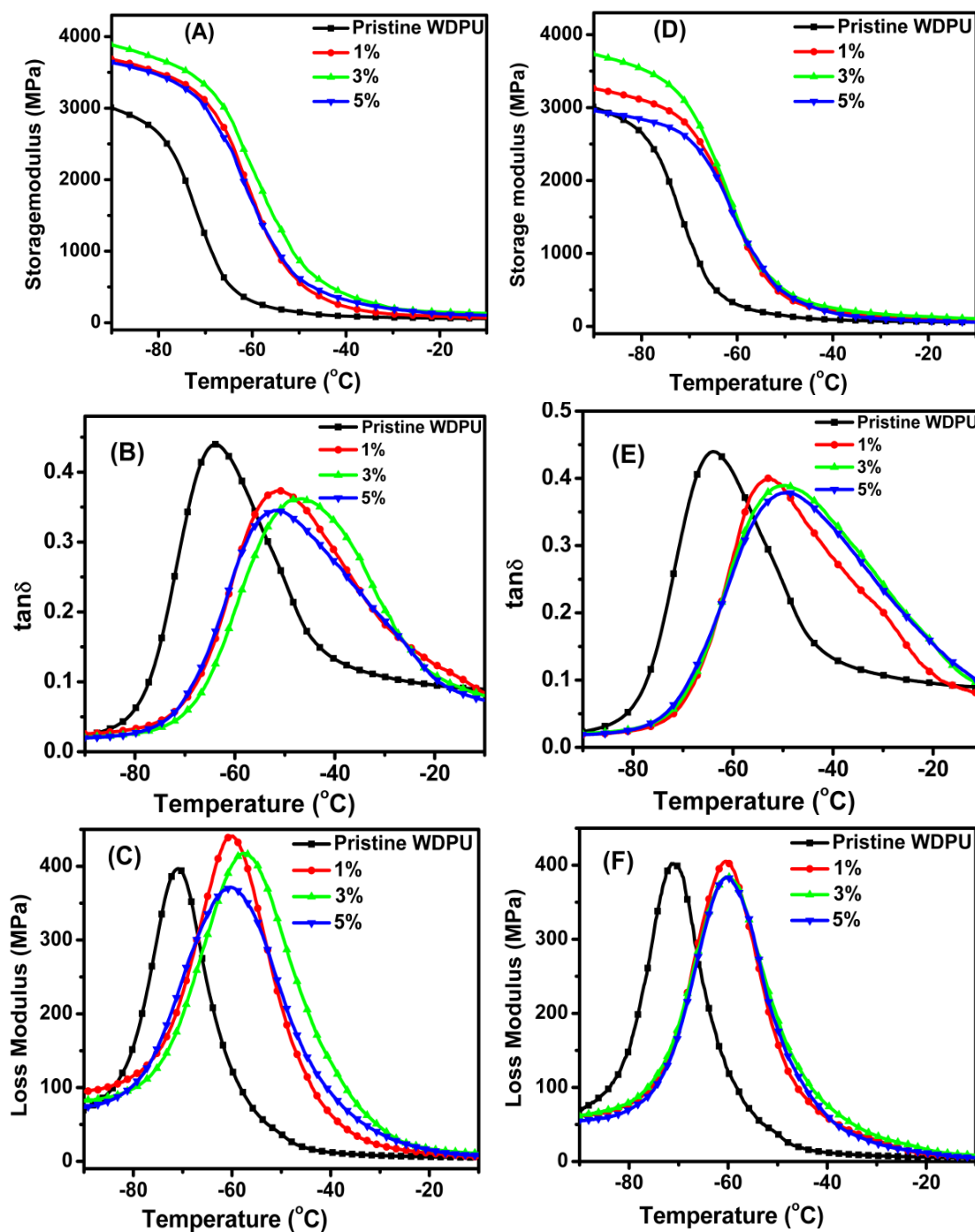


Figure 5.12. DMA plots of all nanocomposites; (A) storage modulus, (B) $\tan\delta$, (C) loss modulus of WDPU/Cloisite-30B and (D) storage modulus, (E) $\tan\delta$, (F) loss modulus of WDPU/OKao with indicated clay loading in figure.

However, we noticed that the E' value slightly decrease when Cloisite-30B loading is 5 wt % (Table 5.3.). We do not know the reason behind this but may be due to partial exfoliation of Cloisite-30B clay layers. On the otherhand, it is observed that 5 wt % OKao composite E' at -90°C is almost similar to pristine WDPU (Table 5.3) and this may be due to longer aggregates of clay at this composition. It is also to be noted that the percentage of increase in modulus is more prominent below T_g for the both the cases which may be due to the difference in chain segmental motion below T_g and after T_g which in turn alter the nature of interactions between the PU chain and silicate layers and hence result in variation of modulus.

The glass transition temperature (T_g) of all the nanocomposites samples are obtained from the peaks of $\tan\delta$ and E'' vs temperature plots are tabulated in Table 5.3. The T_g values decreases with increasing clay loading in both the clay nanocomposites. The reason behind this may be due to the interactions between the clay layers and PU chain which makes the PU chain segmental motions more restricted and hence require lower temperature to overcome this segmental barrier T_g obtained from temperature dependent $\tan\delta$ and E'' are not exactly matching and this is fairly common observation for many polymer nanocomposites. The T_g values of all the WDPU/clay composites are well below the room temperature and hence these nanocomposites display rubbery behaviour at room temperature and hence these nanocomposites are suitable for applications such as coating material.

Table 5.3. Various thermo-mechanical data of all WDPU/clay nanocomposite PU films

Sample Identification	% Clay	Storage modulus (E') ^a	T_g^b	T_g^c	T_g^d
Pristine PU	0	3220	-63.95	-70.68	-78.26
WDPU/Cloisite-30B	1	3876	-50.65	-60.15	-77.27
	3	4069	-47.07	-56.94	-76.60
	5	3785	-52.36	-60.72	-76.12
WDPU/OKao	1	3405	-53.39	-60.18	-76.84
	3	3901	-50.24	-59.75	-76.04
	5	3056	-48.97	-58.86	-75.23

^a Storage modulus at -90°C obtained from DMA, ^b T_g obtained from $\tan\delta$ plots of DMA ,

^c T_g measured from loss modulus plots of DMA and ^d T_g values measured from DSC.

To reconfirm the T_g values and rubbery nature of our nanocomposite WDPU films, we further carried out differential scanning calorimetry experiment to measure the T_g values. The DSC thermograms of clay nanocomposite WDPU samples of varying wt % of both clays are represented in Figure 5.13. and the T_g values are summarized in Table 5.3. The results clearly indicate that T_g values is in the subambient range at around -70°C suggesting the elastic rubbery nature of our composite PU films. However, we could not identify any significant variation in T_g values with clay loading from DSC results.

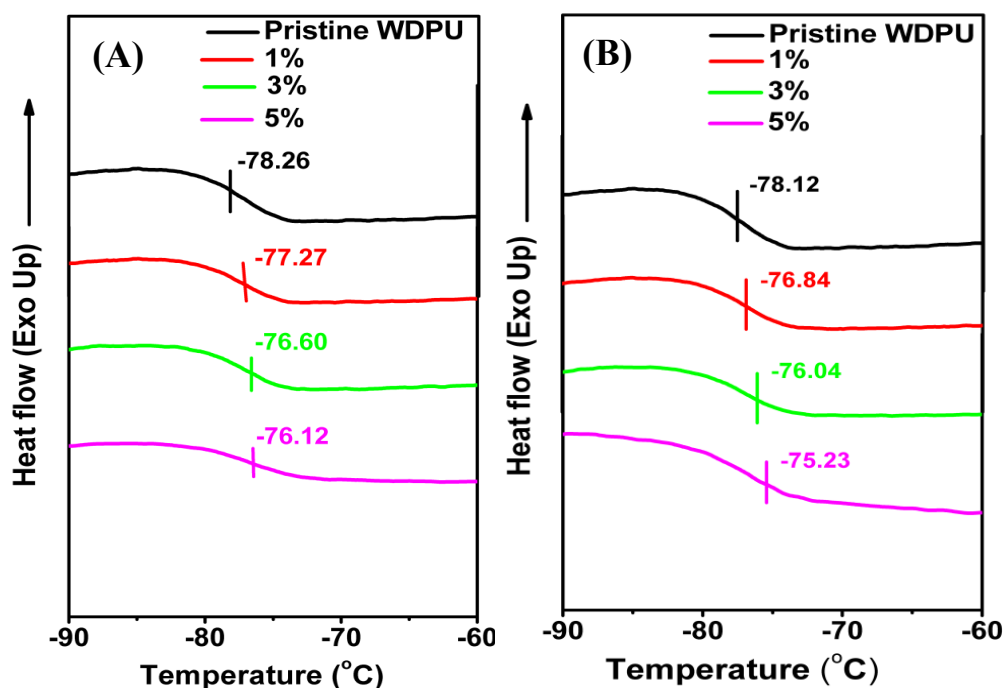


Figure 5.13. DSC plots of WDPU/clay nanocomposites; (A) WDPU/Cloisite-30B (B) WDPU/OKao. Clay loadings are indicated in the figure.

5.4.9. Surface hydrophobicity of nanocomposite films

We have prepared films from WDPU/clay nanocomposites and all the films show good thermal, mechanical and elastic properties as described in the previous sections. We have checked the hydrophobic properties of the films surfaces by measuring contact angle. Wettability is the surface property of the films and this is used for measuring the hydrophobicity of the film surface. This property mainly depends on surface energy and the geometrical arrangement or microstructure of the

surface which can be determined by measuring water contact angle. The measured contact angle images are shown in the Figure 5.14. The results show that the contact angle increases with increasing clay loading in both the cases. The maximum contact angle obtained is $\sim 107^\circ$ in case of WDPU/Cloisite-30B-5% sample. The contact angle $>100^\circ$, indicates that samples are having good hydrophobic surfaces.

The increase in hydrophobicity in nanocomposite samples is due to the hydrophobic nature of silicate layers of clay and as well as the structure formation of nanocomposite which enhances the surface roughness and hence increases the water contact angle. It is to be noted that hydrophobicity (contact angle) of WDPU/Cloisite-30B nanocomposites is more than WDPU/OKao nanocomposites. This is because of the intercalated/exfoliated structure of former and as well as the presence of long alkyl chain in the Cloisite-30B clay. The highest contact angle achieved in case of 5% nanocomposite of Cloisite-30B is because of exfoliated structure at this composition of nanocomposite.

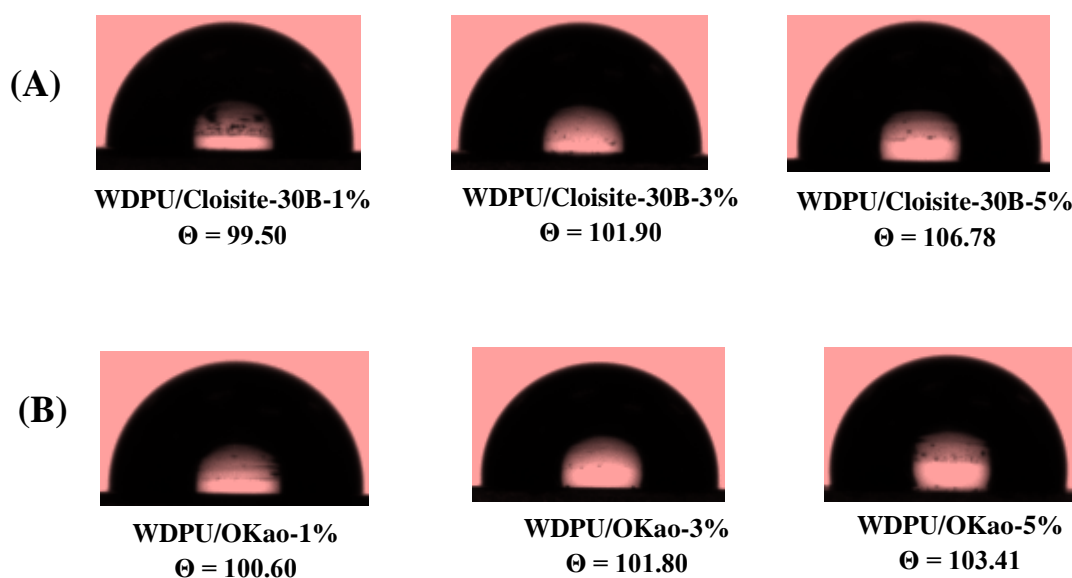


Figure 5.14. Images of water contact angles of HTPB-DNB based WDPU/clay nanocomposite PUs which varying clay loading; (A) WDPU/Cloisate-30B (B) WDPU/Oka. Measured contact angles are shown in the figure.

5.5. CONCLUSION

A series of modified HTPB based WDPU/Clay nanocomposites using two types clays namely Cloisite-30B and OKao have been prepared and thoroughly characterized. Formation of well dispersed nanometer size spherical particles has been confirmed using TEM and Zetasizer measurements and also variation of particle size was observed with change in clay structure and loading in the nanocomposite. FTIR and solid state NMR data clearly prove the presence of interactions between silicate layers of clay with carbonyl group of PU chain. Detailed structural analysis using WAXD, TEM and FESEM studies attributed the formation of intercalated (at lower loading) and exfoliated (at higher loading) structure in case of Cloisite-30B nanocomposite, whereas aggregated (microcomposite) structure has been formed in case of OKao composites. The thermal, mechanical and tensile properties of nanocomposites were found to be governed by the structure of nanocomposite. Also, the segmental motion (T_g) of PU chains has been greatly affected by the structure of nanocomposite. Finally, it has been found that the formation of nanocomposite of HTPB-DNB based WDPU significantly influenced the hydrophobic character of cured PU films. The surface contact angle of WDPU/Clay composite increased with increasing clay loading and maximum value close to 110° has been achieved in case of highest (5wt%) Cloisite-30B loading because of exfoliated nanostructure in this composition with the clay. In summary, our current study demonstrated a newer approach to obtain highly hydrophobic WDPU from the butadiene diol based polyol.

5.6 REFERENCES

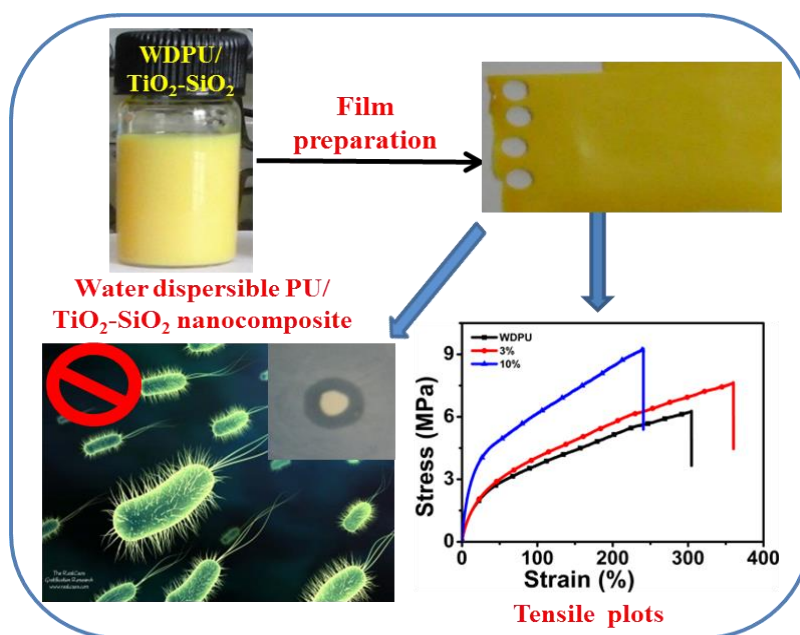
- (1) Madbouly, S. A.; Xia, Y.; Kessler, M. R. *Macromolecules*, **2013**, *46*, 4606–4616
- (2) Florian, P.; Jena, K. K.; Allauddin, S.; Narayan, R.; Raju, K. V. S. N. *Ind. Eng. Chem. Res.*, **2010**, *49*, 4517–4527
- (3) Chattopadhyay, D. K.; Raju, K. V. S. N. *Prog. Polym. Sci.*, **2007**, *32*, 352–418
- (4) Polyurethane handbook. In Oertel G, editor. 3rd ed. vol. 7. *Munich, Hanser publishers*, **1993**.
- (5) Kobayashi, S.; Song, J.; Silvis, H. C.; Macosko, C. W.; Hillmyer, M. A. *Ind. Eng. Chem. Res.*, **2011**, *50*, 3274–3279
- (6) Liu, Q.; Singh, A.; Liu, L. *Biomacromolecules*, **2013**, *14*, 226–231
- (7) Agirre, A.; Heras-Alarcon, C.; Wang, T.; Keddie, J. L.; Asua, J. M. *ACS Appl. Mater. Interfaces*, **2010**, *2*, 443–451
- (8) Im, H.; Roh, S. C.; Kim, C. K. *Ind. Eng. Chem. Res.*, **2011**, *50*, 7305–7312
- (9) Romero, G.; Estrela-Lopis, I.; Zhou, J.; Rojas, E.; Franco, A.; Espinel, C. S.; Gao, C.; Fernandez, A. G.; Donath, E.; Moya, S. E. *Biomacromolecules*, **2010**, *11*, 2993–2999
- (10) Podsiadlo, P.; Kaushik, A. K.; Arruda, E. M.; Waas, A. M.; Shim, B. S.; Xu, J.; Nandivada, H.; Pumphlin, B. G.; Lahann, J.; Ramamoorthy, A.; Kotov, N. A. *Science*, **2007**, *318*, 80–83
- (11) Wang Z, Pinnavaia T. J. *Chem Mater*, **1998**, *10*, 3769–3771.
- (12) Phua, S. L.; Yang, L.; Toh, C. L.; Huang, S.; Tsakadze, Z.; Lau, S. K.; Mai, Y.; Lu, X. *ACS Appl. Mater. Interfaces*, **2012**, *4*, 4571–4578
- (13) Chen, W.; Xu, Q.; Yuan, R. Z. *Compos Sci Technol*, **2001**, *61*, 935–939
- (14) K.B. Brandt, T.A. Elbokl, C. Detellier, *J. Mater. Chem*, **2003**, *13*, 2566–2572
- (15) Subramani, S.; Choi, S.; Lee, J.; Kim, J. *Polymer*, **2007**, *48*, 4691–4703
- (16) Subramani, S.; Lee, J.; Choi, S.; Kim, J. *Polym. Sci. Part B: Polym. Phys.*, **2007**, *45*, 2747–2761
- (17) Maiti, P.; Yamada, K.; Okamoto, M.; Ueda, K.; Okamoto, K. *Chem. Mater*, **2002**, *14*, 4654–4661
- (18) Luo, X.; Zhang, P.; Ren, J.; Liu, R.; Feng, J.; Ge, B. *J. Appl. Polym. Sci.*, **2015**, *132*, 42005–42013
- (19) Sethi, S.; Dhinojwala, A. *Langmuir*, **2009**, *25*, 4311–4313.
- (20) Zhao, L.; Liu, W. L.; Zhang, L. D.; Yao, J. S.; Xu, W. H.; Wang, X. Q.; Wu, Y. Z. *Colloids Surf. A. Physicochem. Eng. Asp.*, **2013**, *423*, 69–76.
- (21) Wang, L.; Yang, S.; Wang, J.; Wang, C.; Chen, L. *Mater. Lett.*, **2011**, *65*, 869–872.

- (22) Feng, X. J.; Jiang, L. *Adv. Mater*, **2006**, *18*, 3063-3078
- (23) Reshmi, S.; Arunan, E.; Nair, C. P. R. *Ind. Eng. Chem. Res*, **2014**, *53*, 16612-16620.
- (24) Subramanian, K. *J. Polym. Sci. Part-A; Polymer Chem*, **1999**, *37*, 4090–4099.
- (25) Krishnan, P. S. G.; Ayyaswamy, K.; Nayak, S. K. *J. Macromol. Sci. Part A: Pure Appl. Chem*, **2013**, *50*, 128–138.
- (26) Ganesh, K.; Sundarrajan, S.; Kishore, K.; Ninan, K. N.; George, B.; Surianarayanan, M. *Macromolecules*, **2000**, *33*, 326-330.
- (27) Shankar, R. M.; Roy, T. K.; Jana, T. *J. Appl. Polym. Sci*, **2009**, *114*, 732-741.
- (28) Sankar R. M.; Saha, S.; Meera K. S.; Jana T. *Bull Mater Sci*, **2009**, *32*, 507–514.
- (29) Sankar R. M.; Roy T. K.; Jana T. *Bull Mater Sci*, **2011**, *34*, 745– 754.
- (30) Rao, B. N.; Yadav, P. J. P.; Malkappa, K.; Jana, T.; Sastry, P. U. *Polymer*, **2015**, *17*, 323-333
- (31) Malkappa K.; Jana T. *Ind. Eng. Chem. Res*, **2013**, *52*, 12887–12896
- (32) Malkappa K.; Jana T.; *Ind. Eng. Chem. Res*, **2015**, *54*, 7423–7435
- (33) Ghosh, S.; Sannigrahi, A.; Maity, S.; Jana. T. *J. Phys. Chem. C*, **2011**, *115*, 11474–11483
- (34) Y. A. Elabd, J. M. Sloan, T. A. Barbari. *Polymer*, **2000**, *41*, 2203-2212.
- (35) Lee H. T.; Li-Huei Lin. *Macromolecules*, **2006**, *39*, 6133-6141.
- (36) Chakraborty, C.; Sukul, P. K.; Dana, K.; Malik. S. *Ind. Eng. Chem. Res*, **2013**, *52*, 6722–6730.
- (37) Yang, C.; Liu, F.; Liu, Y.; Liao, T. *J. Colloid. Inter. Sci*, **2006**, *302*, 123–132
- (38) Mirzataheri, M.; Mahdavian, A. R.; Atai, M. *Colloid Polym. Sci*, **2009**, *287*, 725–732
- (39) Gorrasi, G.; Tortora, M.; Vittoria, V.; *J. Polym. Sci. Part B: Polym. Phys*, **2005**, *43*, 2454-2467
- (40) Xu, R.; Manias, E.; Snyder, A.; Runt, J. *Macromolecules*, **2001**, *34*, 337-339.
- (41) Osman, M. A.; Mittal, V.; Morbidelli, M.; Suter, U. W. *Macromolecules*, **2003**, *36*, 9851-9858.
- (42) Finnigan, B.; Jack, K.; Campbell, K.; Halley, P.; Truss, R.; Casey, P.; Cookson, D.; King, S.; Martin. D. *Macromolecules*, **2005**, *38*, 7386-7396.
- (43) Rao, K. K. S. V.; Naidu, V. K. B.; Subha, M. C. S.; Sairam, M.; Aminabhavi. T. M. *Carbohydr. Polym*, **2006**, *66*, 333.
- (44) Wang, M. S.; Pinnavaia, T. J. *Chem. Mater*, **1994**, *6*, 468–474.
- (45) Letaief, S.; Leclercq, J.; Liu, Y.; Detellier, C. *Langmuir*, **2011**, *27*, 15248–15254
- (46) Alvi, M. U.; Zulfiqar S.; Yavuz C. T.; Kweon, H.; Sarwar, M. I.; *Ind. Eng. Chem. Res*, **2013**, *52*, 6908–6915
- (47) Maiti P.; Yamada K.; Okamoto M.; Ueda K.; Okamoto K. *Chem. Mater*, **2002**, *14*, 4654-4661

- (48) Mirzataheri, M.; Mahdavian, A. R.; Atai, M. *Colloid Polym Sci*, **2009**, 287, 725–732
- (49) Kim B. K.; Seo J. W.; Jeong H. M. *Eur. Poly. J.*, **2003**, 39, 85–91
- (50) Chu C.; Chiang, M.; Tai, C.; Lin, J. *Macromolecules*, **2005**, 38, 6240–6243
- (51) Letaief, S.; Elbokl, T. A.; Detellier, C. J. *Colloid. Inter. Sci*, **2006**, 302, 254–258.
- (52) Shah, R. K.; Hunter, D. L.; Paul, D. R. *Polymer*, **2005**, 46, 2646–2662
- (53) Barmar, M.; Barikani, M.; Fereidounnia, M. *Iranian. Polym. J.*, **2006**, 15, 709–714
- (54) Chung, H.; Washburn, N. R. *ACS Appl. Mater. Interfaces*, **2012**, 4, 2840–2846.
- (55) Becker, O.; Varley, R. J.; Simon, G. P. *Eur. Polym. J.*, **2004**, 40, 187–195.
- (56) Burnside, S. D.; Giannelis, E. P. *Chem. Mater*, **1995**, 7, 1597–1600

CHAPTER 6

Organic/Inorganic hybrid nanocomposites of water dispersible polyurethanes for antibacterial coating



Malkappa, K.; Rao, B. N.; Suresh, G.; Jana, T.; Ramana, C. V.
(Manuscript under preparation)

6.1. INTRODUCTION

The water dispersible polyurethanes (WDPU) are widely used for coating applications because of environmental consideration and hence many researchers are putting their efforts to prepare the WDPU with improved properties.¹⁻⁶ Despite many advantages of WDPU, there are several disadvantages such as the thermal stability, insolubility and mechanical properties which need to be addressed.^{3,7-9} In addition, hydrophobicity and antibacterial activity of the cured films of WDPU would be of very useful since they are good for coating applications. Several researchers have used nanoscale inorganic fillers which are dispersed into the polymer matrix to form a hybrid nanocomposite so that the above properties can be achieved.¹⁰⁻¹⁵

In Chapter 4, we have developed a novel method to prepare anionic water dispersible PUs¹⁶ from HTPB (hydroxyl terminated polybutadiene) and modified HTPB in which DNB (dinitrobenzene) is attached at the terminal position (called as HTPB-DNB) based polymer diols.²¹ We have observed that HTPB-DNB based WDPU has got better properties in terms of thermal, mechanical and hydrophobic character. In another work, (Chapter 5) we have further enhanced these physical properties of HTPB-DNB based WDPU by preparing nanocomposite with various clay types and by varying the clay loading in the nanocomposites. In addition to significant improvement in thermo-mechanical properties, the clay nanocomposites of HTPB-DNB based PU display the contact angle as high as ~110°. However, since the primary application of WDPU is for coating and hence antibacterial activity of WDPU along with other properties would be more interesting, challenging and useful.

The aim of the current work is to develop HTPB-DNB based WDPU with strong antibacterial activity, high hydrophobic surface and good thermo-mechanical properties. To do this we need to make nanocomposites with a such inorganic fillers so that these fillers can introduce antibacterial properties in the nanocomposites along with other physical properties.

A literature search on antibacterial coating suggests that titanium dioxide (TiO₂) nanoparticle might serve our objective. However, it is also observed that TiO₂ particles coated with SiO₂ in which TiO₂ acts as core and SiO₂ is a shell exhibit better antibacterial properties.^{4,17-20} In addition, SiO₂ is known to have influence on thermo-mechanical properties of polymer. Several reports elaborated that loading of SiO₂ in to the polymer matrix can significantly improve thermal, mechanical and chemical stabilities.

Based on these observations in this Chapter we prepared nanocomposites of HTPB-DNB based WDPU with TiO₂ (core)-SiO₂ (shell) nanoparticle. We have altered the loading of nanoparticles

and characterised the nanocomposite by measuring their thermal, mechanical, surface hydrophobicity and antibacterial activity.

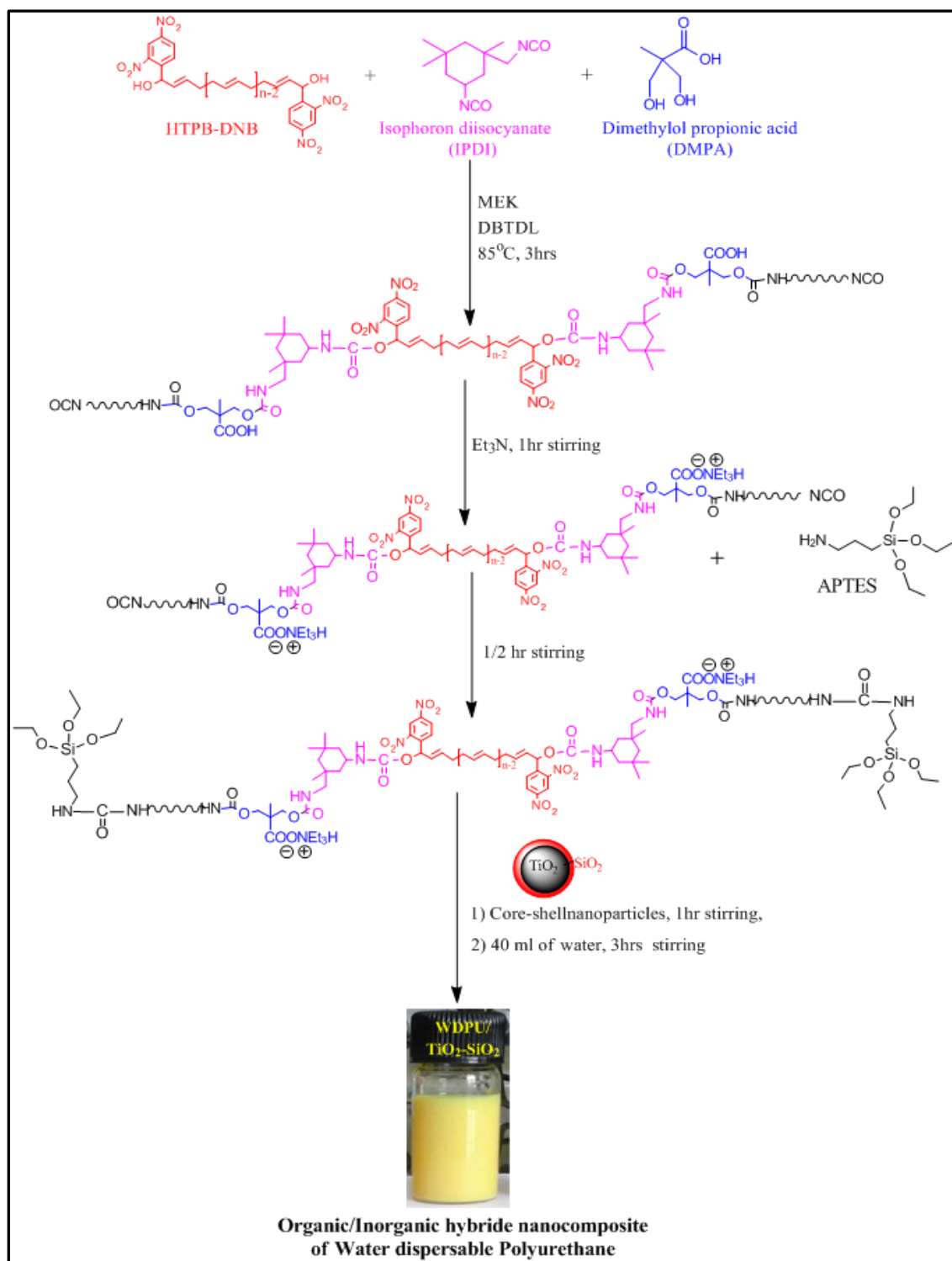
6.2. SYNTHESIS

6.2.1. Preparation of TiO₂ (core)-SiO₂ (shell) nanoparticles

2g of TiO₂ nanoparticles dispersed in isopropanol and stirred for 30 min. Then 0.6 mL of NH₄OH solution (pH=11) and 4 mL of water added and stirred for 12 h Then we added 20 mL of ethyl alcohol and reaction mixture was sonicated for 30 min. After this we added 4 mL of tetraethyl orthosilicate (TEOS) slowly drop by drop to the reaction mixture and stirring was continued for 24 h. After the reaction, we separated nanoparticles by the centrifuge.²²⁻²⁴ Then, we washed the product (nanoparticles) several times with water and EtOH until neutral pH was obtained in filtrate and we kept the product in vacuum oven for 24 h at 70°C for complete drying.

6.2.2. Preparation of water dispersible PU (WDPU) nanocomposite with TiO₂ (core)-SiO₂ (shell) particles

The WDPU/TiO₂-SiO₂ nanocomposites were prepared by using HTPB-DNB as polymer diol source with different wt% of TiO₂ (core)-SiO₂ (shell) particles content. The process is quite similar to our previous reported procedures.¹⁶ The preparation process is an *in-situ* nanocomposite preparation method.²⁵ The detailed reaction scheme is shown in Scheme 6.I. Briefly the procedure is as follows: the polymer diol (HTPB-DNB), DMPA (dimethylol propionic acid), IPDI (Isophorone diisocyanate) and catalytic amount (20 µL) of DBTDL were added into the reaction mixture. The reaction was continued by stirring at 85°C in presents of N₂ atmosphere for 3 h With progress of reaction, a viscous liquid was formed and to avoid further viscosity development ~3-5 mL of MEK (methyl ethyl ketone), at about 2 h during the reaction progress. After 3 h of reaction, -NCO terminated prepolymer was formed, which was confirmed by the presence of urethane linkage and -NCO peak frequencies in the IR spectra of the prepolymer sample. The whole reaction mixture containing -NCO terminated PU prepolymer was cooled down to room temperature. Then (triethyl amine) TEA (1.2 equivalents of DMPA) was added to the prepolymer to neutralize the carboxylic acid group because of DMPA present in the -NCO terminated PU prepolymer and one hour stirring was continued. This prepolymer further chain extended by adding required quantity of (3-Aminopropyltriethoxysillane) APTES and stirring was continued for about 30 minutes.

Scheme 6.1. Synthesis of WDPU/ TiO₂(core)-SiO₂(shell) nanocomposite

All the remaining –NCO, formed urethane urea bond with APTES which was confirmed by the complete disappearance of –NCO peak in the IR spectra at 2270 cm⁻¹ of the reaction mixture. After that, we added calculated wt% of TiO₂ (core)-SiO₂ (shell) nanoparticles to the PU polymer and continued stirring for another one hour. Then we added 40 mL of water slowly to the reaction mixture with vigorous stirring which resulted the milky water dispersion of PUs and continued for stirring another 3 h. In this reaction scheme, we varied only wt % of (1 to 10 %) of the core-shell nanoparticles of the reaction mixture and all other parameters kept constant. The calculated hard segment (HS) content was 40 %.

6.2.3. Preparations of PU films from WDPU/TiO₂-SiO₂ nanocomposites

The water dispersible nanocomposite samples were poured in a glass plate and dried at room temperature for 24 h. After that, the glass plate with the sample was kept at 70° C inside oven for 2 days for further curing of PU chains. After 2 days, free standing elastic films were pilled off from the glass Petri dish and the thicknesses of the films were about 200 μm. The films were stored in the desiccator for all further characterization.

6.3. CHARECTERIZATION TECHNIQUES

All the information about the characterization techniques which include spectroscopic characterization by fourier transform infrared spectroscopy (FT-IR) and solid state ¹³C-NMR, X-ray diffractions (WAX), transmission electron microscopy (TEM), particle size analyser (PSA), field emission scanning electron microscope (FE-SEM), thermogravimetric analysis (TGA), differential scanning coloremtry (DSC), dynamic mechanical analysis (DMA), contact angle measurement (CA), antibacterial activity and universal testing measurement (UTM) analysis studies for all the polymer samples are discussed in the Chapter 2.

6.4. RESULTS AND DISCUSSION

6.4.1. Synthesis of HTPB-DNB based WDPU and its nanocomposites with TiO₂ (core)/SiO₂ (shell) particles

In our earlier work (Chapter 5), we have observed that the HTPB-DNB based PU and their nanocomposites with clay can be readily made into water dispersible PU by introducing ionic monomers in the PU chain. We also noticed that the terminal groups (DNB) of HTPB-DNB plays a significant role in enhancing the several physical properties especially tensile strength and hydrophobicity of cured WDPU films. In Chapter 5, we also demonstrated that clay nanocomposites

of HTPB-DNB based WDPU display very high hydrophobicity with contact angle $\sim 110^\circ$. Therefore, we concluded that this type of WDPU may be suitable for aqueous based hydrophobic coating applications. We also wish to introduce the antibacterial properties into this WDPU which may be value added advantage for coatings. To do this we can introduce the TiO₂ nanoparticle, which is known for its antibacterial activity and hence we can achieve the antibacterial WDPU. However, TiO₂ nanoparticles will not interact with PU polymer unless we functionalize the TiO₂ surface. And for this we made TiO₂ (core)/SiO₂ (shell) particles which may interact with PU provided PU chain has Si-O-functionality.²⁶⁻²⁸ Figure 6.1 show the TEM images of TiO₂ and TiO₂ (core)-SiO₂ (shell) particles. Dark field image clearly proves the formation of TiO₂ (core)-SiO₂ (shell). The procedure for core-shell particles synthesis has been described in the experimental part. The particle size of these particles is in range of ~ 80 nm as obtained from TEM.

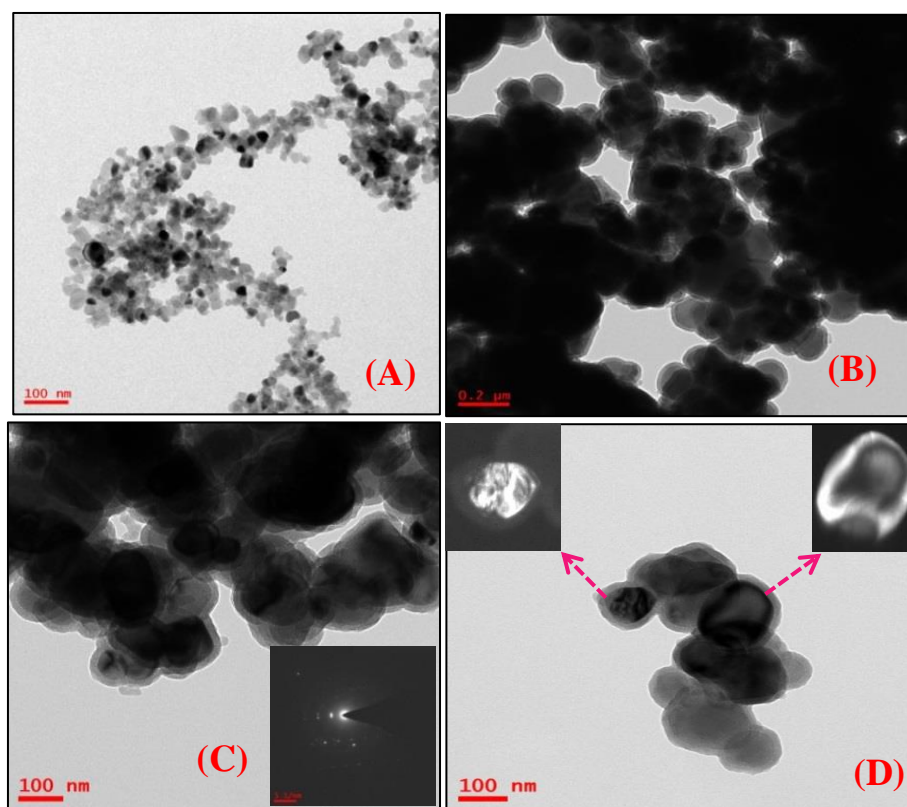


Figure 6.1. TEM images of (A) TiO₂ nanoparticle (B, C) TiO₂/SiO₂ core-shell nanoparticles low and high magnification and SAED pattern showed in the inset of image (C), (D) dark field image of TiO₂ (core)/SiO₂ (shell) nanoparticles.

To introduce the Si-O- groups in WDPU chain, in this chapter we followed the similar reaction scheme as described earlier with a little bit modification in the second stage (Scheme 6.1). We have chain extended the –NCO terminated prepolymer by reacting with APTES to form urethane-urea linkage in the polymer chain and also this reaction allows us to introduce the silicon (Si-O-) functionality in the main PU chain. After this in the 3rd stage, we added the TiO₂ (core)-SiO₂ (shell) nanoparticles (Scheme 6.1) with a hope that silicate PU chain would be interacting with silica modified TiO₂ and yield to homogeneous nanocomposite. The introduction of Si-O- in the PU chain and their interaction with core-shell nanoparticles have been studied using spectroscopic techniques and will be discussed in the next section. It is important to know the particle size and shape of WDPU/TiO₂-SiO₂ nanocomposite. Figure 6.2 and 6.3 represent the results obtained from the zetasizer and TEM, respectively. Table 6.1 lists the size and PDI obtained from zetasizer. These results clearly indicate the formation of particles with nearly spherical shape. It is to be noted that the particles size increases with increasing TiO₂-SiO₂ loading and the particle size is quite different from the TiO₂-SiO₂ particles. The PDI also increases with increasing loading of core-shell particles. We could not separately identify only the TiO₂ (core)-SiO₂ (shell) particles may be because of either very low loading of particle in the composite or the WDPU particles overshadowed the core-shell particles.

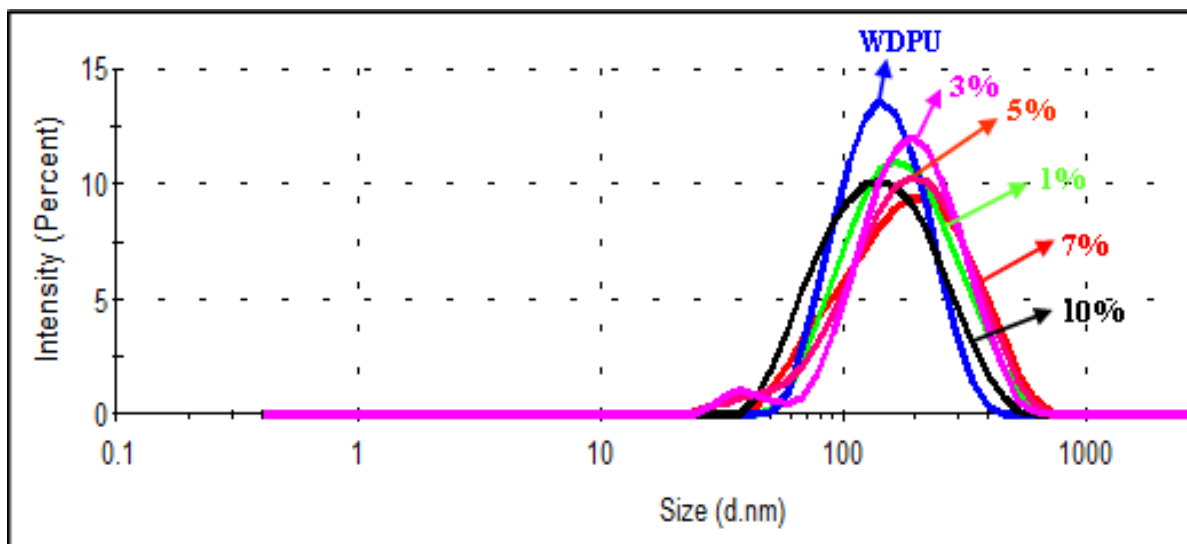


Figure 6.2. Particle size and size distribution plots (obtained from Zetasizer) of HTPB-DNB based WDPU/TiO₂-SiO₂ composites with different wt% of TiO₂-SiO₂ content.

Table 6.1. Particle size and PDI of HTPB-DNB based WDPU/TiO₂-SiO₂ nanocomposites with different wt% of TiO₂-SiO₂ nanoparticle content.

Sample Identification	TiO ₂ -SiO ₂ (Wt%)	Particle Size ^a (nm)	PDI ^a
WDPU	0	152	0.176
WDPU composites	1	155	0.210
	3	156	0.230
	5	156	0.254
	7	158	0.256
	10	155	0.258

^a Measured from zetasizer

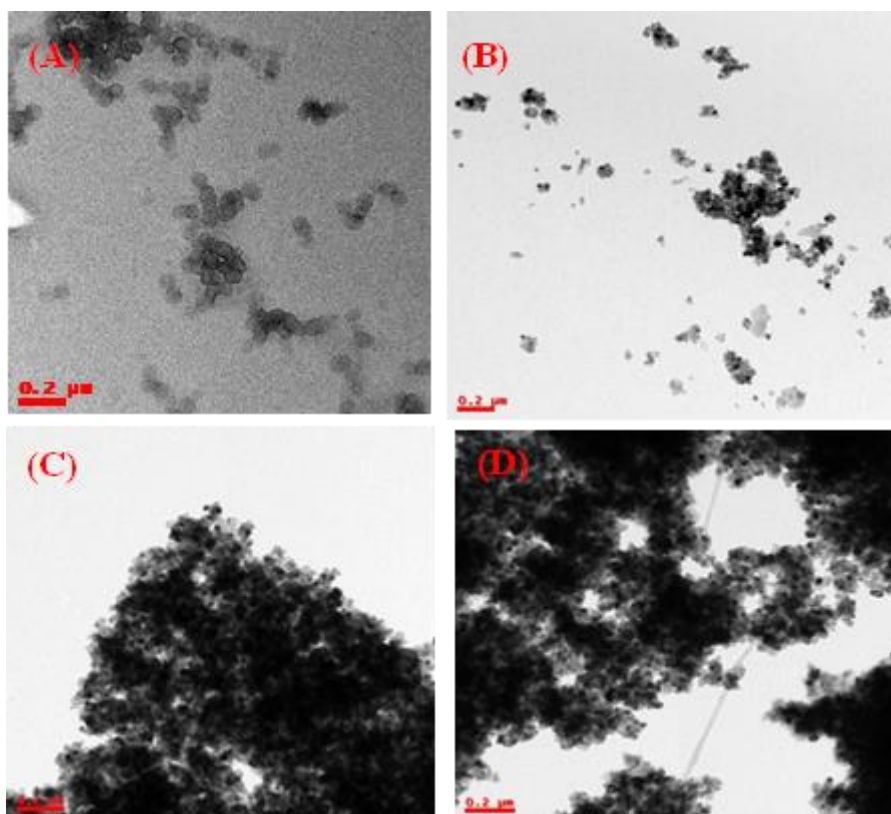


Figure 6.3. TEM images of HTPB-DNB based WDPU/TiO₂-SiO₂ nanocomposites with different wt% of TiO₂-SiO₂ content. (A) WDPU (B) 1% (C) 5% (D) 10%

6.4.2. Spectroscopic study of WDPU/TiO₂-SiO₂ nanocomposites

Both IR and SS-NMR studies were carried out on the cured film of WDPU/TiO₂-SiO₂ nanocomposite to understand the nature of interaction between the PU chain and TiO₂-SiO₂ particles. IR spectra of nanocomposite PU films with different wt% nanocomposites are shown in Figure 6.3. The three peaks (1726, 1711 and 1695 cm⁻¹) owing to -C=O region of pristine WDPU^{16,25} changes to only one peak at 1704 cm⁻¹ in case of nanocomposites. This attributes that carbonyl groups are involving in some kind of interaction with nanoparticles. The sharp peak at around 1048 cm⁻¹ in nanocomposite samples is corresponding to O-Si-O stretching frequency²⁹ and the peak intensity gradually increases with increasing TiO₂/SiO₂ nanoparticles loading in nanocomposite PU films. This indicates the insertion of nanoparticle in the composite.

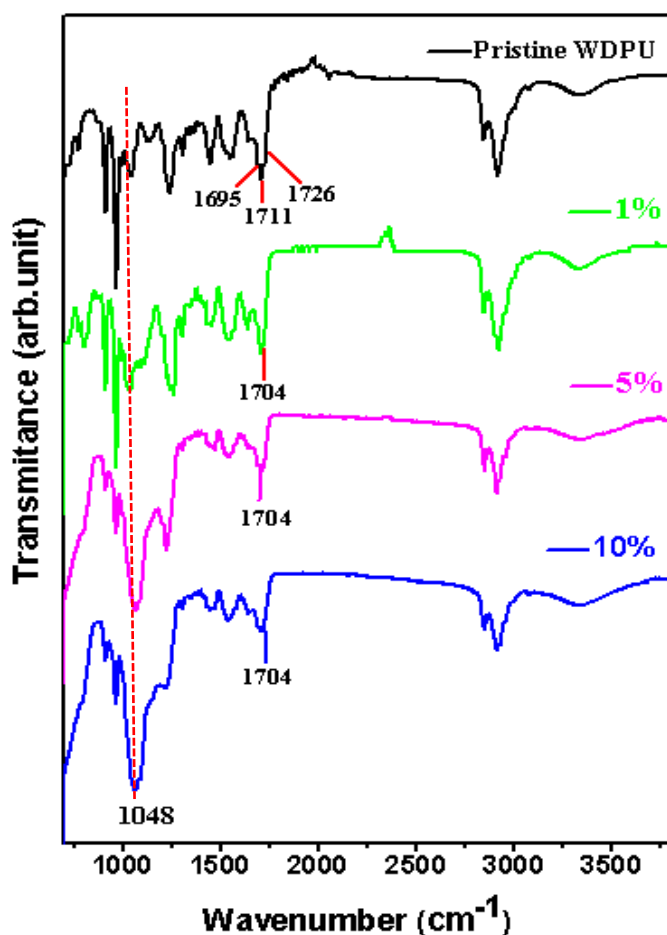


Figure 6.3. FT-IR spectra of HTPB-DNB based WDPU/TiO₂-SiO₂ nanocomposite with different wt% as indicated in the figure.

The pristine WDPU and nanocomposite samples were studied by recording ¹³C solid state NMR and the magnified portion of the spectra (δ 100-200 ppm) are shown in the Figure 6.4. The spectral characteristic peaks observed here are similar to our previously reported results.^{30,16,25} The two important peaks at around 156 and 175 ppm are corresponding to carbonyl carbon of urethane and carboxylate, respectively. These two peaks are slightly shifted at lower side with peak broadness due to interactions between the carbonyl carbon and shell part of the TiO₂-SiO₂ nanoparticles. We measured the full width at half maximum (FWHM)³¹ of both peak regions at 156 and 175 ppm to find out the broadness of peaks and listed in Table 6.2.

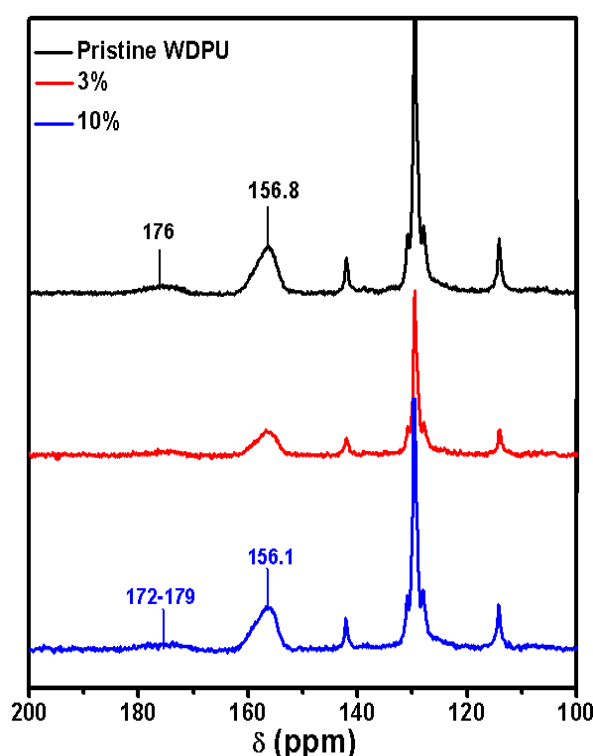


Figure 6.4. Solid state NMR of pristine WDPU and nanocomposite of different wt% of TiO₂-SiO₂ as indicated in the figure.

The value of FWHM at 156 ppm, region for pristine WDPU is 450 Hz, 3 wt % composite of WDPU is 456 Hz and highest nanoparticle content, i.e. 10 wt % composite is 473 Hz. The value of FWHM increases from pristine WDPU to composite WDPU and hence, clearly indicates the broadness of the peak with increasing nanoparticle content in the composite. Similarly, the peak at 175 ppm shows significant line broadening and the values of FWHM at that peak region for pristine

WDPU is 640 Hz, 3wt% composite WDPU is 768 Hz and 10 wt% is 989 Hz. This attributes that with increasing the TiO₂-SiO₂ nanoparticle content in the WDPU matrix the value of FWHM also increases and line broadening takes place. Both the peak regions from WDPU to nanocomposite PUs, the peak broadness was observed and with increasing wt% of the TiO₂-SiO₂ nanoparticle content the broadness also increases because of the broad distribution of the carbonyl group in the PU chain.

Table 6.2. The calculated FWHM values of HTPB-DNB based WDPU and nanocomposites of WDPU with different wt% of TiO₂-SiO₂ nanoparticle content.

Sample	FWHM (Hz)	
	Peak at 156 ppm	Peak at 156 ppm
WDPU	450	640
3%	456	768
10%	473	989

6.4.3. Wide angle X-ray diffraction (WAXD) studies

The diffraction pattern of bare SiO₂, TiO₂ and silica coated TiO₂ core-shell nanoparticles are shown in Figure 6.5(A). A series of characteristic peaks of TiO₂ nanoparticles are observed and all peaks are in good agreement with the standard diffraction pattern of TiO₂ as reported previously.^{32,22,24} However, the intensities of SiO₂ coated nanoparticles decreases little than that of bare TiO₂ because of the amorphous SiO₂ which shows broad amorphous peak at around $2\theta = 23^\circ$. After coating of SiO₂ on surface of TiO₂ nanoparticles, the characteristic peaks of TiO₂ in TiO₂ (core)-SiO₂ (shell) nanoparticles did not change.^{32, 33} This indicates that the crystal structure of TiO₂ is not effected due to the presence of amorphous SiO₂. The WAXD pattern of HTPB-DNB based WDPU and its nanocomposite with TiO₂-SiO₂ nanocomposites are shown in Figure 6.5(B). We observed some diffraction peaks owing to DNB moiety³⁰ and also in the nanocomposite of WDPU with different wt% core-shell nanoparticles display several diffraction peaks. These peaks include all the characteristics peaks of TiO₂-SiO₂ along with pristine WDPU peaks. The peak at $2\theta = 25$, which is corresponding to TiO₂-SiO₂ nanoparticles and the peak intensity increases with increasing wt% of nanoparticle loading. This clearly shows that the TiO₂/SiO₂ core-shell nanoparticles are dispersed in WDPU matrix.

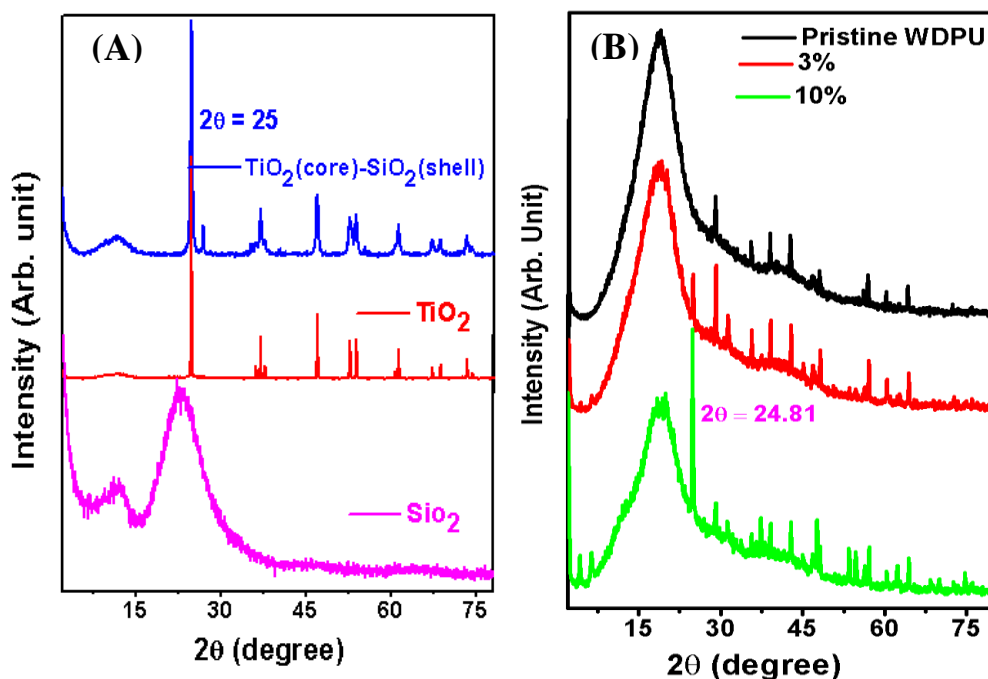


Figure 6.5. WAXD pattern (A) TiO₂, SiO₂ and TiO₂ (core)-SiO₂ (shell) nanoparticles (B) HTPB-DNB based WDPU/TiO₂-SiO₂ nanocomposite with different wt% as indicated in the figure.

6.4.4. FE-SEM studies

FESEM studies along with EDX analysis was carried out to confirm the presence of added TiO₂-SiO₂ nanoparticles in the nanocomposite WDPU films and the images are shown in Figure 6.6. EDX spectra of one of 10 wt % nanocomposite along with the elemental analysis are also presented in Figure 6.6 (E and F). Comparison of the surface morphology of pristine WDPU and the different nanocomposite of WDPU films clearly indicating the presence of nanoparticles. In all the composites, we could see that the small white dots corresponding to the nanoparticles are present and dispersed in the PU which we could not see in the pristine WDPU.²⁶ And also with increasing nanoparticles content the amount of white dots increases. The images confirm that a homogeneous and well dispersion of the nanoparticles in the WDPU matrix. This uniform dispersion of nanoparticles has taken place in the WDPU matrix plays an important role to enhance the thermal and mechanical properties of nanocomposite WDPU films which we will discuss in the later section. Figure 6.6 (E and F), clearly shown the presence of Si and Ti along with C and O. These analyses prove the presence of TiO₂-SiO₂ nanoparticles present in the WDPU matrix.

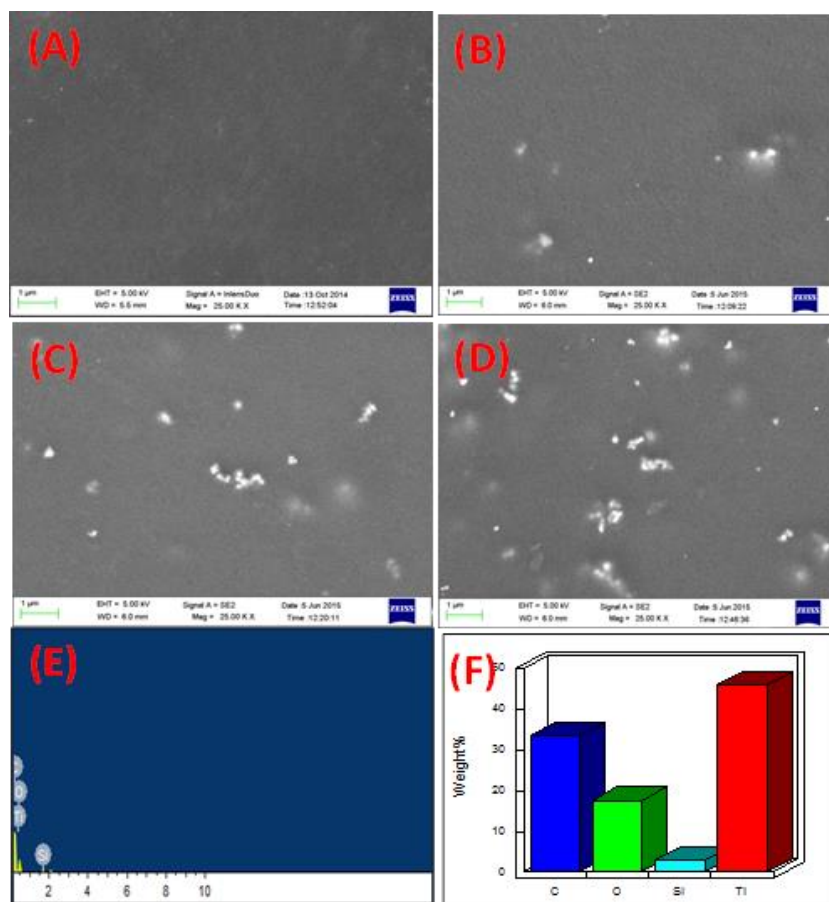


Figure 6.6. FESEM images of HTPB-DNB based WDPU/TiO₂-SiO₂ nanocomposites: (A) Pristine WDPU and nanocomposite with loading (B) 1wt% (C) 5wt% (D) 10wt% and (E) EDX spectra of 10 wt% nanocomposite. The bar diagram of different elemental wt% are presented in (F).

6.4.5. Tensile properties of WDPU/ TiO₂-SiO₂ nanocomposites

The stress-strain profile of all nanocomposite films with different wt% of TiO₂ (core)-SiO₂ (shell) are shown in the Figure 6.7. and we measured the tensile strength (σ_b), elongation at break (ϵ_b), toughness and young modulus (E) from these tensile plots. All these values are summarized in Table 6.3. The tensile strength (σ_b) and elongation at break (ϵ_b) of nanocomposite films increases for 1 and 3 wt% loading because of good interactions between the nanoparticles and WDPU matrix. However, beyond 3 wt % loading the elongation at break (ϵ_b) decreases and tensile strength (σ_b) increases with increasing wt % of the TiO₂/SiO₂ nanoparticles in the WDPU matrix. The young modulus and toughness which are responsible for materials resistance to fracture when stressed are calculated

stress-strain profile and Tableted in Table 6.3. Toughness value increases till 3 wt% and then decreases. On the otherhand Young modulus value gradually increases with increasing filler wt % in the matrix. In addition, the effective crosslinking (N) is calculated from the Figure 6.7. using the rubber elasticity theory,³⁴ in which the number of network stands for unit volume (N, effective crosslinking density) can be estimated from the relation $E = 3NK_B T$, where the E is the young modulus obtained from the stress-strain plots, K_B the Boltzmann constant and T is the absolute temperature in kelvin. N values are listed in Table 6.3, for all nanocomposites and are showing an increasing trend with loading. All these above results clearly attribute the influence of TiO₂ (core)-SiO₂ (shell) nanoparticles on the nanocomposite mechanical properties and microstructure.

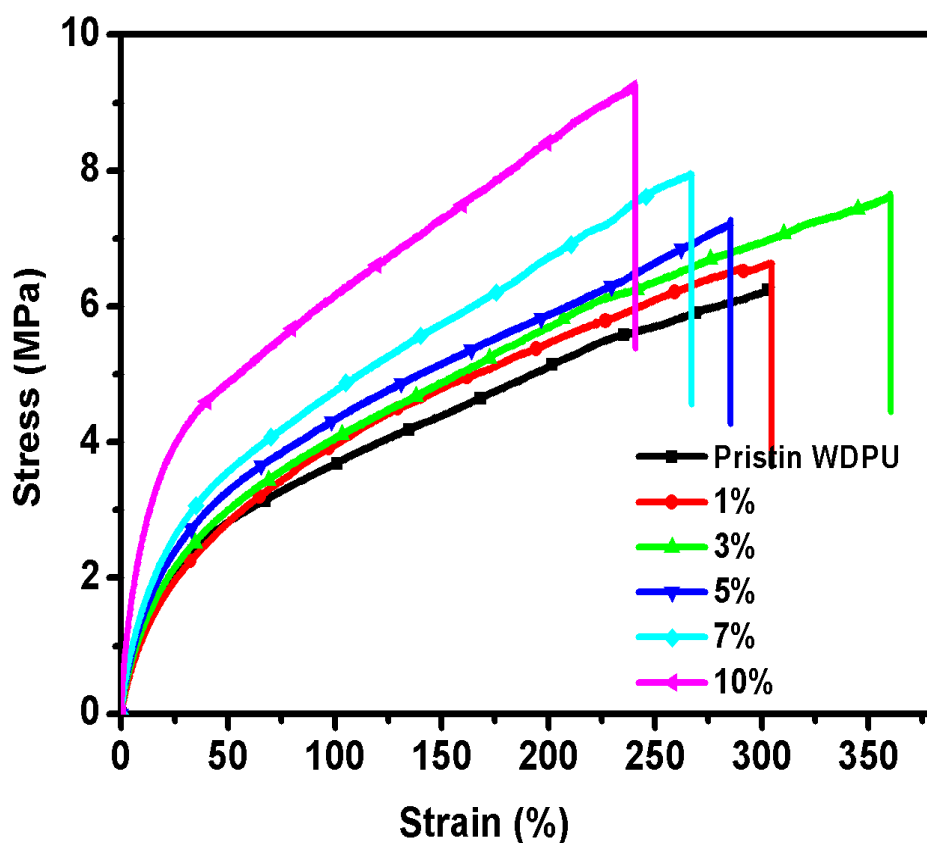


Figure 6.7. Stress-strain profile of all HTPB-DNB based WDPU/TiO₂-SiO₂ nanocomposite films with different wt% of core-shell nanoparticles as indicated in the figure.

Table 6.3. Various mechanical data obtained from stress-strain plots of all nanocomposite films.

Sample Identification	TiO ₂ (core)-SiO ₂ (shell) nanoparticle (%)	Tensile strength (MPa)	Elongation at break (%)	Toughness (MPa)	Young modulus (MPa)	Effective crosslinking (N/M ³) × 10 ²²
Pristine WDPU	0	6.24	307.79	1298.65	0.179	1420
Nanocomposite PUs	1	6.63	303.11	1377.28	0.186	1480
	3	7.64	360.17	1840.14	0.193	1540
	5	7.22	285.84	1373.59	0.227	1810
	7	7.94	267.25	1396.47	0.239	1900
	10	9.24	240.80	1543.72	0.463	3700

6.4.6. Thermo-mechanical studies of WDPU/TiO₂-SiO₂ nanocomposites

The influence of TiO₂ (core)-SiO₂ (shell) nanoparticles on the thermos-mechanical properties of the HTPB-DNB based WDPU nanocomposite films was evaluated by DMA analysis. The storage modulus (E'), Loss modulus (E'') and $\tan\delta$ of these samples as a function of temperature are shown in the Figure 6.8. The important data like T_g , E' at -100° C obtained from these figures are summarized in Table 6.4. The storage modulus (E') of all the nanocomposites are more compared to the pristine WDPU and also shows increasing trend with increasing nanoparticles loading. This increase in E' values is because of reinforcement of WDPU matrix with the TiO₂ (core)-SiO₂ (shell) nanoparticle. With increasing wt % of nanoparticles, the interaction between the PU chain and particle surface become stronger and hence the final nanocomposite becomes mechanically stronger and this data is in agreement with previous tensile data (Table 6.3.). The T_g values of all the nanocomposite PUs are shown in the Figure 6.8(B) and (C). The T_g values are shifted to somewhat higher T_g (Table 6.4) with decreasing the peak intensity than pristine WDPU because of restricted chain mobility in the PU with silica fillers. Observation on T_g values from both E'' vs temperature and $\tan\delta$ vs temperature are almost similar in nature.

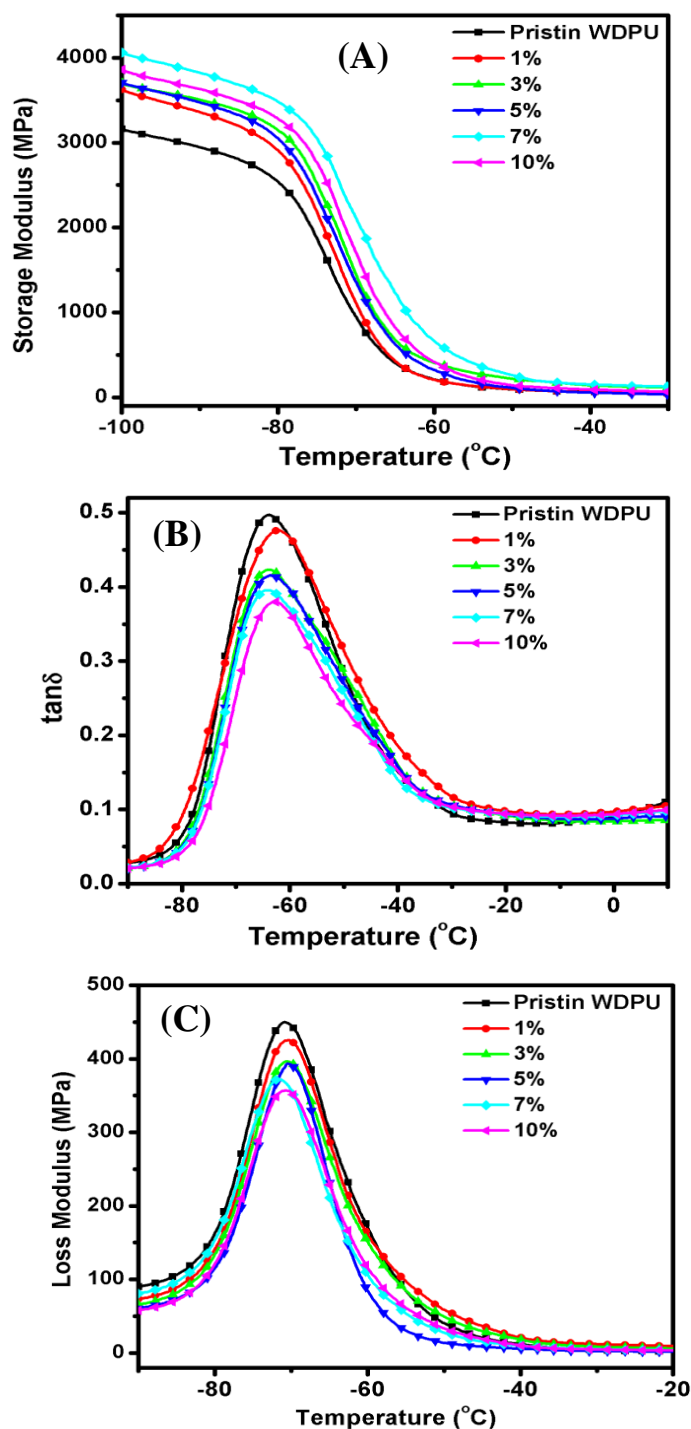


Figure 6.8. (A) Storage modulus (B) $\tan \delta$ and (C) Loss modulus as a function of temperature plots for the HTPB-DNB based WDPU/TiO₂-SiO₂ nanocomposite with different wt% of TiO₂-SiO₂ nanoparticles.

Table 6.4. Various thermo-mechanical data of all nanocomposite films obtained from DMA, DSC, and TGA studies.

Sample Identification	TiO ₂ /SiO ₂ nanoparticle (%)	^a Storage modulus (MPa)	Tan δ^b (°C)	T _g ^c (°C)	TGA data (°C)		
					^d T ₂₀	^e T ₃₀	^f T _{max}
Pristine PU	0	3160	-63.54	-76.12	290	318	464
Nanocomposite PUs	1	3615	-62.83	-75.42	312	339	481
	3	3698	-63.42	-74.84	305	340	478
	5	3731	-63.42	-73.14	307	362	524
	7	4065	-63.81	-73.64	313	366	526
	10	3879	-62.51	-72.38	309	358	549

^a measured storage modulus at -100° C, ^b obtained from tan δ vs temperature plot of DMA study,

^c measured from DSC thermograms, temperature at which ^d20% weight loss and ^e30% weight loss are obtained. ^f Temperature of maximum weight loss.

To reconfirm the T_g values and elastic nature of nanocomposite films, we further carried out differential scanning calorimetry (DSC) experiment to measure the T_g values. The DSC thermograms of nanocomposite films of different wt % loading of TiO₂-SiO₂ nanoparticles are represented in Figure 6.9 and the T_g values are summarized in Table 6.4. From the results it is clear that the T_g values is in the subambient range at around -75° C suggesting that the rubbery nature of our composite and similar to the DMA results as explained in the previous section. From the results it is evident that T_g values increase with increasing loading though change is not very significant. This is because of the interaction between the nanoparticles and PU matrix which alters the segmental motion by changing the free volume of PU chains resulting in the higher T_g in case of nanocomposites.

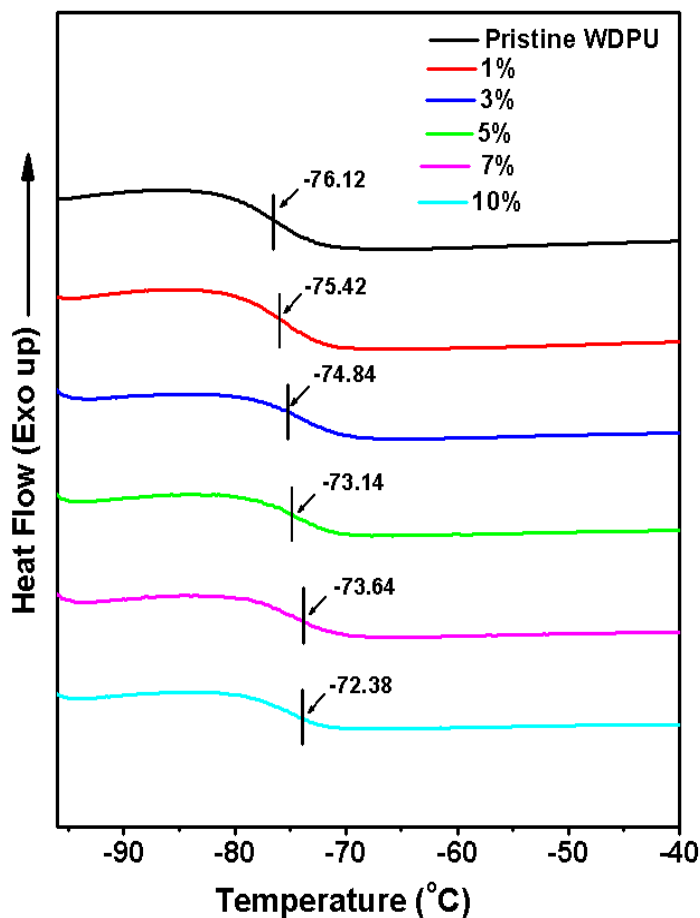


Figure 6.9. DSC thermograms of HTPB-DNB based WDPU/TiO₂-SiO₂ nanocomposite films.

The TGA curves of the WDPU and its nanocomposite film samples are shown in Figure 6.10. It is clear from the TGA plots and Table 6.4 data that the thermal stability of all the composite are more compared to pristine WDPU and with the increasing nanoparticles loading in composites the thermal stability also increases. From Figure 6.10, we could observe that the thermal degradation of nanocomposites started at around 225 °C for all the nanocomposite films. The other important weight loss at different percentage are summarised in Table 6.4 and the data clearly attributes to the higher thermal stability of nanocomposite compared to pristine WDPU. Hence, it can be concluded that the TiO₂-SiO₂ nanoparticles enhances thermal stability by acting as barrier layers and inhibiting heat and mass transfer.³⁵

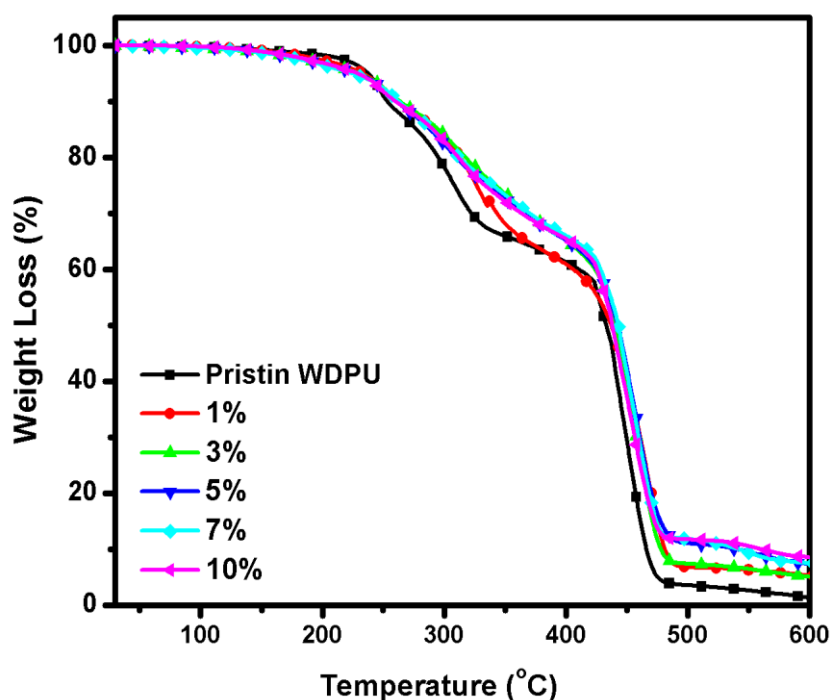


Figure 6.10. TGA curves of HTPB-DNB based WDPU/ TiO₂-SiO₂ nanocomposite films.

6.4.7. Surface hydrophobicity of WDPU/TiO₂-SiO₂ nanocomposite films

As discussed in the previous section, it has been found that nanocomposite WDPU films show good thermal, mechanical, elastic behaviour. To find out the hydrophobicity of the film surface, we have measured the surface water contact angle of all the nanocomposite PU films. The results are shown in Figure 6.11 along with the contact angle data. Although we expected increasing contact angle in nanocomposite as we have observed previously with clay nanocomposite (Chapter 5) however, the data presented in Figure 6.11 display decrease in contact angle with increasing loading of nanoparticles. This may be due to the surface SiO₂ on the nanoparticle which contains -OH functional groups which has moderate hydrophilic nature.³⁶⁻³⁸

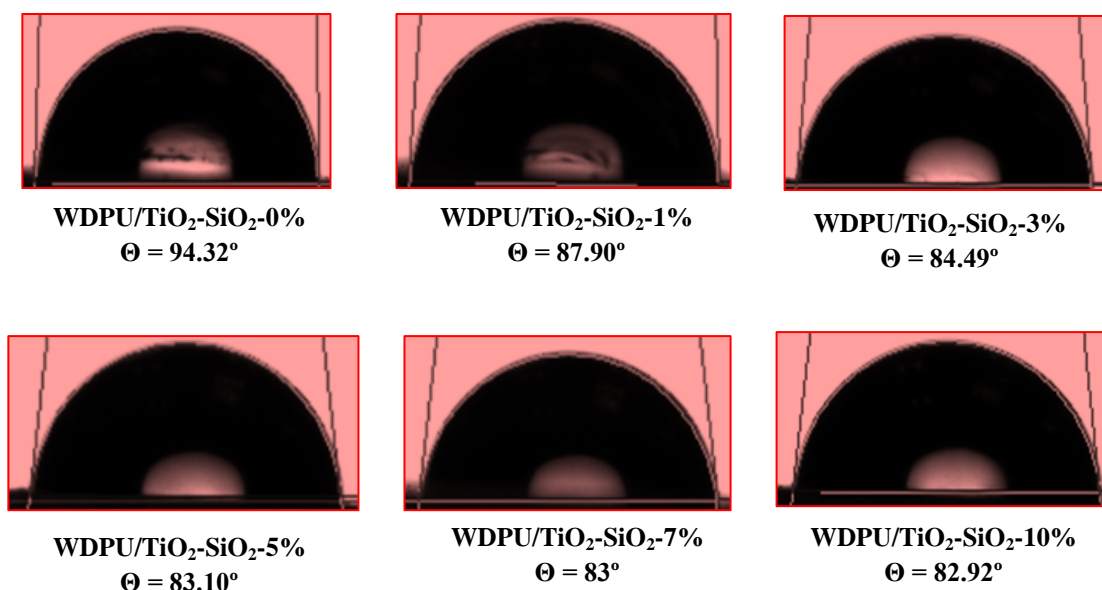


Figure 6.11. Contact angle images of of HTPB-DNB based WDPU/TiO₂-SiO₂ nanocomposite films with different wt% TiO₂-SiO₂ nanoparticle loading.

6.4.8. Antibacterial activity

The antibacterial activity of the nanocomposite films was evaluated against *Escherichia coli* (gram-negative) and *Staphylococcus aureus* (gram-positive) bacteria after 16 h of incubation period using the disc diffusion method. All the composite films antibacterial activity measurements are shown in the Table 6.5. and Figure 6.12. The antibacterial activity of the composite films was determined based on the formation of a zone which is inhibiting bacterial growth surrounding the film and beneath the films placed on a nutrient agar medium. The antibacterial activity of the composite films increases with increasing nanoparticle loading in the composite films as observed from the Figure 6.12 and Table 6.5. The zone of inhibition increases in both the cases with increasing loading. It is to be noted that the zone of inhibition is more clear and bigger in size in case of gram positive than gram negative. So the results indicate that these nanocomposites have strong affinity to the cells of *S. aureus* than *E. coli*. This may be due to difference in membrane structure of bacteria.^{26,3,39-43}

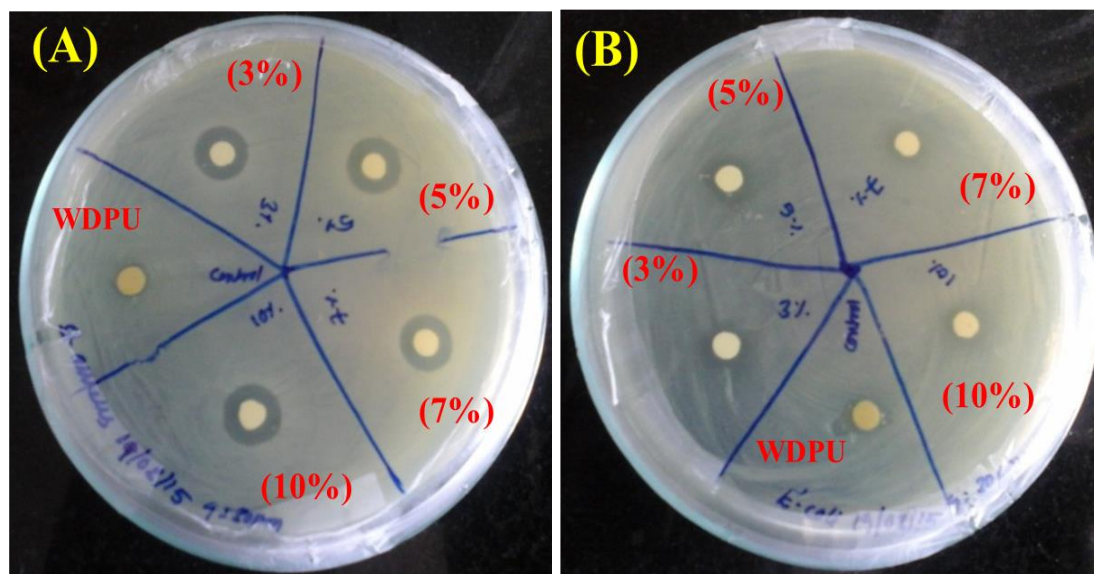


Figure 6.12. The antibacterial activity of HTPB-DNB based WDPU/ TiO₂-SiO₂ nanocomposite films with two types of bacteria: (A) *Staphylococcus aureus* (B) *Escherichia coli*.

Table 6.5. Zone of Inhibition data of antibacterial activity of all nanocomposite films

Sample Identification	TiO ₂ -SiO ₂ nanoparticle (%)	Zone of Inhibition diameter (mm)	
		<i>S. aureus</i>	<i>E. coli</i>
Pristine PU	0	6	6
Nanocomposite PUs	3	8.30	7.60
	5	10.70	8.30
	7	11.20	7.40
	10	11.30	8.10

6.5. CONCLUSION

TiO₂ (core)-SiO₂ (shell) nanoparticles were prepared by sol-gel process and these particles have been used as inorganic nanofillers to prepare the nanocomposites of modified HTPB (HTPB-DNB) based water dispersible PUs. We identified the strong interactions between the TiO₂-SiO₂ nanoparticles and the carbonyl group of PU matrix with FTIR and solid-state ¹³NMR study. From WAX study, it is clearly proved that TiO₂-SiO₂ is present in the composite WDPU. From UTM analysis, we found out the mechanical strength of the nanocomposite PUs and quantified based on Young modulus, toughness, and tensile strength of the cured films. It has been observed that with increasing TiO₂-SiO₂ nanoparticles in composite, tensile strength and young modulus increases but elongation at break decreases. Similarly, thermal stability and glass transition temperature increases with increasing TiO₂-SiO₂ content in the nanocomposite. The antibacterial activity studies were carried out using disc diffusion method with two microorganisms: *Staphylococcus aureus* and *Escherichia coli* and found that the nanocomposite samples inhibit *S. aureus* more compared to *E. coli*, because of its different cell structures and also we could observe the clear zone of inhibition circles in case of *S. aureus*. Therefore, these WDPU/TiO₂-SiO₂ nanocomposites are useful for antibacterial hydrophobic coating and biomedical applications.

6.6 REFERENCES

- 1) Armelao L., Barreca D., Bottaro G., Gasparotto A., Gross S., Maragno C., Tondello E. *Coordination Chemistry Review*, **2006**, 250, 1294–1314.
- 2) Noble, K. L.; Prog Org Coat, 1997, 32, 131–136.
- 3) Xue-Yong Ma, Wei-De Zhang. *Polym Degrad Stab*, **2009**, 94, 1103–1109
- 4) Chen, Y. R. M.; Zhang, Y. Wu, L. *Langmuir*, **2010**, 26, 11391–11396
- 5) Zhang, X. T.; Sato, O.; Taguchi, M.; Einaga, Y.; Murakami, T.; Fujishima, A. *Chem. Mater*, **2005**, 17, 696–700.
- 6) H. Kong, J. Jang, *Langmuir*, **2008**, 24, 2051–2056.
- 7) Chou, C. W.; Hsu, S. H.; Chang, H.; Tseng, S. M.; Lin, H. R. *Polym Degrad Stab*, **2006**, 91, 1017–24.
- 8) Cao, X. D.; Dong, H.; Li, C. M. *Biomacromolecules*, **2007**, 8, 899–904.
- 9) Jeon, H. T.; Jang, M. K.; Kim, B. K.; Kim, K. H. *Colloid Surface A*, **2007**, 302, 559–567.
- 10) Zhu, J.; Wei, S.; Haldolaarachchige, N.; Young, D. P.; Guo, Z. *J. Phys. Chem. C*, **2011**, 115, 15304–15310
- 11) Kuan, H. C.; Ma, C. C.; Chang, W. P.; Yuen, S. M.; Wu, H. H.; Lee, T. M. *Compos Sci Technol*, **2005**, 65, 1703–1710.
- 12) El-Sayed, M.; Mahmoud, W. M.; Davis, E. M.; Coughlin, R. W. *Int. Biodeterior Biodegrad* **1996**, 37, 69–79
- 13) Kim, B. K.; Seo, J. W.; Jeong, H. M. *Eur Polym J*, **2003**, 39, 85–91.
- 14) Hsu, S. H.; Chou, C. W.; Tseng, S. M. *Macromol Mater Eng*, **2004**, 289, 1096–1101.
- 15) Zhao, C. X.; Zhang, W. D. *Eur Polym J*, **2008**, 44, 1988–1995.
- 16) Malkappa K.; Jana T.; *Ind. Eng. Chem. Res*, **2015**, 54, 7423–7435
- 17) Liga, M. V.; Maguire-Boyle, S. J.; Jafry, H. R.; Barron, A. R.; Li, Q. *Environ. Sci. Technol*, **2013**, 47, 6463–6470
- 18) Michael V. Liga, Samuel J. Maguire-Boyle, Huma R. Jafry, Andrew R. Barron, Qilin Li. *Environ. Sci. Technol*, **2013**, 47, 6463–6470
- 19) Permpoon, S.; Berthome, G.; Baroux, B.; Joud, J. C.; Langlet, M. *J. Mater. Sci*, **2006**, 41, 7650.
- 20) Yunchen Du, Wenwen Liu, Rong Qiang, Ying Wang, Xijiang Han, Jun Ma, Ping Xu, *ACS Appl. Mater. Interfaces*, **2014**, 6, 12997–13006
- 21) Shankar, R. M.; Roy, T. K.; Jana, T. *J. Appl. Polym. Sci*, **2009**, 114, 732–741.

- 22) Yu Lu, Yadong Yin, Brian T. Mayers, Younan Xia. *Nano Lett*, **2002**, 2, 183-186
- 23) Sotiriou, G. A.; Hirt, A. M.; Lozach, P.; Teleki, A.; Krumeich, F.; Pratsinis, S. E. *Chem. Mater*, **2011**, 23, 1985–1992
- 24) Yonghui Deng, Dawei Qi, Chunhui Deng, Xiangmin Zhang, and Dongyuan Zhao. *J. Am. Chem. Soc*, **2008**, 130, 28-29
- 25) Malkappa K.; B. N. Rao.; Jana T. (Communicated to *J. Phys. Chem. C*)
- 26) Kishore K. J.; Narayan, R.; Raju, K. V. S. N. *Polym Int*, **2012**, 61, 1309–1317
- 27) Chattopadhyay, D. K.; Muehlberg, A. J.; Webster, D. C. *Progress in Organic Coatings*, **2008**, 63, 405–415
- 28) Ennaoui, A.; Sankapal, B. R.; Skryshevsky, V.; Lux-Steiner, M. Ch. *Sol. Energy Mater. Sol. Cells*, **2006**, 90, 1533–1541
- 29) Ghosh, S.; Sannigrahi, A.; Maity, S.; Jana. T. *J. Phys. Chem. C*, **2011**, 115, 11474–11483
- 30) Malkappa K.; Jana T. *Ind. Eng. Chem. Res*, **2013**, 52, 12887–12896
- 31) Yang, C.; Liu, F.; Liu, Y.; Liao, T. *J. Colloid. Interface. Sci*, **2006**, 302, 123–132
- 32) Vladimir V.; Bojana M, Milan N.; Stevan O. *Proces. Appl. Ceram*, **2013**, 7, 45–62
- 33) Balachandran, K.; Venckatesh, R.; Sivaraj, R. *Inter. J. Res. Eng. Tech*, **2013**, 02, 46-51.
- 34) Chung, H.; Washburn, N. R. *ACS Appl. Mater. Interfaces*, **2012**, 4, 2840–2846.
- 35) D. K. Chattopadhyay, D. C. Webster, *Prog. Polym. Sci*. **2009**, 34, 1068-1133.
- 36) Zhang, X. T.; Sato, O.; Taguchi, M.; Einaga, Y.; Murakami, T.; Fujishima, A. *Chem. Mater*, **2005**, 17, 696-700.
- 37) Wier, K. A.; McCarthy, T. J. *Langmuir*, **2006**, 22, 2433-2436
- 38) Tricoli, A.; Righettoni, M.; Pratsinis, S. E. *Langmuir*, **2009**, 25, 12578-12584.
- 39) Shah, S. A. S.; Nag, M.; Kalagara, T.; Singh, S.; Sunkara, V. M. *Chem. Mater*, **2008**, 20, 2455–2460
- 40) Jin, C.; Jiang, Y.; Niu, T.; Huang, J. *J. Mater. Chem*, **2012**, 22, 12562–12567
- 41) Yang Hou.; Xinyong Li.; Qidong Zhao.; Guohua Chen.; Colin L. Raston. *Environ. Sci. Technol*, **2012**, 46, 4042–4050
- 42) Sheikha, F. A.; Kanjwalb, M. A.; Saranc, S.; Chung, W.; Kim, H. *Appl. Surf. Sci*, **2011**, 257, 3020–3026
- 43) Jafry, H. R.; Liga, M. V.; Qilin, Li.; Barron, A. R. *Environ. Sci. Technol*, **2011**, 45, 1563–1568

CHAPTER 7

Summary & Conclusions

7.1. SUMMARY

This thesis entitled “*Studies of Polybutadiene diol based Water Dispersible Polyurethanes and their Nanocomposites*” describes the methods to prepare polyurethane, water dispersible polyurethanes and their nanocomposites using HTPB and modified HTPB (HTPB-DNB) as a polymer diols. The thesis contains the seven chapters. The summary of the contents of each chapter are described below.

Chapter 1

This chapter deals with the brief introduction of about different types of polyurethanes that is in solvent based and water based PUs, described the different types of water dispersible PUs, described about different polyols and diisocyanates, about HTPB and modified HTPB, history of the polyurethanes, briefly discussed about their applications in various fields, and physical and chemical properties. A brief introduction about hydrophobic water dispersible PU coating materials and other applications like antibacterial applications and challenges involved to improve the hydrophobicity of the PU coating material and antibacterial activity for the use of hydrophobic antibacterial coating applications. Finally the aim of the present work is given.

Chapter 2

Describes the details the source of all the materials which were used for all the working chapters and the details instrumentation methods for characterization, and properties evaluation of the synthesized different types of polyurethanes and their nanocomposites.

Chapter 3

Chemical modifications of hydroxyl-terminated polybutadiene (HTPB) with hydrogen bond forming functionalities were used as tactics to improve both tensile strength and elongation of polyurethanes (PUs) simultaneously. PUs were prepared using various diisocyanates with modified HTPB in which dinitrobenzene (DNB) groups are attached to terminal carbon atoms. The spectroscopic studies revealed the presence of an additional hydrogen-bonding network between DNB and the urethane backbone, which resulted into supramolecular cross-linking and was found to be responsible for significant improvement in mechanical properties of HTPB-DNB-PUs. Also, substantial improvement of elongation at break was observed in the case of HTPB-DNB-PUs. Small angle X-ray scattering (SAXS) and thermodynamical studies indicated a strong segmental mixing

between the hard and soft segments of HTPB-DNB-PU. Growth of partial crystalline character in HTPB-DNB-PU was believed to be responsible for “fibrous-assembly” morphology. In summary, modification of HTPB induced extra cross-linking through supramolecular hydrogen bonding which in turn concurrently enhanced both strength and elongation of PUs.

Chapter 4

Preparation of stable, freestanding elastic film with hydrophobic surface from water dispersible polyurethanes (WDPU) is a challenging task. Here, we have prepared WDPU from Polybutadiene based diols and the resulting PU films are satisfying the requisites. Two types of diols, namely, hydroxyl-terminated polybutadiene (HTPB) and terminal-functionalized HTPB with dinitrobenzene (DNB) [HTPB-DNB], were used to make WDPU and the effects of diol structures were investigated. The synthesized WDPU displayed particle morphology with size in the range of ~130–270 nm and more than 1 year storage stability. WDPU yielded stable and free-standing films upon curing and the resulting films showed high thermal and mechanical stabilities. The contact angle of the films is in the range of ~80–100°, attributing the hydrophobic nature of the surface. Hard segment content of the PU varied from 30 to 40% (by weight) to tune the properties of WDPU and the resulting films.

Chapter 5

In this chapter, we wish to further enhance the hydrophobicity and mechanical properties of HTPB-DNB-WDPU. To do this we have chosen two different organically modified clays, such as Cloisite-30B and Kaolinite (OKao) and we observed that the effect of clay structures on the nanocomposite morphology and other properties. The structure of the clay composites were analysed using PXRD and FESEM, TEM microscopic studies, and suggested that different morphological structures from different clays. In case of Cloisite-30B composite PUs, at lower percentage of clay intercalated structure and at higher percentage of clay, exfoliated structures were obtained. In case of OKao composite PUs, we could expect one of the situations either intercalated or exfoliated nanocomposites. However, in this case, we observed one of the interesting observations that are the displacement of DMSO from the interlayer space without intercalation of the polymer and it forms aggregated structure (microcomposite). The tensile properties of all elastomer clay composite PU films, with organically modified different types of organo clays with different wt% loadings were found to have remarkable reinforcing effect in both composite PUs because of good interaction

between the silicate layers and the PU matrix. The prepared clay composite PU samples displayed very high water contact angle, which indicates the hydrophobicity of the composite PU films.

Chapter 6

In this chapter, we have prepared the organic/inorganic hybrid nanocomposites of HTPB-DNB-WDPUs with $\text{TiO}_2/\text{SiO}_2$ core-shell nanoparticles to improve the thermo-mechanical properties along with to use as an antibacterial applications. The nanocomposite of HTPB-DNB-WDPU/ TiO_2 - SiO_2 core-shell nanocomposites displays high mechanical strength and more thermal stability than pristine WDPU. The FT-IR and ^{13}C -NMR, analysis revealed that the existence of strong hydrogen-bonding interactions between the carbonyl carbons of WDPU chain and TiO_2 - SiO_2 core-shell nanoparticles resultant that significant improvement in mechanical properties such as Young modulus, tensile strength and toughness and also all these properties increases with increasing TiO_2 - SiO_2 nanoparticles content in WDPU matrix because of reinforcement. The DMA study showed that all the composite WDPUs are elastic and those T_g values around at -68°C . The entire composite PU films shows contact angle around 90° indicates these are hydrophobic and all the WDPU/ TiO_2 - SiO_2 nanocomposites showed antibacterial activity. Therefore, all the studies revealed that the WDPU/ TiO_2 - SiO_2 composite PUs could use as an antibacterial coating material in the field of coating applications.

7.2 CONCLUSION

The following conclusions are drawn from the “*Studies of Polybutadiene diol based Water Dispersible Polyurethanes and their Nanocomposites.*”

1. A series of HTPB and modified HTPB (HTPB-DNB) based PUs were synthesised using different types of diisocyanates and characterized.
2. The terminal modification of HTPB highly influences the properties of the PUs such as thermal, mechanical and other properties.
3. The soft and hard segmental mixing of all the PUs were studied with the help of SAXS and DMA studies. The DMA study clearly demonstrates the presence of two T_g values from all the HTPB-DNB-PUs because of segmental phase mixing.
4. The partial crystalline nature was obtained in case of HTPB-DNB-PUs because of fibrous-assembly like morphology then ordering.
5. A series of HTPB and modified HTPB (HTPB-DNB) based water dispersible PUs were synthesised with varying the percentage of hard segment content and the required properties for coating material were characterized using different instrumental techniques.

6. All the water dispersible PUs are longer time stable (more than a year) with nanoparticle morphology. The TEM and PSA (particle size analyzer) study revealed that spherical nanoparticle morphology and narrow PDI distribution.
7. The hydrophobic properties of the PU films surfaces were studied based on contact angle measurement. All the PU film surfaces shows around 90° contact angle indicating hydrophobic character and with increasing percentage of HS content the contact angle also increases.
8. The tensile strength of the PU films increases with increasing % HS content while elongation decreases.
9. The surface roughness of the films was studied with AFM, the surface roughness increases with increasing the % HS content of the PUs which is responsible to increases the contact angle.
10. The properties of WDPUs can be efficiently controlled by varying the percentage of HS content such as varying the weights of initial monomers during the synthesis of water dispersible PU.
11. The nanocomposite of PU with two types of organically modified clays (Cloisite-30B and OKao), have been developed by *in-situ* method and characterized.
12. The morphology and properties of the WDPU/Clay nanocomposites were found to be governed by the structure of the clay and the percentage of the clay loading.
13. The incorporation of the nanoclay in the WDPU matrix resulted into highly improvement in mechanical, thermal and hydrophobic properties.
14. The incorporation of $\text{TiO}_2\text{-SiO}_2$ core-shell nanoparticles into the WDPU matrix enhanced thermal and mechanical properties compared to pristine WDPU and with increasing nanoparticle content the thermo-mechanical properties also increases.
15. All the WDPU/ $\text{TiO}_2\text{-SiO}_2$ composite PU films displayed antibacterial activity.

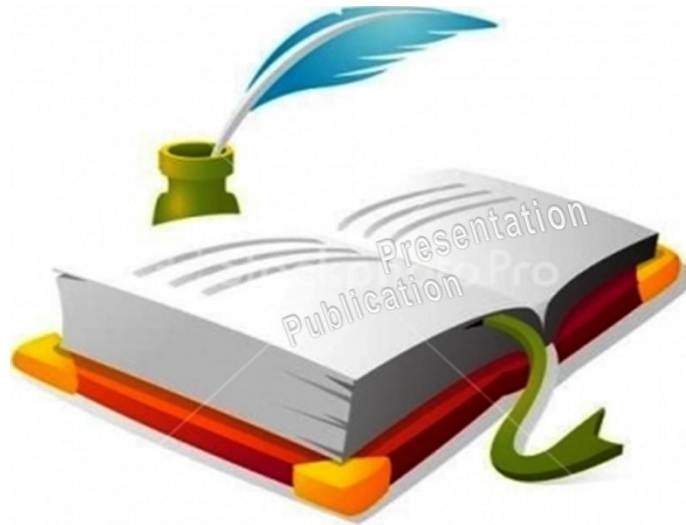
7.3 SCOPE OF FUTURE WORK

The present thesis has addressed various issues in the synthesis of polyurethanes from HTPB and modified HTPB (HTPB-DNB) used as polymer diols in different mediums such as solvent and water based PUs. The effect of terminal modification of HTPB polymer diols, the structure property relationship of the PUs, soft and hard segmental mixing, particle morphology, mechanical and hydrophobic properties of PUs play a significant role. Throughout this study, we have experienced several issues which need to be addressed and more importantly, the thesis work has been motivated

us to think in the new directions. Overall, the thesis has following outcome and the potential, which may be addressed by the researchers in future.

1. Different types of modified HTPB based water dispersible PUs and solvent based PUs can be synthesized using established methods in this thesis.
2. More systematic efforts must be given to understand the simultaneous improvement of tensile strength and elongation at break in PU chemistry.
3. The structure property relationship and segmental phase mixing need to be studied with the help of SAXS, microscopy and DMA studies.
4. Efforts can be made to synthesis water dispersible PUs with the help of established methods in this thesis.
5. A variety of water dispersible PUs can be synthesized.
6. Flame retardant HTPB based water dispersible PUs can be synthesized.
7. Efforts may be made to synthesis of super hydrophobic HTPB based water dispersible PUs through introducing fluorine containing functionalities into the PU backbone.
8. Efforts must be made to understand the longer time stability of water dispersible PUs.
9. Efforts must be made for the use of varieties of nanofillers into the PU matrix to improve the properties such as thermal, mechanical, hydrophobic and antibacterial properties.

Publications & Presentations



PUBLICATIONS

- (1) *Particle-size-dependent properties of sulfonated polystyrene nanoparticles.* Mousumi Hazarika, **Kuruma Malkappa**, Tushar Jana. *Polymer Int.* **2012**, 61, 1425-1432.
- (2) *Simultaneous improvement of tensile strength and elongation: An unprecedented observation in case of HTPB polyurethanes.* **Kuruma Malkappa**, Tushar Jana. *Ind. Eng. Chem. Res.* **2013**, 52, 12887-12896.
- (3) *Hydrophobic, water dispersible polyurethane: Role of polybutadiene diol structure.* **Kuruma Malkappa**, Tushar Jana. *Ind. Eng. Chem. Res.* **2015**, 54, 7423-7435.
- (4) *Functionalized polybutadiene diol based hydrophobic, water dispersible polyurethane nanocomposite: Role of Organoclays structure.* **Kuruma Malkappa**, Billa Narasimha Rao, Tushar Jana. (*Communicated to J. Phys. Chem. C*).
- (5) *Organic/Inorganic hybrid nanocomposites of water dispersible polyurethanes for antibacterial coating.* **Kuruma Malkappa**, Billa Narasimha Rao, G. Suresh, Ch. Venkata Ramana, Tushar Jana. (*Manuscript under preparation*).
- (6) *Triazine functionalized hydroxyl terminated polybutadiene polyurethane: influence of triazine structure.* Billa Narasimha Rao, Yadav, P. J. P.; **Kuruma Malkappa**, Tushar Jana, Sastry, P. U. *Polymer.* **2015**, 77, 323-333.
- (7) *Non-chain extended, non-hydrogenbonding segmented Polyurethanes and studies of their morphological and mechanical properties.* Billa Narasimha Rao, **Kuruma Malkappa**, Sastry, P. U.; Tushar Jana. (*Manuscript under preparation*).

Note: Only publication numbers 2, 3, 4 and 5 are included in this thesis as Chapter 3, 4, 5 and 6, respectively.

CONFERENCE PRESENTATIONS

- (1) Poster Presented on “Polymer Template Assisted Synthesis of Hollow Fe₂O₃/Fe₃O₄ Spherical Nanoparticles” **Frontiers of Polymers & Advanced Materials: MACRO 2010**; December 15-17, 2010, Indian Institute of Technology, and New Delhi, India.
- (2) Poster Presented on “Synthesis of polyurethanes from Butadiene based diols” **9th Annual in-house Symposium: CHEMFEST 2012**; February 24-25, 2012, School of Chemistry, University of Hyderabad, Hyderabad, India.
- (3) Poster Presented on “Polyurethanes synthesized from terminal functionalized butadiene-diol oligomers” **10th Annual in-house Symposium CHEMFEST 2013**; February 15-16, 2013, School of Chemistry, University of Hyderabad, Hyderabad, India.
- (4) Poster Presented on “Synthesis and characterization of HTPB and modified HTPB based polyurethanes” **Polymers on the Frontiers of Science and Technology: APA 2013**; February 21-23, 2013, Punjab University, Chandigarh, India.
- (5) Poster Presented on “Water Dispersible Polyurethanes from butadiene diols: Morphology and Self-cleaning Properties” **3rd FAPS Polymer Congress and MACRO-2013**; May 15-18, 2013, Indian Institute of Science, Bangalore, India.
- (6) Poster Presented on “Water Dispersible Polyurethanes from butadiene diols: Morphology and Biodegradable studies” **11th Annual in-house Symposium: CHEMFEST 2014**; February 21-22, 2014, School of Chemistry, University of Hyderabad, Hyderabad, India.
- (7) Poster Presented on “Simultaneous improvement of tensile strength and elongation: An unprecedented observation in case of HTPB polyurethanes” **International Symposium on Polymer Science and Technology: MACRO-2015**; January 23-26, 2015, Indian Association for the Cultivation of Science, Kolkata, India.
- (8) Oral Presented on “Water Dispersible Polyurethanes from Butadiene diols” **12th Annual in-house Symposium: CHEMFEST 2015**; February 21-22, 2015, School of Chemistry, University of Hyderabad, Hyderabad, India.